No. COO-1617-27

THE UNIVERSITY OF NEBRASKA

DEPARTMENT OF CHEMISTRY

HALOGEN ATOM REACTIONS ACTIVATED BY RADIATIVE NEUTRON CAPTURE AND $^{82}Br^{m}$ AND $^{128}I^{m}$ ISOMERIC TRANSITION

PROGRESS REPORT NO. 5

FEBRUARY 15, 1971

THIS WORK WAS SUPPORTED BY:

The Department of Chemistry,
University Research Council,
The United States Atomic Energy Commission
Contract No. AT(11-1)-1617

Lincoln, Nebraska 68508

DISCLAIMER

THE UNIVERSITY OF NEBRASKA

Department of Chemistry

Progress Report No. 5

February, 1970 - February, 1971

HALOGEN ATOM REACTIONS ACTIVATED BY RADIATIVE NEUTRON CAPTURE AND $^{82}Br^{m}$ AND $^{130}I^{m}$ ISOMERIC TRANSITION

Edward P. Rack, Project Director

Supported by

The Department of Chemistry,

University Research Council,

and

The U. S. Atomic Energy Commission

Contract No. AT(11-1)-1617

February, 1971

PREFACE

The following is a report of the work completed during the period February 15, 1970 to February 14, 1971. These studies were supported by the U. S. Atomic Energy Commission, Division of Research, Contract No. AT(11-1)-1617, the Department of Chemistry of the University of Nebraska, and the University Research Council. Most of the material for this report has been accepted, submitted, or will be submitted for journal publication. Because of the U. S. Atomic Energy Commission's depository library system and the facilities of the Technical Information Service at Oak Ridge, it is possible to make available through a progress report the extensive original data only summarized in journal publications and results of unsuccessful experiments. It is hoped that this report will be of added value to workers in the field.

TABLE OF CONTENTS

LIST OF TABLES

LIST OF FIGURES

LIST OF FIGURES (Cont.)

I. FACILITIES

A. Triga Mark II Reactor

All enutron irradiations were made in the Triga Mark II "swimming pool" nuclear reactor at the Veteran's Administration Hospotal at Omaha, Nebraska. A flux of 1 x 10" thermal neutrons $cm.^{-2}$ $sec.^{-1}$ was present at an operating power of 15.5 kilowatts. Various positions in the "lazy susan" sample holder were employed and the assembly was rotated to ensure that all samples received the same neutron flux and radiation dose. In very short irradiations the assembly was not rotated, but samples were all irradiated in the same position. The radiation dose was approximately 3×10^{17} $e.v.g.^{-1}$ $min.^{-1}$ using Fricke dosimetry. This was confirmed by studying the ^{131}I organic uptake in $c\text{-}C_6H_{12}$, due to radiation.

This past year the reactor operated routinely for at least four eight-hour days a week at 15.5 kilowatts. The radiochemistry group has used for the period from August 1, 1968 to July 31, 1969, 300 hours (integrated time in reactor) at 15.5 kilowatts power making 2,500 irradiations.

B. Radiochemistry Laboratory

All sample preparation and most of the radioassaying were performed in a well-equipped, specially-designed radiochemistry laboratory in the new Hamilton Hall Chemistry building. The two hot laboratories contains four six foot "Oak Ridge-Type" hoods, several radioactive waste sinks, radiation safety equipment, seven separate vacuum lines for preparing gas, liquid and solid state systems, and the usual laboratory facilities. The counting room is equipped with two radiogas chromatographs, three single-channel analyzers with sev-

eral 2" x 2" NaI crystals, four GM counting stations, four gas-flow counters, and a Nuclear-Data 128-Channel analyzer with a 3" x 3" NaI crystal specially housed in a concrete, cadium and lead cave.

If and when we get a neutron generator we have a specially-constructed room for its housing. This room is presently used for equipment storage.

For most of our ^{80}Br, ^{38}Cl and ^{128}I experiments, we used the radiochemistry facilities and radioassaying equipment of the Omaha VA Hospital. The use of their RIDL 400-channel analyzer with 3" x 3" NaI crystal was most helpful in many of our studies.

II. INSTRUMENTATION

Radiogas Chromatograph

The first radiogas chromatograph utilized in this laboratory was constructed by Merrigan and Nicholas. This initial instrument was completely redesigned and extensively modified during the summer of 1967, resulting in improved reliability, sensitivity, and versatility of the chromatograph. This instrument has been in day-to-day use since it was placed in operation and has been used for all the product distributions determined reported in this progress report.

After a year of extensive usage, a critical evaluation of the above instrument's performance suggested a number of improvements or modifications in the original design. On the basis of this evaluation a new chromatograph was constructed in order to incorporate the suggested qualifications. Figures 1, 2, and 3 show the basic features of this chromatograph. The helium carrier gas is obtained from a pressurized steel cylinder and passed through a two-stage pressure regulator, shut-off valve, stream splitter, flow-meters, constant flow controllers, bulblet breaker and/or preheated injection ports, and into the reference and analytical columns. After separation in the analytical column, the eluted fractions enter the sensing portion of the thermal conductivity detector, where macroscopic amounts are detected. The signal from the thermal conductivity detector is routed through an attenuator to one pen potentiometric strip chart recorder. After passage through the thermal conductivity cell the analytical and reference carrier gas streams are combined for passage through the radiation detectors. The radiation detector is a window-type proportional flow-counter, housed in a heated enclosure to prevent condensation of the

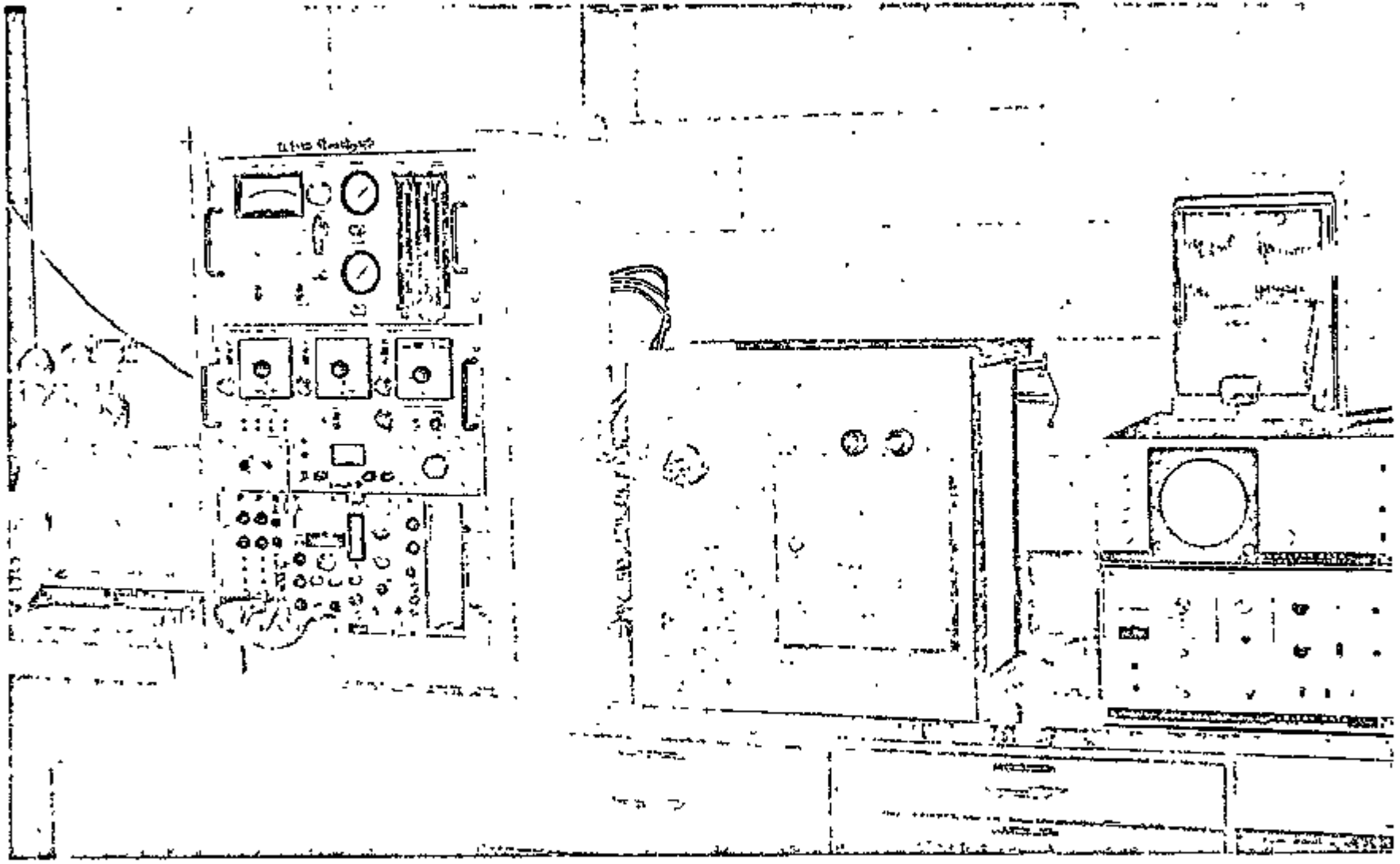

Figure 1 View of the Complete Instrument.

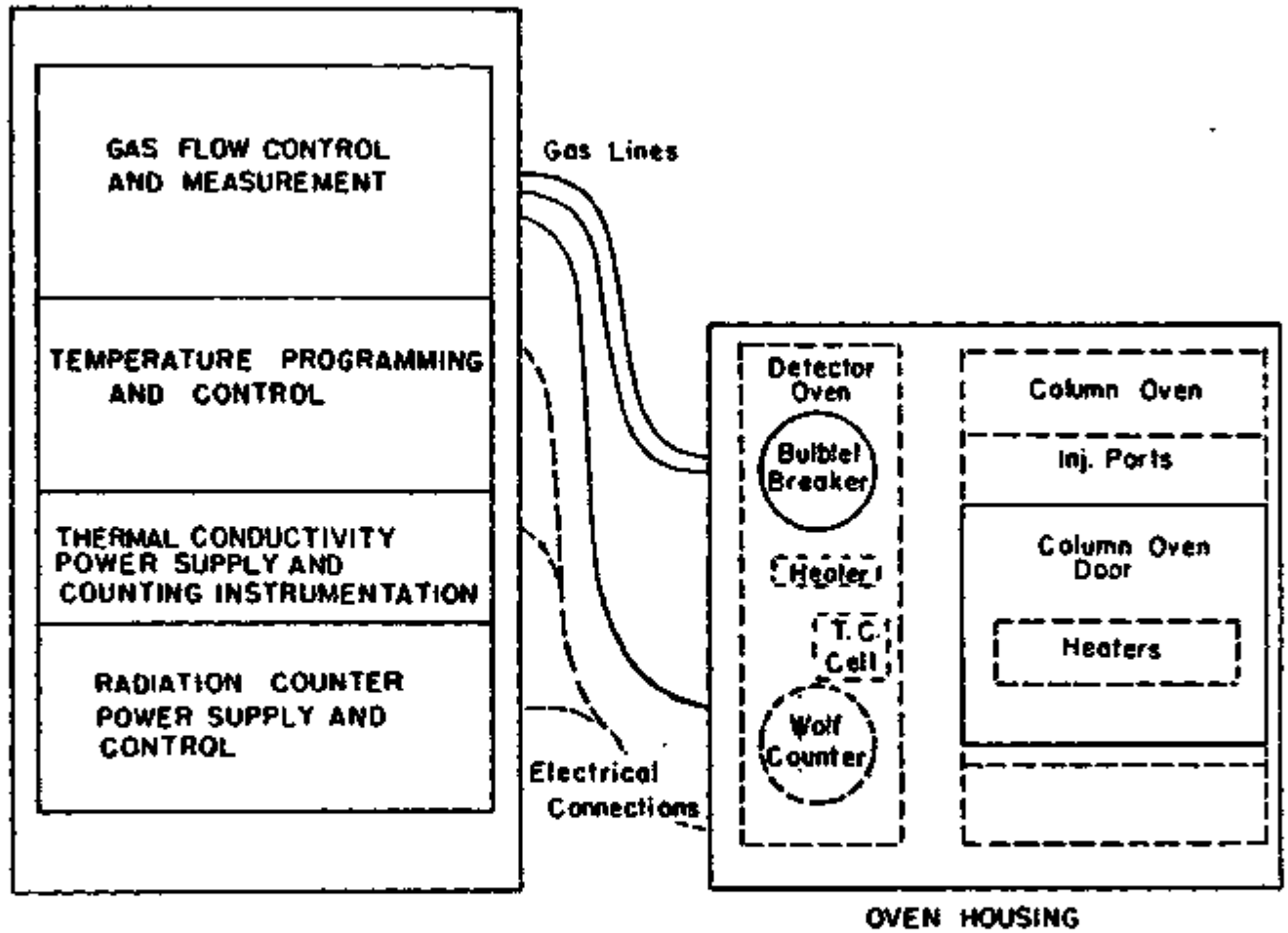

Figure 2. Block diagram of the radiogas chromatograph.

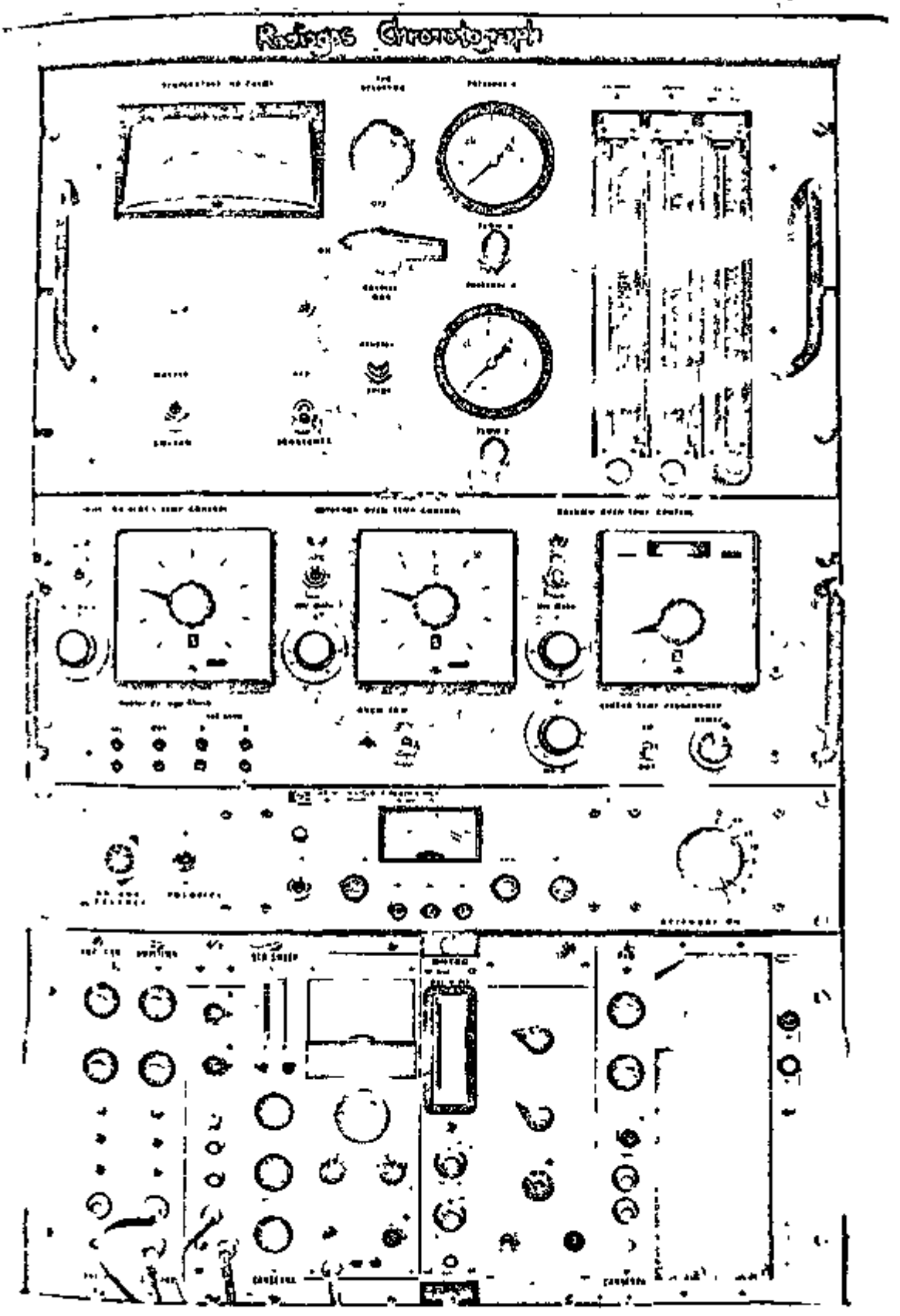

Figure 3. View of control console.

products. Trace quantities (~ 10^{-3} g.) of eluted products are detected by monitoring the beta and/or gamma radiation emitted.

The signal from the proportional counter is directed through a preamp, amplifier, single-channel analyzer, ratemeter, and to a multichannel analyzer for digital storage of the output. The analog output of the count-rate meter is directed to the second pen of the strip chart recorder. From the proportional counter the eluted products flow through heated tubing to liquid N_2 cold traps, where the radioactive materials are removed from the carrier gas stream. After passage through the cold traps the carrier gas may be routed to a fume hood to insure that no radioactive species escape into the laboratory atmosphere.

The columns are housed in an insulated temperature controlled oven of a plenum chamber design. The temperature of the column oven is controlled by a 0-400° C potentiametric temperature controller possessing linear programming capabilities. The thermal conductivity cell, proportional counter, and bulblet breaker are located in a separate heated detector oven. The location of the detectors in an enclosure thermally isolated from the column oven, permits variation of the column oven temperature without any accompanying thermal effects in the various detector signals.

Carrier Gas Measurement and Control

Figure 4 shows in schematic form, the gas flow-through the instrument. Gas tank (A) and pressure reduction valve (B) furnish the supply of He carrier gas at a constant pressure of 50 psig. The carrier gas enters the flow control panel through shut-off valve (C) and is then split into two streams for entrance into the flow meters (F & G). The flow-meters are Brooks Sho-Rate "150"

Purgemeters with direct reading scales, having a ± 17 full scale accuracy for He at 50 psig and 25°C. These meters are protected from particulate contaminants by Brooks Model 1390 filters (D & E) attached to the inlets of the individual meters. After passage through the flow-meters the carrier bas streams pass through two Brooks ELF Flow Rate Controllers (H & I). These controllers provide valves for the control of the individual carrier gas flow rates and, after an initial flow rate has been set, automatically compensate for any increase in downstream pressure such as would be encountered in temperature programming. Individual (0-60 psig) pressure gauges (J & K) monitor the downstream pressures and are located between the flow controllers and the carrier gas exits from the control panel.

After exiting from the control panel the carrier gas streams are routed to the oven assembly. Here one stream enters a bulblet breaker assembly (1), housed in the detector oven and proceeds to inlet of a separately heated injection port (M). The other carrier gas stream proceeds directly to the inlet of a matching injection port (N). The carrier bas streams then pass through interchangeable reference and analytical columns (O & P) located in the column oven. From there the carrier bases enter the detector oven and pass through the thermal conductivity cell (Q) and are recombined for passage through the radiation detector (R). After exiting from the radiation detector (and the detector oven) the carrier gas is routed through a series of two liquid N_2 cold traps (S & T) and then exited into the atmosphere.

All tubing and tubing fittings used prior to the entrance of the carrier gas into the various injection ports were of copper construction. Similarily all materials that would be contact with the sample gases were constructed of stainless steel, teflon, or glass. The use of direct reading flow meters

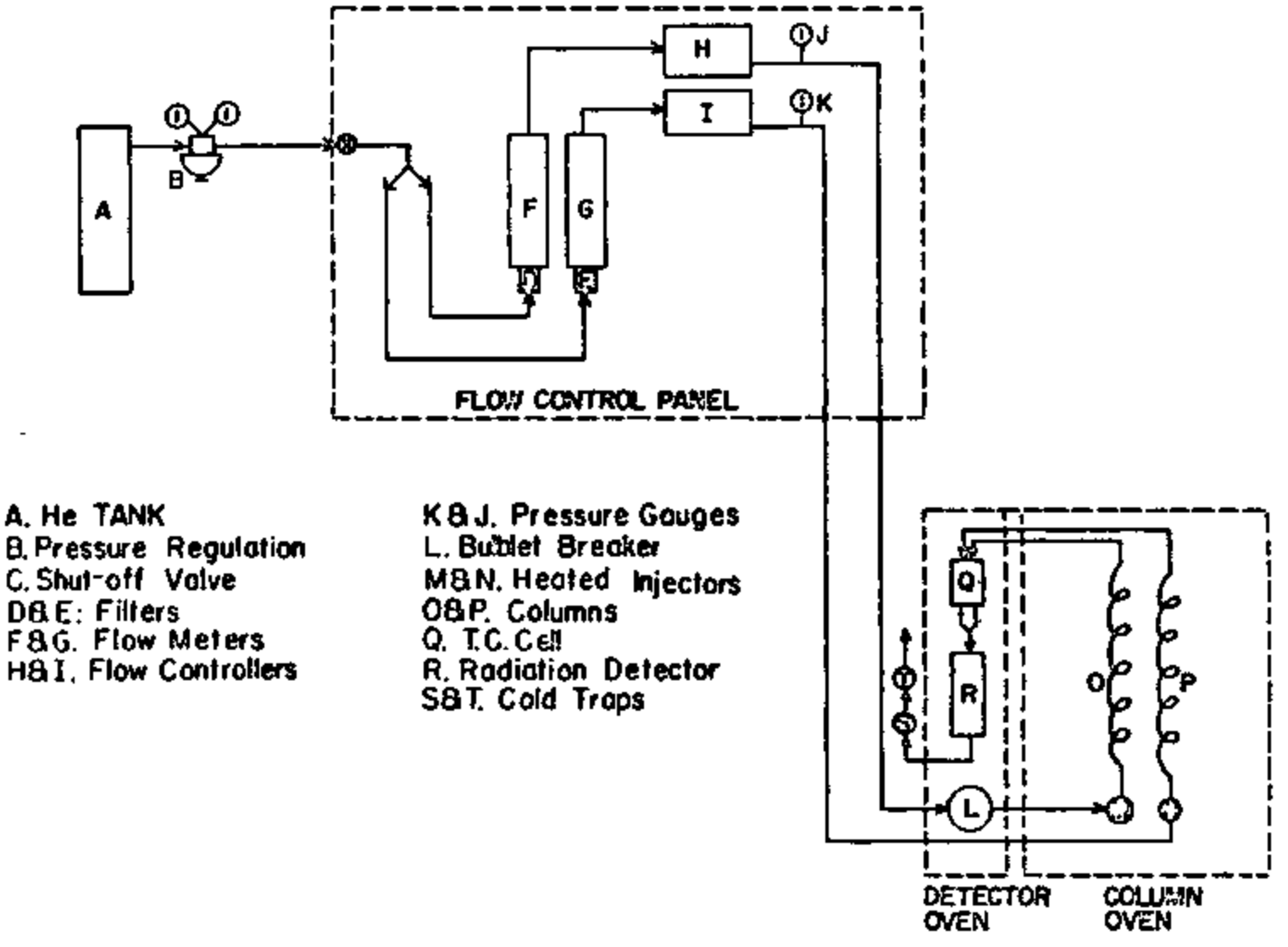

Figure 4. Instrument carrier gas flow.

greatly simplifies the determination of the carrier bas flow rates through the columns and the radiation detector. The inclusion of the constant flow controllers permits the automatic maintenance of the initial flow rate over a downstream pressure variation of 0-40 psig to within ± 0.3% of the instantaneous rate. Thus providing the convenient and accurate flow control essential in radiogas chromatography due to the direct dependence of the hot product peak intensities on the rate of passage of the sample gases through the detector.

Injectors

Two different types of sample introduction techniques are employed. Provision for the introduction of liquid samples is provided via two heated injection ports (Fig. 5), and quartz encapsulated gaseous systems are introduced directly into the carrier gas stream with a bulblet breaker (Fig. 6).

Measured quantities of liquid samples are introduced by syringe through a silicon rubber septum located in the injection ports. The individual injection ports were constructed using a bored through Swagelok fittings for the outlet connections to the columns and/or separate inserts. Thus either flash vaporization or direct on column injection of the sample is permitted by the selection of the appropriate column to injector connection and injector temperature. The injectors are heated by two 50 watt cartridge heaters and the temperature controlled by a Weathermeasure Corporation Model TPC-N potentiometric temperature controller with an accuracy of ± 0.5% of the set point. A large brass heat sink is used to minimize rapid temperature fluctuation in the injectors and to simultaneously provide a heat source for preheating

the carrier gas before entrance into the injectors. This is necessary to prevent condensation of the sample.

The capability of directly introducing gaseous samples, incapsulated in ~ 10 ml. quartz ampoules, into the carrier gas stream is provided by the specially constructed bulblet breaker shown in Fig. 6. In addition to the bulblet breaker itself a 1/4 in. dia. by 5 in. removable stainless steel pre-column is located between the bulblet housing (Teflon) and the outlet of the assembly. This pre-column is packed with fine mesh potassium ferracyanide which removes inorganic halogens from the sample prior to entrance into the analytical column; thus, preventing internal contamination of the instrument by the reactive inorganic products. The bulblet breaker assembly is housed in the detector oven, thereby, eliminating the necessity of providing separate heating and temperature control.

Columns

The analytical columns, packed with an appropriate support and stationary phase, are coiled stainless steel or glass tubes 1/4 in. in diameter, 10 ft. in length, with a spiral diameter of 6 to 8 in. The diameter of the spiral is large enough to prevent loss of separating power attributable to the longer path which a gas has to transverse along the outer wall of the column. Either glass or stainless steel are used because of their relative inertness toward halogenated compounds as compared to other commonly used materials. The column inlets and outlets are connected to the chromatograph by way of 1/4 in. Swagelok fittings. When glass columns are used the stainless steel ferrules are replaced with teflon ferrules. As a result of the small separation between

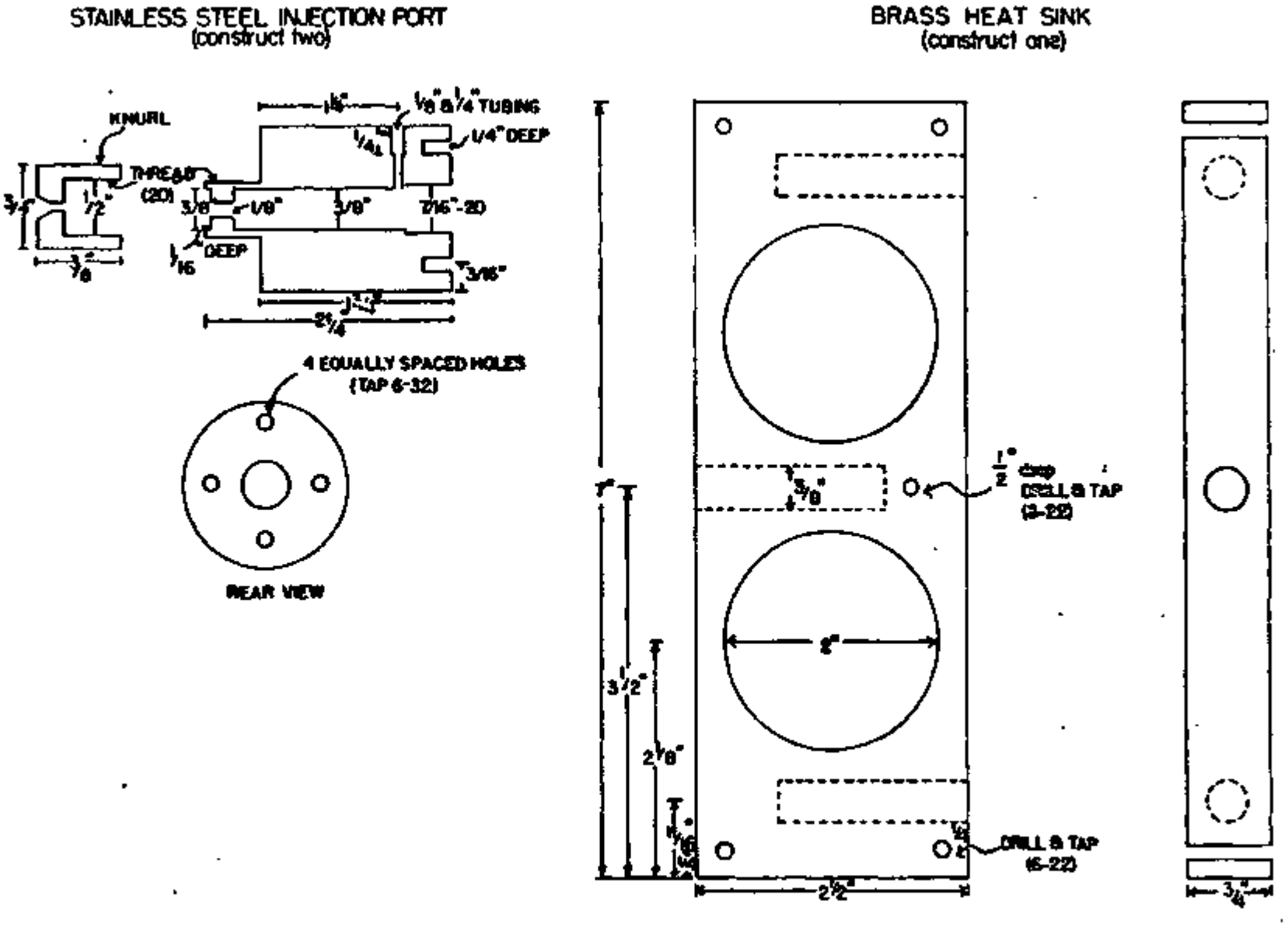

Figure 5. Injection port assembly.

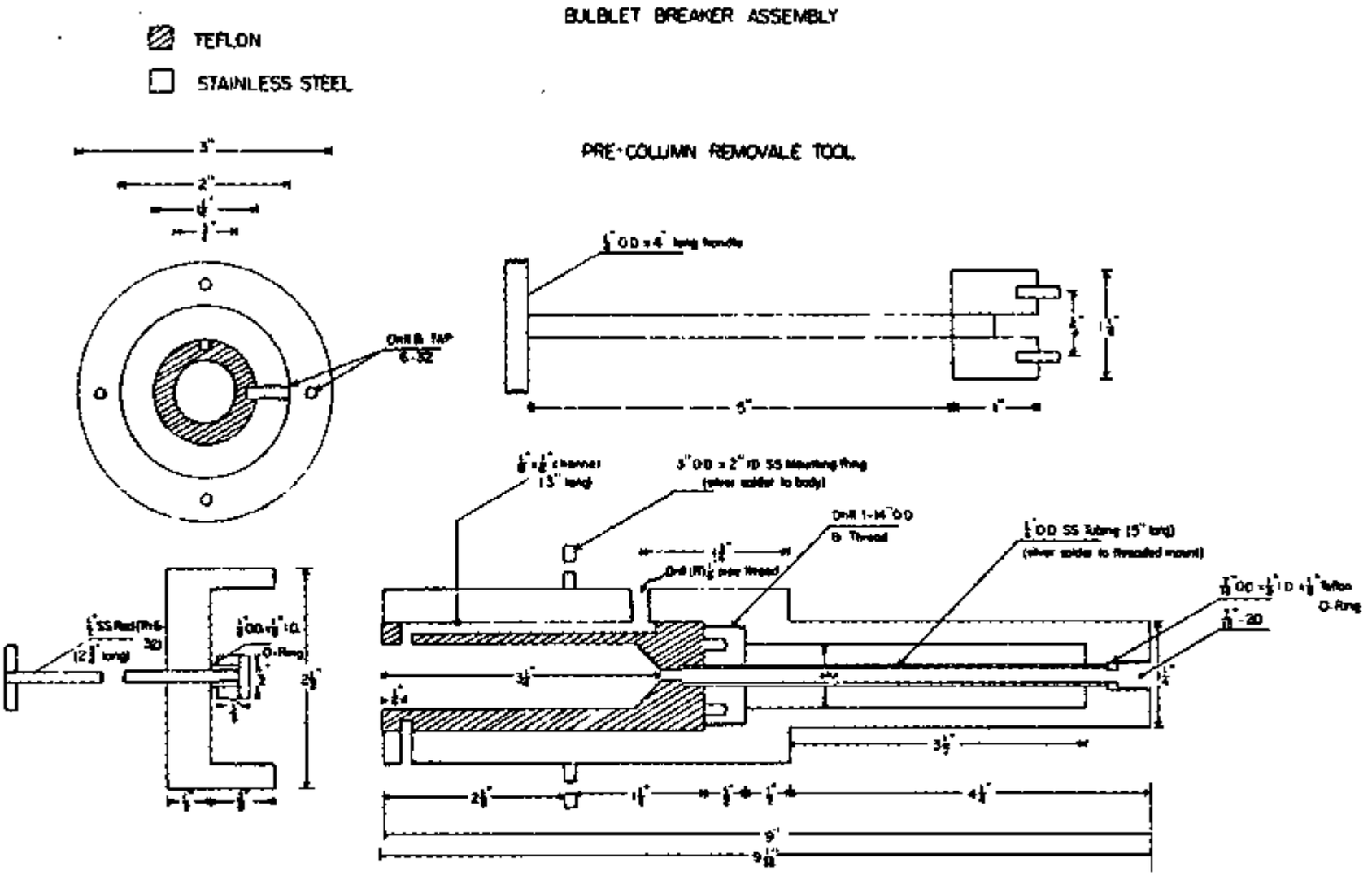

Figure 6. Bulblet breaker and pre-column assembly.

the injection ports, the individual columns must be coiled in opposite directions, i.e., the left column must be coiled in such a manner that its spiral extends to the left when connected and the right column such that its spiral extends to the right. Filling of the columns was accomplished by applying suction to the outlet end along with vibration during the addition of the column packing to the inlet.

Detectors

Two detectors are present for the identification and quantitative treatment of fractions which elute from the column. A thermal conductivity cell was selected to detect macroscopic amounts of eluents because:

1. The measurements could be readily monitored with simple instrumentation.
2. The detector, because of its simplicity could be readily installed.
3. The sensitivity is high and adjustable.
4. The detector is sensitive to nearly all gases.
5. The wide operating temperature range of the cell.
6. The signal is linearly proportional to the concentration of the components eluting from the analytical column.

Since the thermal conductivity cell measures the presence of a component by a physical means, i.e., thermal conductivity, the sample was not destroyed and could be recovered for subsequent measurement of the component possessing a radioactive label.

The outlets of the individual columns are directed into the respective wiring and reference inlets of the thermal conductivity detector. The

detector used is a Model 10-285, supplied by Gow-Mac, and consists of a stainless steel block with two matched sets of 48 ohm gold plated tungsten filiments, one set each for the reference and sensing portions of the bridge. As a result of the gold plating on the tungsten filiments of this detector the filiments are insensitive to air oxidation when hot. This permits continuous operation when exposed to air, as can easily occur when using the bulblet breaker, thereby eliminating a serious source of instrument down time. Because the sensing and reference portions of the bridge are identical in all respects they may be readily interchanged; thus, in a dual column instrument either column may be used for the reference column simply by reversing the polarity of the bridge output. This provision has been included as shown in the complete thermal conductivity circuitry diagram (Fig. 7).

In this research, the thermal conductivity detector was used only for qualitative determinations of compounds so calibration of the detector output as a function of sample composition and operating conditions was ignored.

After passage through the thermal conductivity cell the reference and sensing carrier gas streams are recombined just prior to entrance into the radiation detector. Thus, fractions eluted from either column pass through the detector, again permitting either column to be employed in the analytical column for the quantitative and qualitative assay of the radioactively labeled products eluted.

The radiation detector is a cylindrical window flow-through proportional counter. The basic design of this counter and a number of its characteristics have been previously reported by Welch, et. al.[1] The design and dimensions

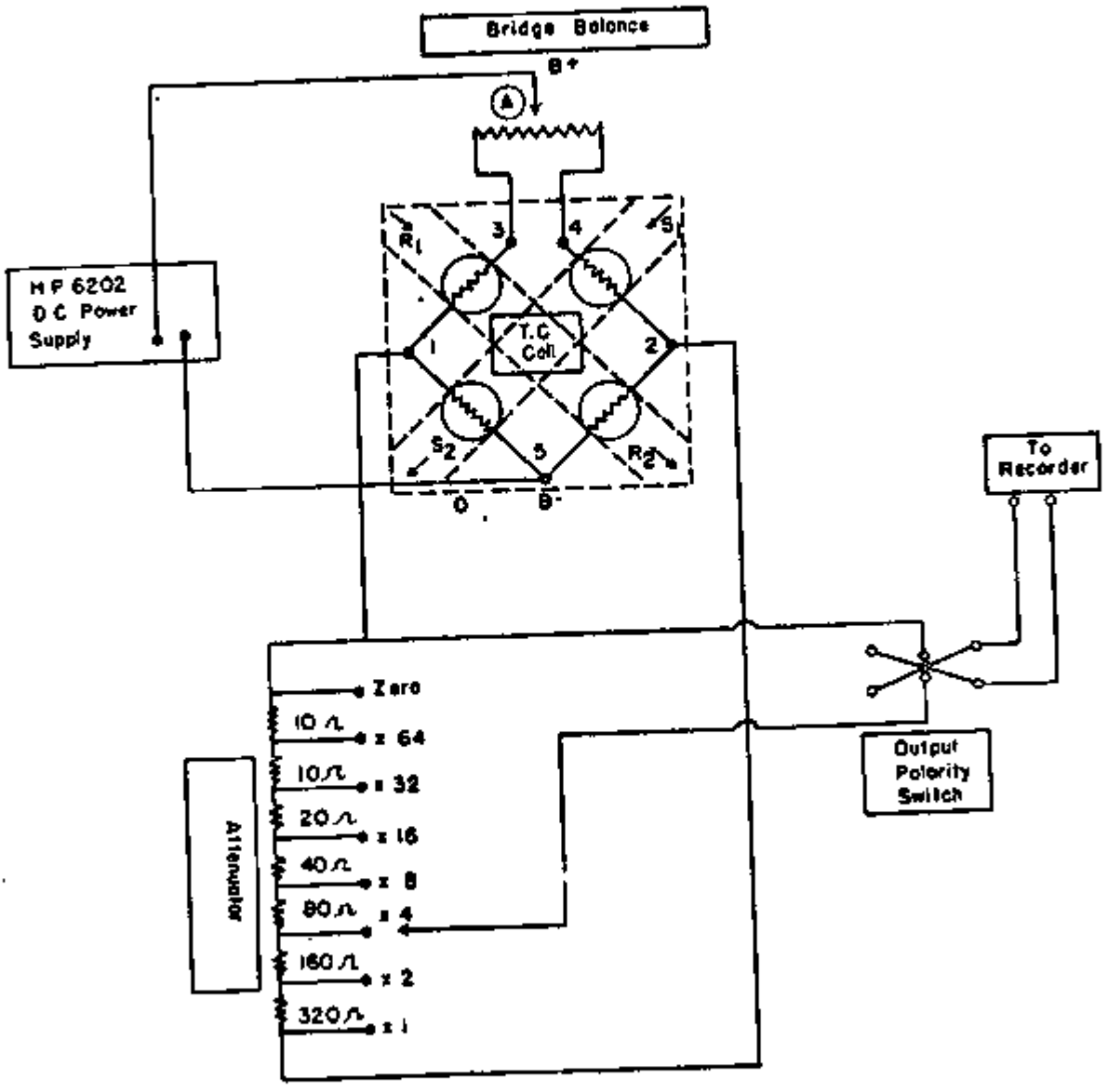

Figure 7. Circuit diagram of the thermal conductivity detector.

of our counter are shown in Figs. 8, 9 and 10. The design of the counter incorporates a number of modifications in the original, such that the counter may be placed in a heated enclosure and to improve its operation with the labeled halogen compound obtained in this research.

The principle modifications are as follows:

1. The counter was constructed so that it could be completely disassembled from one end, thus permitting easy access for repairs, when mounted in its oven enclosure.
2. A removable center support rod was employed in the window insert, thereby, permitting the window insert inlets and outlets to be modified in such a manner as to minimize any possible internal dead space in the flow assembly.
3. Use of stainless steel or titanium for construction of all components that are in contact with the sample because of their relative inertness to high temperatures and halogenated compounds.
4. Six equally spaced (60° apart) high voltage (0.0035 in tungsten wire) anodes, supported by Teflon insulators, were used to provide a uniform electrostatic field around the window containing the sample gases.

The previously reported[1] maximum operating temperature of the original design was 150°C. Since many of the possible products of systems under investigation by this laboratory have boiling points higher than 160°C, several of the modifications on the original design, were implemented in an effort to increase the maximum operating temperature of the counter.

There are two restrictions placed on the maximum operating temperature

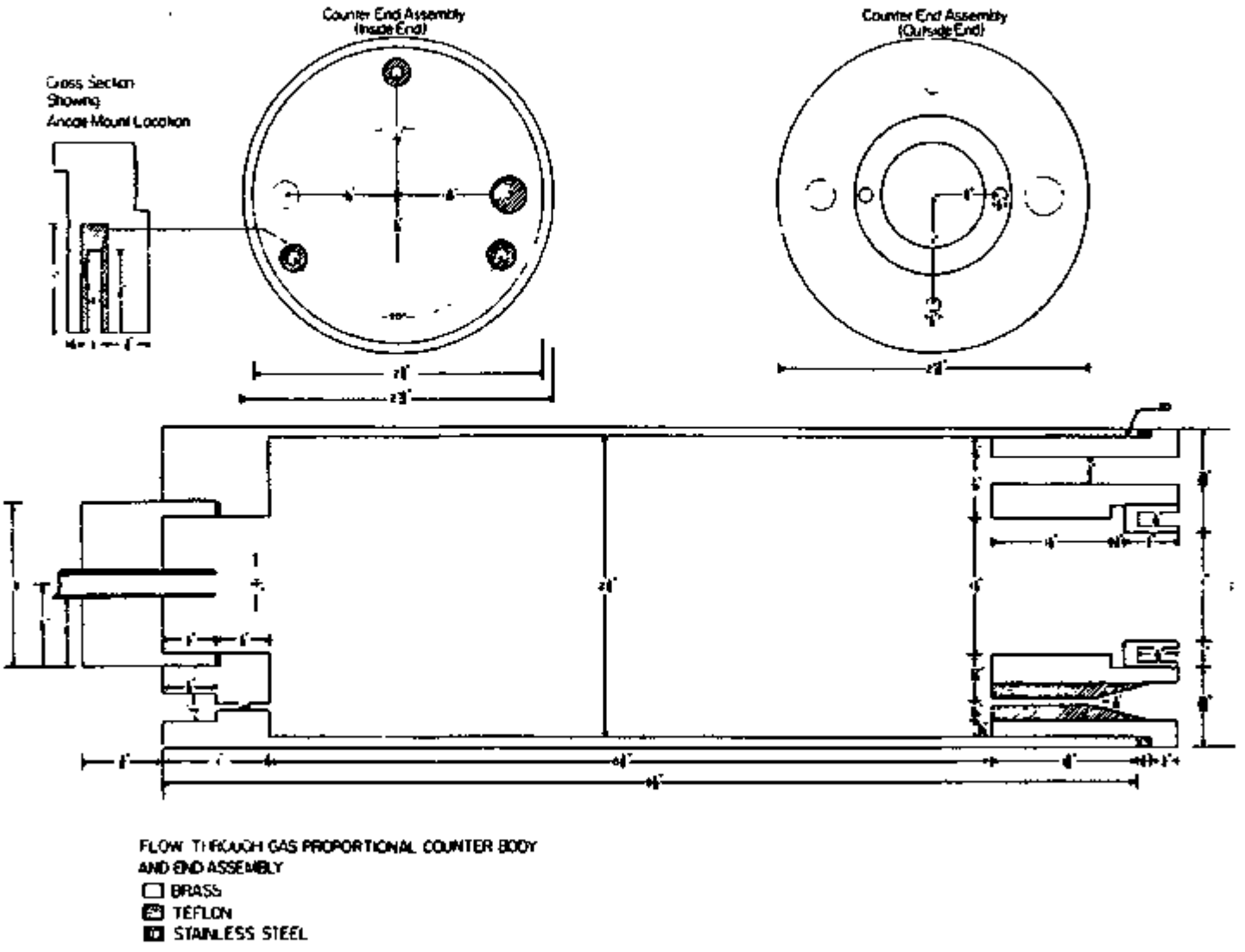

Figure 8. Dimensions and design of the counter body.

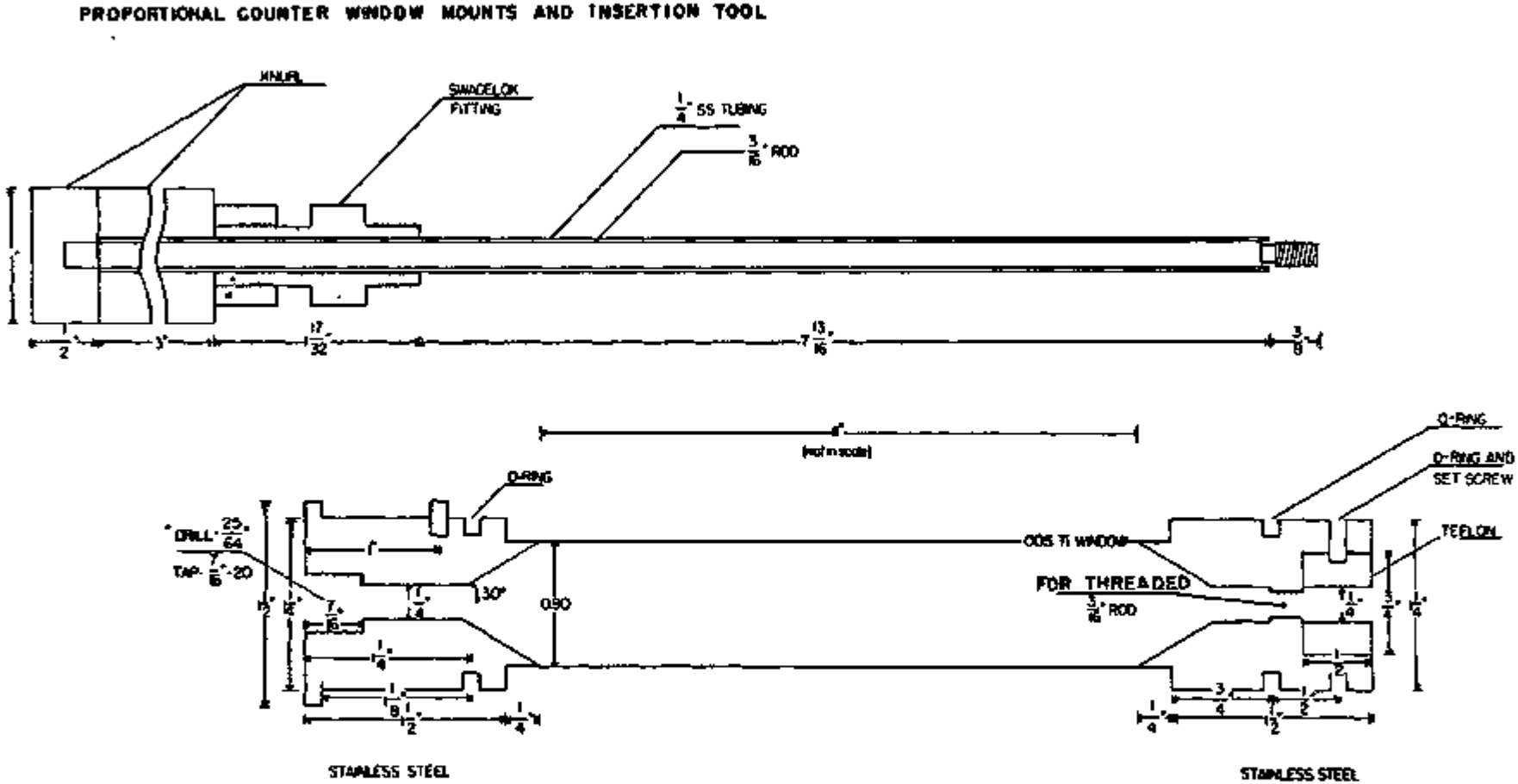

Figure 9. Window insert and insertion-removal tool.

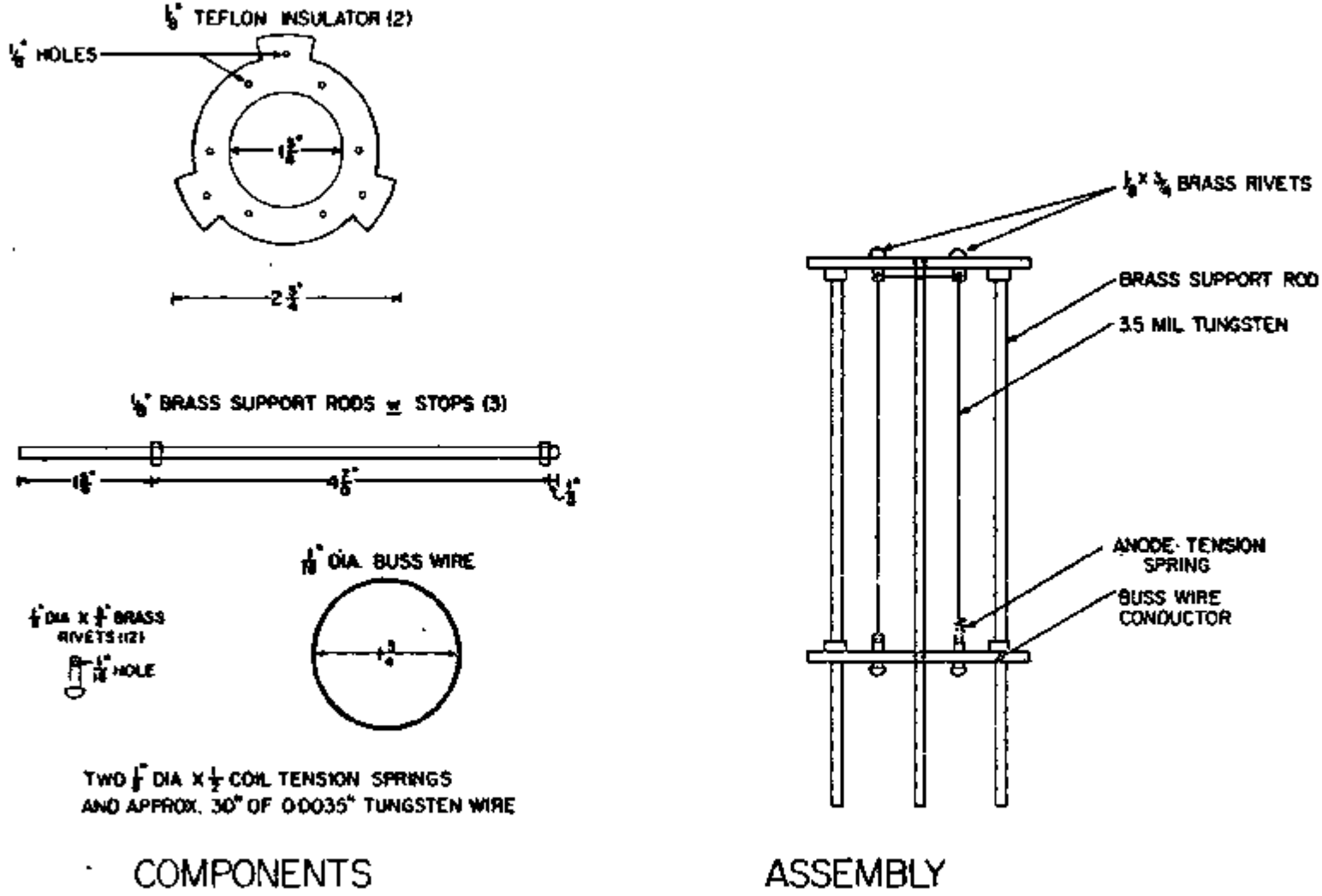

Figure 10. High voltage anode components and assembly.

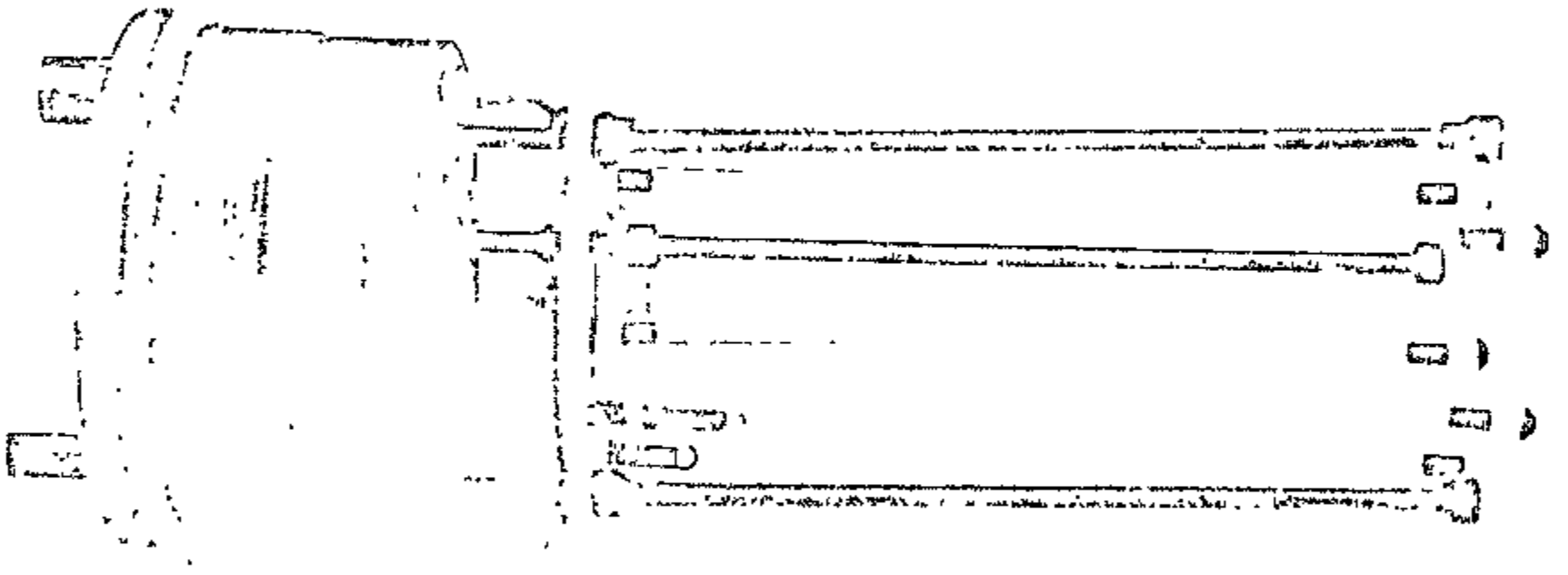

Figure 11 View of assembled high voltage anode assembly mounted in counter endcap.

of this type of counter. The first being the upper temperature limits of the materials used in the construction of the counter. This would be approximately 250°C due to the use of Teflon for the construction of several of the counter components. However, this physical temperature limitation can be readily increased by replacing the Teflon components with components constructed from materials possessing higher thermal stabilities such as a ceramic.

The second temperature limitation is imposed by maximum temperature at which a usable plateau may still be achieved. The usable plateau length decreases with increasing temperature of the counter as shown in Fig. 12. This is a result of increasing ease of ionization of the counting gas mixture (90% Ar + 10% CH_4) with increasing temperature, thus shifting the plateau to a lower voltage range and decreasing its length. Once the temperature has reached a certain point the length of the voltage plateau will decrease to zero, thereby restricting the counter to operation below this temperature. Although the counter may be operated at temperatures in excess of this limit by using a voltage in the sharply rising region prior to the onset of the plateau, the resulting accuracy would be poor because of large changes in sensitivity caused by small voltage fluctuations in the power supply.

For a cylindrical counter the largest voltage gradient exists in the vicinity of the anode wires and is a function of e^{-r}, where r is the radius of the anode wire. Thus by using a larger diameter anode wire (3.5 mil.) and increasing the applied voltage the voltage gradient between the cathode (outer body) and the anodes would be reduced. This should result in a corresponding decrease in the sensitivity of the plateau region to the temperature of the counting gas.

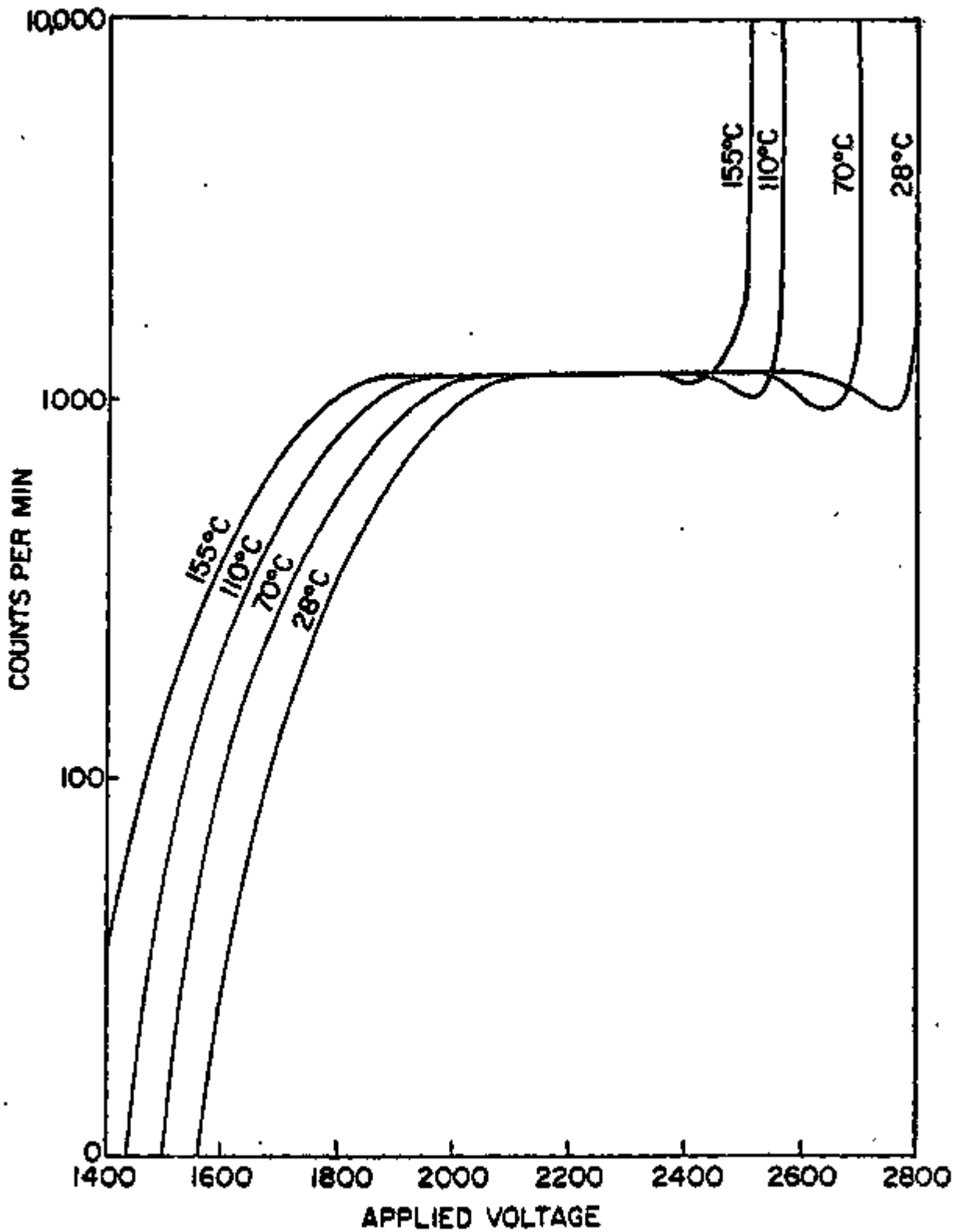

Figure 12. Counter voltage plateaus as a function of temperature.

Using the 3.5 ml. tungsten anode wires the voltage plateaus as a function of temperature were determined using a 5 mCi ^{137}Cs source located in the center of the counter and a mixture of 90% argon and 10% methane, at a flow rate of 10 ml. per minute, as the counting gas. As shown in Fig. 14 the plateau narrows from ~ 650 volts at 28° C to ~ 550 volts at a temperature of 155° C. Using the plateau voltage values given above, the decrease in the length of the voltage plateau with increasing temperature was found to be 0.8 volts per degree C. This would give an extrapolated maximum operating temperature of approximately 650° C for the proportional counter. However, as discussed previously, the present operation of the counter is limited to 250° C by the Teflon construction material.

In the operation of an earlier model counter, which contained a window insert identical in design to the original, problems with false efficiencies and contamination or sticking, with labeled halogen compounds possessing detected activities in excess of 10,000 counts per min., were encountered. This resulted in failure of the detector signal to return to the baseline after the illusion of the component possessing a high activity.

In an effort to determine the cause of this problem the counter was deliberately contaminated by introducing large quantities of ^{82}Br labeled organic bromides. The window insert was then dismantled and the individual components inspected for contamination. It was found that the stainless steel window, window support surfaces, and (to a greater extent) the exposed epoxy used to form and attach the window were contaminated. However, the degree of contamination of these surfaces was small in comparison to that observed during operation of the counter.

Examination of the design[1,2] and of this window insert showed the existance

of a small dead volume (~ 1-2 ml.) between the entrance and/or exit gas ports and the window to insert seal. The trapping of a portion of the activity being detected in this dead volume would account for the appearance of contamination when high specific activity compounds are passed through the counter.

The counter contamination was observed to decrease at a rate independent of the half-life of the isotope responsible. This observation would support the contention that the principle cause of the observed "sticking" in the counter resulted from the trapping of a portion of the compound in these dead volumes rather than actual contamination of the counter surfaces. This could also contribute to the false efficiencies observed by Welch, et. al.[1], in this type of counter.

In an effort to correct these difficulties a new window insert (Fig. 9) was designed. By elimination of the counter support rod, which is unnecessary once the window insert is in place, the amount of stainless steel surface exposed to the sample gases for possible contamination was reduced. In addition, a slight improvement in the counting geometry was obtained.

The elimination of the center support rod also permitted an improved inlet and outlet design, which minimizes or eliminates any dead volume associated with the detection volume in the earlier design, thus eliminating the suspected major source of contamination.

A new 0.5 mil, titanium window was used in this counter in place of the 1.0 mil. stainless steel window used previously, thereby, eliminating all exposed stainless steel surfaces in the counting volume. This window material was found to be more inert to organic halides than the previously used stainless steel and, in addition, the smaller attenuation coefficient, for the

β-radiation detected, of this thinner and lower Z material window resulted in a two-fold increase in the detection sensitivity of the counter.

The use of high temperature silicon O-rings to seal the window to the insert (tested and found to form a gas tight seal of the thin window material to the stainless steel surfaces) eliminates the major portion of the epoxy surface on the inside of the window. The only remaining epoxy (Good year Pliobond HT-30) used in the construction of the window insert was that used to form the thin titanium foil into a cylinder. Other joining the edges of the foil together to form the cylinder and allowing the adhesive to partially set, the interior of the cylinder was carefully cleaned with ethyl acetate solvent to remove any excess adhesive. Thus, the maximum surface area of exposed epoxy in the window assembly consisted of a very thin line (<0.05 in.) the length of the cylinder. Subsequent operation of the counter has shown these measures to be successful in eliminating or greatly reducing the contamination problems previously encountered with the earlier design.

The relative sensitivity of the proportional counter as compared to the NaI(Tl) scintillation well employed previously in the laboratory was determined for a number of halogen isotopes. The results are shown in Table I. As shown the relative sensitivities for the various isotopes differ greatly due to their dissimilar modes of decay; i.e. the ratio of the average number γ-photons emitted to the number of β^- particles (one) in a single decay. Since the proportional counter is relatively insensitive to γ-radiation (∿ 1% efficient) and close to 100% efficient for the detection of the β^--radiation the sensitivity of the Wolf counter would not be expected to vary appreciably for the various isotopes tested. However, the scintillation well is insensitive to β^- particles and detects incident γ-radiation only (with ∿ 20% efficiency) thus the large variation found for the relative sensitivity of the two counters can be largely attributed to the wide variation in the γ/β^- intensities (shown in Table I,

column 5) for the three isotopes.

One of the most important results from the determinations of the relative sensitivities is the consistently higher sensitivity of the Wolf counter, particularly for the ^{128}I isotope of interest in this research. The greater counting efficiency, or sensitivity, of the proportional counter over that of the scintillation well, is the cumulative effect of a number of factors. A few of the more important ones are: (1) improved geometry (~ 4π); (2) inherently greater static efficiency (a maximum of 5:1); and a larger active volume (~ 42 ml.) with a resultant increase in the flow counting efficiency. This greatly increased sensitivity has permitted the previously unobtainable analyses of low activity samples.

The efficiency of the flow-through proportional counter could be greatly improved by eliminating the window and passing the radioactive effluent directly through the counter, thereby eliminating all attenuation of the emitted β^- radiation by the window material. However, halogen containing compounds are effective quenching agents and preclude radioassay in a windowless counter.

The heating and temperature control of the counter is provided by the detector oven enclosure in which it is housed. The counter is shielded from background radiation by wrapping with eight turns of 1/8 in. thick sheet lead. The operating high voltage is supplied by a NIM Canberra Model 3002 high voltage power supply. Signal detection and amplification is provided by Canberra Models 1406 preamplifier and 816 amplifier, respectively. It was necessary to add a special diode protection network to the input FET transister on the Model 1406 preamplifier in order to prevent destruction of the transister by the input signals from the counter. After amplification the signal was routed to a Canberra Model 1431 single channel analyzer which was used to provide

TABLE I

Comparison of the Relative Sensitivities of the Wolf and NaI(Tl) Well Counters for ^{38}Cl, ^{82}Br, and ^{128}I

Isotope	Activity Wolf Counter	Detected (C/M) NaI(Tl) Well Counter	Relative Sensitivity	Relative γ/β^- Intensity Ratio
^{82}Br	20527	4718	4.4	314
^{38}Cl	33952	973	35.0	85
^{128}I	28143	141	200.0	16

discrimination against low level instrument noise. The SCA output was divided by a BNC "tee" connector and routed to a MecTronics Model 775 103/linear ratemeter and a Nuclear Data ND-110 128 channel analyzer. The output of the ratemeter is connected to one pen of a Dohrmann Instruments Model DC-120 dual pen strip chart recorder from which a permanent analog record of the counter output is obtained. The 128 channel analyzer is operated in the multi-sealing mode with a 10 sec. dwell time, thus the digital record of the counter output, over a time period of 1280 sec. in 10 sec. increments, is obtained from integration of product peak areas. A black diagram of the GC radiation detection system is shown in Figure 8.

Collection Devices

After gaseous fractions flow out of the counter, they are trapped in two tandem cold traps at -196° C. Radioactive compounds enter the top of the trap and are condensed on the sides. Stopcocks are arranged to permit removal of one trap while passing the effluent through the other, or, to pass the effluent through both traps in series. Over 98% of the radioactive compounds were shown experimentally to be trapped in the first cold trap. Even greater percentages were trapped when small amounts of glass wool are placed in the path of the carrier gas through the trap. After passage through the traps the carrier gas is expelled into the room or channeled to a fume hood where it is discharged if there is a possibility that all dangerous quantities of radioactivity were not removed by the cold traps.

Oven Enclosure

The main oven enclosure consists of a 21 in. wide by 20 3/4 in. high by

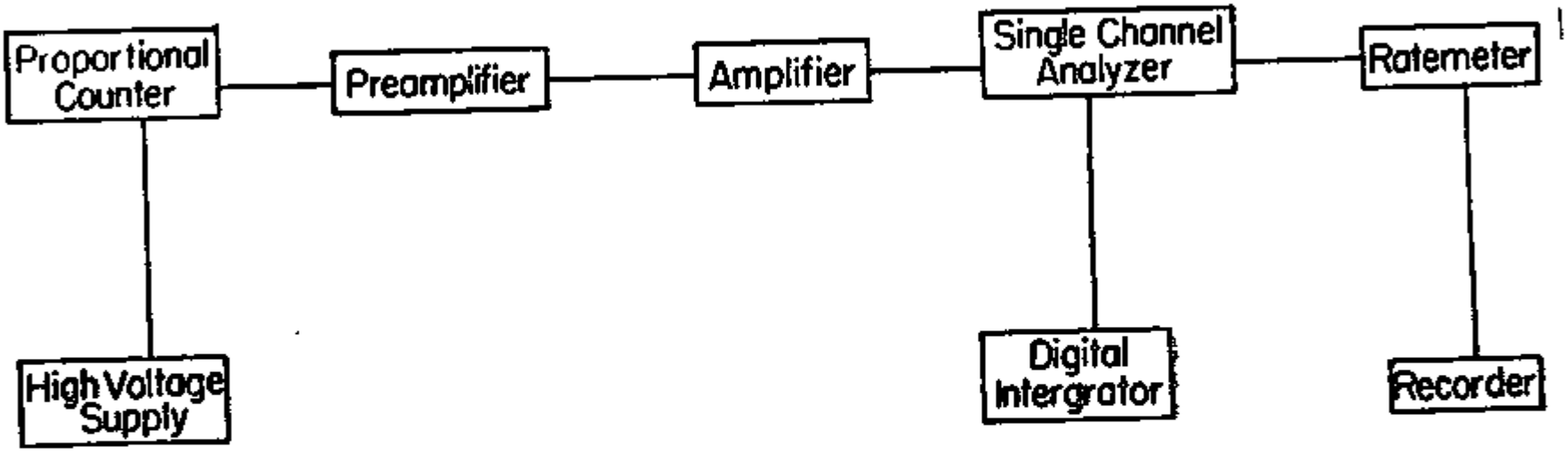

Figure 13. Block diagram of GC radiation detection system.

16 3/8 in. deep box with the front enclosed by a removable 1 3/8 in. thick panel housing the injectors and column oven access door. The main enclosure and front panel were constructed by attaching 3/8 in. thick high density asbestos board insulation to the inside of a 1 in. x 1 in. angle iron frame. Further insulation was provided by completely covering the exterior with a 1 inch thickness of fiberglas. After installation of all components the entire exterior was covered in with sheet metal. The interior of the insulated enclosure was then divided into two thermally isolated compartments (detector and column ovens) with provision for independent temperature control. The thermal barrier used to isolate the separate oven enclosures consisted of two 3/8 in. thick sheets of asbestos board with a 1 3/4 in. space, filled with fiberglas, between the asbestos sheets. The larger of the two compartments (10" x 15" x 18") was used for the column oven and the smaller (5 1/2" x 15" x 18") for the detector oven. A frontal view of the oven with the front panel and sheet metal column housing removed showing the location of several of the interiorly located components of the instrument is presented in Figure 14. The front panel is shown in Figure 15.

The column oven is a plenum chamber design as shown in Figure 16. This design was employed to insure uniform air velocity and has been reported[4] to provide a more uniform column temperature with a substantial reduction in column thermal gradients during temperature programming than other commonly employed oven designs. A three inch squirrel cage blower delivers air at high velocity to the plenum chamber, separated from the column compartment by a perforated metal sheet. The high velocity of the air and the flow resistence offered by the perforated sheet create a uniform pressure across the surface of the perforated sheet. This in turn promotes uniformity of air velocity

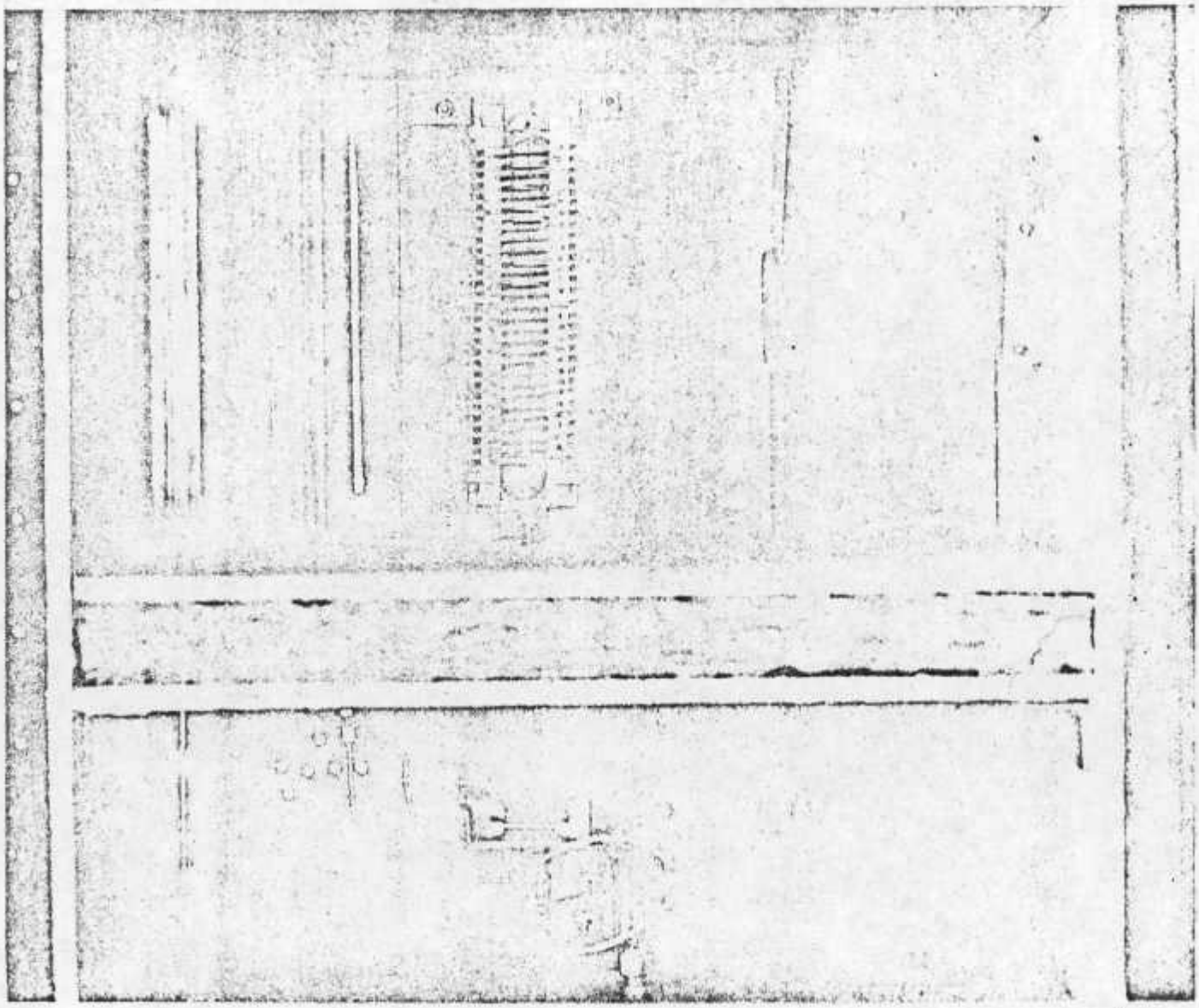

Figure 14. Front view of partially assembled oven with front panel and sheet metal column housing removed.

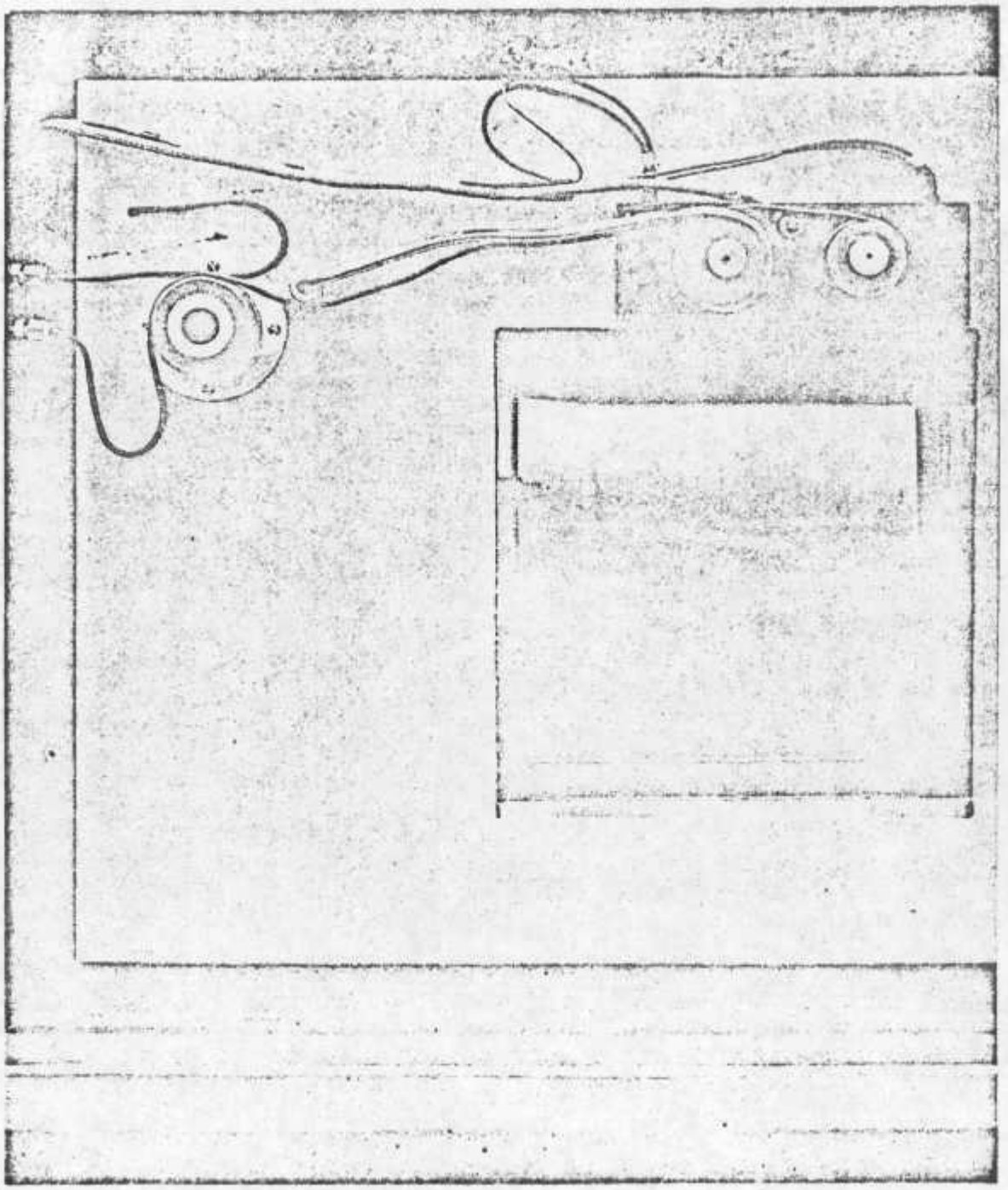

Figure 15. Front panel with cover and insulation removed.

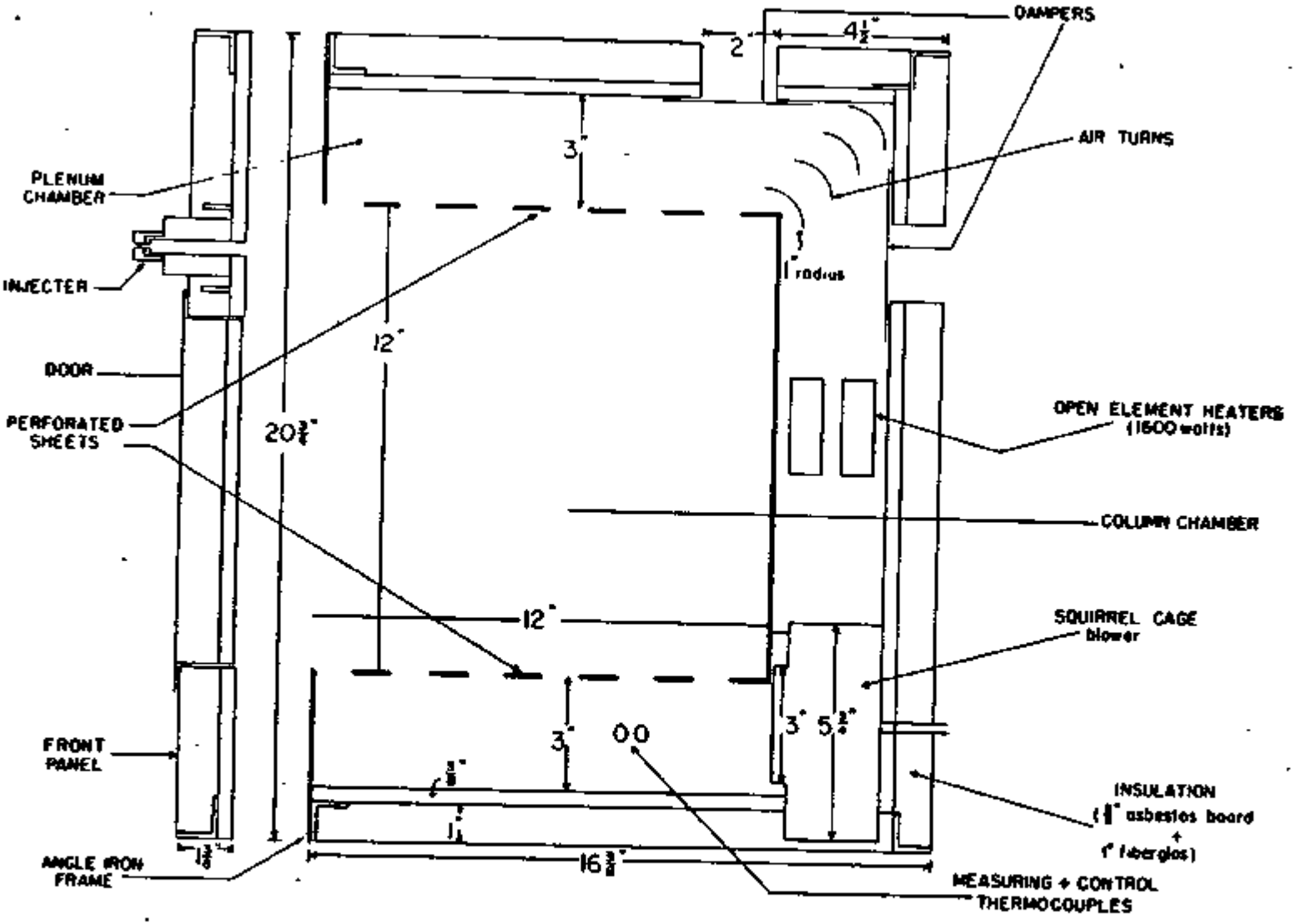

Figure 16. Side view of plenum chamber column bath.

over the entire cross section of the column compartment, minimizing temperature gradients on the column. A perforated sheet is also provided at the exit end of the column compartment to maintain nearly parallel lines of air flow through the column compartment.

Thin gauge stainless steel construction of the column compartment, low mass open wire heaters (two 800 watt, 110 v.), and a high velocity air circulation system permit rapid heating and cooling. Manually operated intake and exhaust dampers enhance the rate of cooling, and may be readily adapted to automatic control. Column temperature equilibrium is quickly achieved after cooling because the dampers permit the front pressure of the bath to remain closed during the cooling phase.

In addition to its superior temperature characteristics, this design also provides convenience of use. The 12 in. x 12 in. x 10 in. oven can accommodate more than 50 ft. of 1/4 in. o.d. tubing. Column diameters may be as large as 9 in. with only one sharp bend required. Convenient accessibility to the column compartment is provided by a 9 in. x 9 in. loged door on the front panel of the oven enclosure, with a compressible silicon rubber gasket on its inner surface to prevent leakage of the air.

Heat is supplied by two 800 watt, 100 volt A.C. open wire heaters wired in parallel. Individual gain (voltage) control is provided for each heater by a pair of General Electric Model S100C5 triac controllers. It is, therefore, possible to vary the heater power continuously from zero to a maximum of 1600 watts. The use of individual triacs was required in order to prevent damage to the controllers by excessive ($\sim$ 16 amp) current requirements at full power.

The detector oven is simply a tightly closed, thermally insulated box

with heat supplied by one 800 watt open wire heater. Provision for gain control of this heater was provided in a manner analogous to that described above. A simplified wiring diagram of the oven heater circuitry is presented in Figure 17. This circuit (four in all) was used in all heaters in the instrument.

Temperature Control and Measurement

Temperature control of the three individually heated areas (column detector oven, and injection ports) was provided for by three Weather Measure Model TPC-I, type J potentiometric temperature controllers. The temperature set point was via a calibrated direct reading dial, spanning a 0-400° C temperature range with an accuracy of ± 0.5% of the set point. Temperature sensing was performed by Iron-Constantan thermocouples with automatic cold junction compensation provided by the controller. The contacts in the thermally located relay of the temperature controller were capable of handling a maximum current of 7.5 amps. since the two sets of oven heaters could exceed this amperage the controller relays for the detector and column ovens were used to operate heavier relays, which controlled the oven heater loads.

Provision for linear temperature programming the column oven was provided by introducing a linearily decreasing negative voltage into the positive thermocouple input of the temperature controller. A -10 to 0 v. D.C. voltage ramp was obtained from a Canberra Model 833 Baseline Sweep, associated with our nuclear counting instrumentation. The circuitry used in the construction of this programmer is shown in Fig. 20. The -10 to 0 v. output sweep of the Model 833 was reduced to a -51 to 0 mv. range by means of a voltage divider. The upper limit of the sweep range may be established at any value between zero and

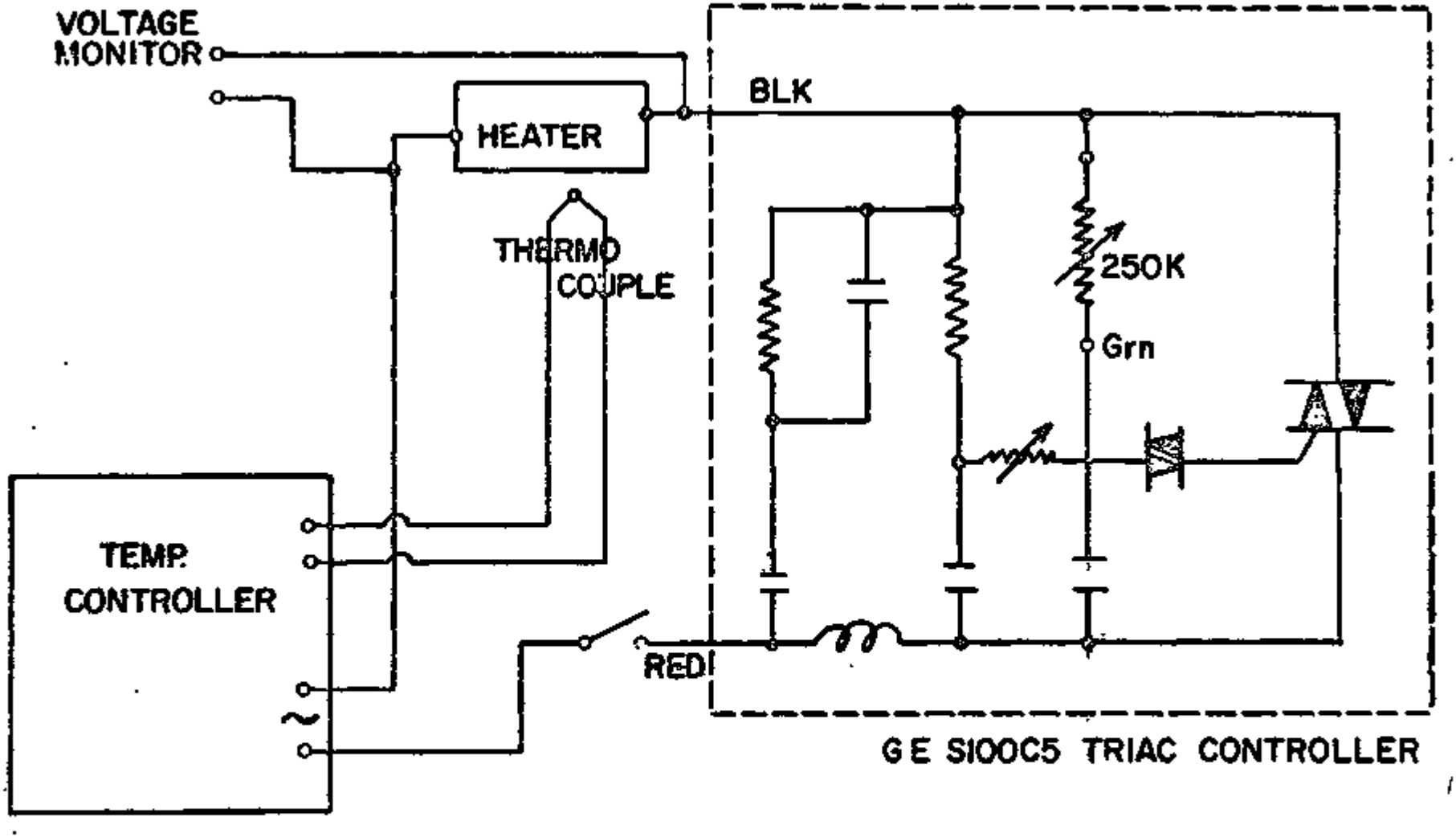

Figure 17. Basic heater wiring diagram.

51 mv by the ten-turn potentiameter incorporated in the voltage divider. This is sufficient to provide equivalent temperature ranges from 0 to greater than 400° C. This increasing (approaching zero from the negative direction) voltage range was then introduced into the positive thermocouple input as a leaking voltage as shown in Fig. 18.

Operation of the programmer is controlled by an in-out switch, the ten turn range control, the sweep time setting of the baseline sweep, and the set point of the temperature controller. First the starting temperature of the column oven is established with the temperature controller. Then the heaters are momentarily switched off and the sweep is switched in and adjusted to provide the maximum (-10 v) output to the input of the voltage divider. The upper temperature limit of the program is then established by setting the temperature controller at the desired temperature. The range control is then adjusted in such a manner that the controller is maintaining the previously established initial temperature while set for the upper temperature limit of the program. This is determined by a zero reading on the deviation indicator of the temperature controller. The heaters are then switched back on. As the entire procedure outlined above can be performed in less than 15 sec., little or no deviation from the initial set point temperature will have occurred. The column oven may then be operated for an indefinite length of time at the initial temperature setting. The program may be initiated at anytime, with its previously established upper and lower limits, by turning the range setting of the baseline sweep to zero and pressing the start button. The sweep rate is established by the sweep time control on the baseline sweep. Presently total sweep times of 1, 3, 10, and 30 minutes are provided for by the sweep time control. However, a large number of other times may be readily obtained by changing the

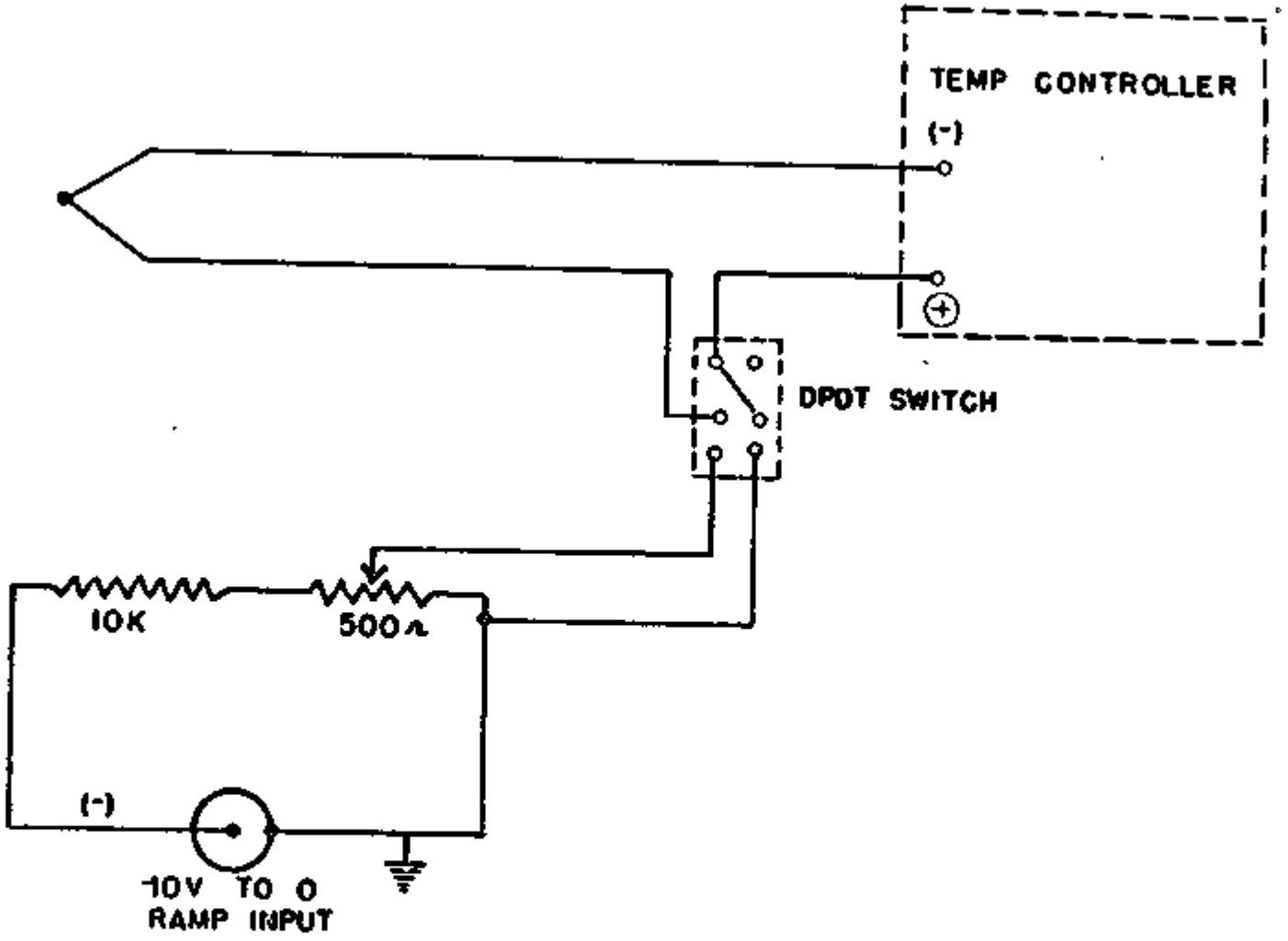

Figure 18. Circuit diagram of the linear temperature programmer.

values of the resisters in the voltage input to the clock in the Model 833 sweep.

Direct temperature readout of the various points of interest is provided for by an Assembly Products, Inc., API, 0-400° C pyrometer. The pyrometer is calibrated for iron-constantan thermocouples with an external resistance of 10 ohms. Adjustment of the thermocouple lead resistances to 10 ohms is accomplished by placing a one-turn 25 ohm trimpot between the positive input of the pyrometer and the thermocouple. The pyrometer has a 1% full scale accuracy and provides internal cold junction compensation.

An eight position selector switch having dual gold plated contacts was used to select a thermocouple located at one of the various points where temperature measurement is desired. The column oven, detector oven, injection ports, radiation counter, and thermal conductivity cell are presently provided with temperature readout, although additional locations may be readily added. The injection port and detector oven thermocouples provide temperature sensing for both measurement and control. Due to the additional circuitry associated with the column oven temperature control thermocouple a separate thermocouple is provided for measurement.

Chromatographic Analysis

Elution techniques were used in conjunction with a differential method of detection of radioactive compounds. An analog display of the differential response of the radiation analyzer showed any eluted activity at the instant of detection and the resultant signal was displayed on a potentiometric strip chart recorder as a nearly Gaussian-shaped elution curve. A typical chromatogram

of products tagged with ^{128}I resulting from the neutron irradiation of CH_3I in the presence of 1-pentene is shown in Fig. 19. The broken line represents the radiation detector signal and the solid trace that of the thermal conductivity detector. The "cold" iodo-products detected by the T. C. cell were added to the irradiated sample just prior to analysis to assist in the qualitative analysis of the "hot" products. The small difference in the recorded elution times of identical "hot" and "cold" compounds is a result of the differential flow time between the two detectors. The decrease in resolution observed for the "hot" peaks over that of the corresponding "cold" peak is a result of the much larger sensitive volume of the radiation detector (~ 40 ml.). There is no baseline drift in this temperature programmed run, since the detectors were operated at a constant temperature. If the proportional counter was improperly heated, some of the labeled products could adhere to the walls and increase the background counting rate, which appears to be a baseline drift. This could generally be rectified by increasing the counter temperature.

The number of theoretical plates or "plate equivalents" of the column was determined by the commonly accepted method[80] of measuring the retention time from the introduction of the sample, tr, and the width of the peak base, Δt. The number of theoretical plates was given by the equation; $n = 16(tr/\Delta t)^2$. The columns used had approximately 4100 plate equivalents. The height equivalent to theoretical plate (HETP) was obtained by dividing column length (10 ft.) by the number of plate equivalents. It was approximately 1.02 mm. The HETP generally decreased slightly with increasing retention time as generally would be expected.[5]

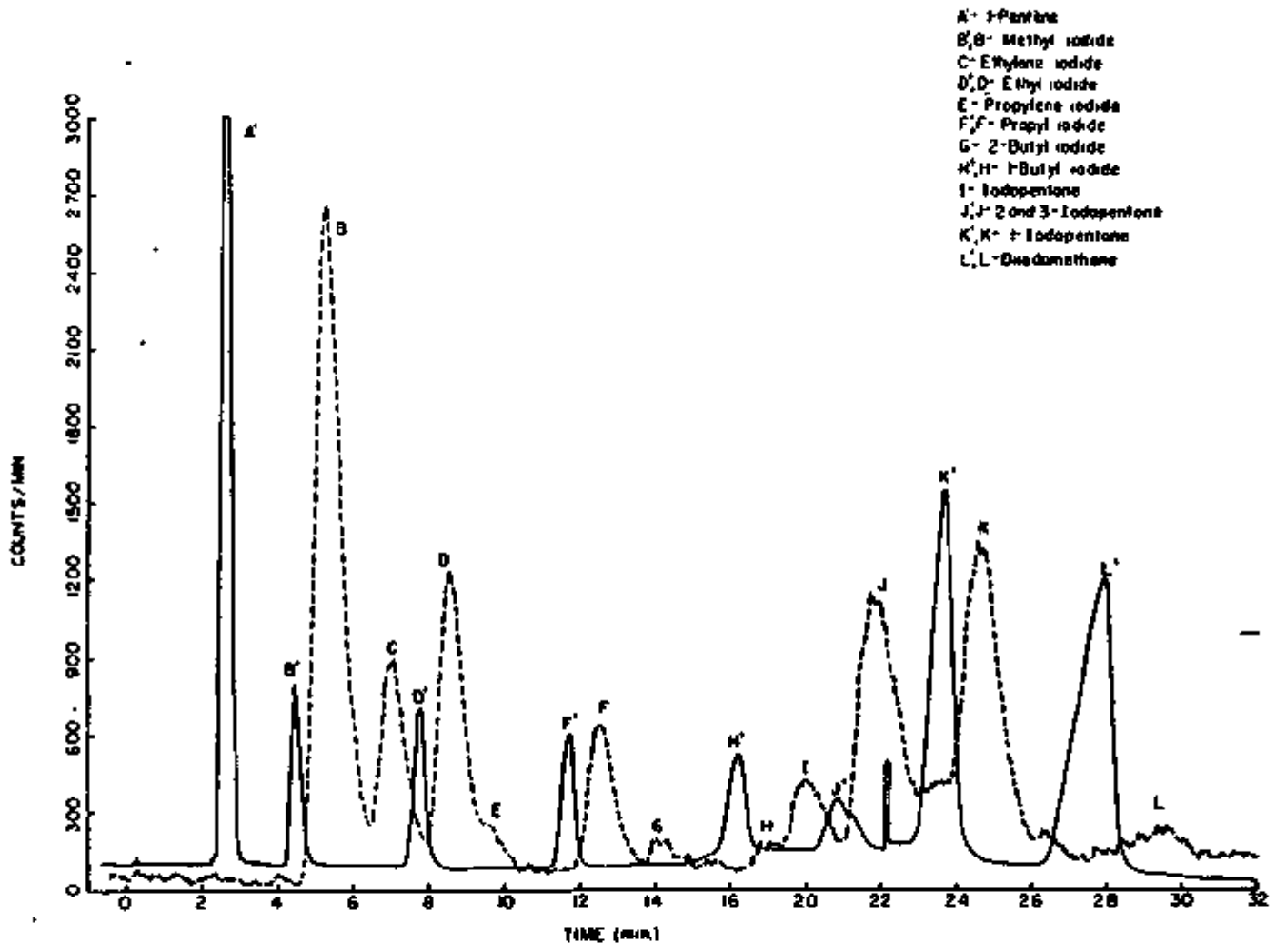

Figure 19. Radiogas Chromatogram of ^{128}I labeled organic products obtained in a 0.1 mole % solution of CH_3I in 1-pentene. "hot" products, ----; added carrier, _____.

Qualitative Identification of Radiocompounds

Since the labeled compounds produced by the nuclear activation were in such small quantities (~ 10^{-13} g.) that they could only be detected by virtue of their radioactive decay, their qualitative identification had to be determined by a type of carrier technique. This technique involved reverse isotope dilution methods in which cold (non-radioactive) carrier compounds, suspected to be identical to the labeled compounds produced by the nuclear activation, were added to the radioactive sample after removal of the inorganic activity by an aqueous sulfite extraction. Thus, in many instances, the qualitative identification could be made on the basis of the coincidental elution and detection (after correction for the time differential between the detectors) of the labeled product with its corresponding added carrier.

For the iodine-pentene systems studied in this research there were no carriers available for many of the unsaturated alkenyl iodides, thus, when possible, estimates of the identity of the peaks could be made on the basis of the boiling point of the compound. It was found that the alkenyl iodides having the iodine bonded to an unsaturated carbon would have a 5-15° C lower boiling point than its saturated analog and would, therefore, elute before the saturated iodide on the columns used. However, the alkenyl and alkyl iodides having the iodine bonded to a saturated carbon were not separated.

Several different techniques were employed in an effort to separate the unsaturated from the saturated C_3 to C_5 iodides. The first was the use of a propylene glycol-silver nitrate (3:1), 5% on Anakrom ABS 50/60 mesh, column packing. The silver nitrate loaded columns are well known for the selectivity towards unsaturated hydrocarbons. However, as determined by the analysis of

1-iodopropane and 3-iodo-propene, this column would not differentiate between the saturated and unsaturated iodides.

The work of Young, et. al.[6] and Coulson[7], in which mercuric perchlorate was found to selectively trap alkenes in a hydrocarbon mixture, suggested a possible alternative. A mercuric perchlorate-treated fire-brick column packing was prepared as described by Coulson[7] and added as a 1/4 in. diameter by 6 in. long column between the analytical column and the detectors. We found, however, that this material removed not only the unsaturated iodides but also a considerable fraction of their saturated analogs. Thus, making this packing worthless for our purposes. It was therefore, not possible to completely isolate and identify all of the possible products of the reaction mixture; thereby, a restricting the analysis of our experimental results to a certain extent.

Quantitative Determinations of Radiocompounds

Since the amounts of radioactive products were the only quantitative results desired, variance of the thermal conductivity cell with conductivity coefficients, temperature, flow rate, ... did not have to be determined. The radiation detector alone was the source of the quantitative values obtained in this study. The chromatogram was recorded by a differential procedure employing the proportional counter and associated electronics, a potentiometric dual-pen recorder, and a digital integrater. Thus, the area under the resultant Gaussian type peaks in the count-rate versus time records was proportional to the quantity of radioactive compound present in the effluent gas stream (when the flow rate was held constant). Since nuclear decay does not significantly depend upon temperature, the chromatograph could be temperature

programmed without any quantitative effects on the results due inherently to the temperature change. However, the flow rate of the carrier gas was seriously affected by changes of column temperature, requiring manual correction during temperature programming to prevent the introduction of error in the quantitative results as the magnitude of a peak resulting from a given amount of a radioactive compound was dependent on the length of time spent in the counter.

The detected radiation was the beta-ray emissions of ^{128}I and ^{131}I. The efficiency of detection was the same for all compounds and no corrections were needed in this regard. The ^{128}I gamma-ray emissions were sometimes monitored for the higher activity samples by a 5 ml. flow-through glass counting cell placed in a NaI(Tl) well counter. Because of the very much lower sensitivity of this detector (Table III) this data was seldom used.

The detector cell geometry was constant during a given run; background counting was relatively constant, and the flow was maintained at a constant rate during the run. The only experimental parameter affecting the relative magnitudes of the detected peaks was the radioactive decay of the relatively short-lived (25 min.) ^{128}I. Thus, all peaks were corrected for the amount of iodine that had decayed prior to detection using the first peak eluted as the zero time marker. Such corrections were unnecessary for the longer-lived (8 day) ^{131}I product analyses. The area of each peak was determined by summing the total counts (in 10 sec. increments from the digital integrator) under the peak and then subtracting the background counts.

The product distributions of the individual samples were reported as the magnitude of the product peak relative to the total of all the organic products observed. Assuming all significant quantities of organic products were detected

and measured, then the relative product distributions may be placed on an absolute basis by comparison with the previously determined organic yields of the respective samples.

CHAPTER III. KINETICS AND MECHANISM OF IODINE ADDITION TO VARIOUS PENTENE ISOMERS

Sumrell, et. al.[8], and Skell and Pavlis[9] have reported that contrary to information commonly found in the literature[10-13], iodine readily adds to 1-pentene and C_4 alkenes, respectively. They have reported that in the presence of a liquid phase and at ordinary room illumination the reaction proceeds via a mildly exothermic reaction which goes essentially to completion:

$$RCH = R^1 + I_2 \qquad RCHICHIR'$$

In their study of the addition-elimination cycle of iodine to cis and trans-2-butenes, Skell and Pavlis[9] proposed a radical chain mechanism, proceeding via a bridged radical intermediate. The basis for their hypothesis was the observed photoacceleration and stereospecific nature of the addition-elimination reactions of iodine with the corresponding 2-butenes.

Benson, et. al.[14] have reported that the I atom catalyzed elimination of iodine from vicinal diiodides must be a concerted process, proceeding by a single step elimination. They further concluded that if the decomposition reactions are concerted processes, then by the principle of microscopic reversibility, the addition reactions also must be concerted processes. However, this microscopic reversibility argument has been shown to be invalid for reasons discussed by Burwell and Pearson.[15]

This controversy over the sequence of the formation of the transtion state has been summerized by Noyes, et. al.[16], without reaching a conclusion as to whether or not all present observations could be explained without assuming

the existence of bridged radicals, as proposed by Skell and co-workers to explain their stereochemical observations.[9, 17-19]

In order to study the radiative neutron capture induced reactions of ^{128}I in the various C_5 alkenes, (see Chapter IV) a knowledge of the rate and mechanism of the thermal reactions of iodine in these systems is essential. In view of the uncertainty in the rate and mechanism of the addition of iodine to various unsaturated hydrocarbons in the condensed phase, the kinetics of the addition process to various C_5 alkene isomers in solution at 25°C was investigated in an effort to shed additional light on the mechanism of the reaction.

Kinetic Experiments

A radiometric procedure was employed to follow the addition of iodine to the various pentene isomers studied. The individual kinetic runs were started by mixing known volumes of tagged iodine in CCl_4 with the pentene of interest. The reactions were initiated by the ordinary white fluorescent lighting of the laboratory. Prior to the use of ^{131}I tagged I_2 in CCl_4 several runs were made by adding tagged molecular iodine directly to the liquid alkene to initiate a run. However, the dissolution time of the molecular iodine was found to affect the rate data obtained, particularly during the initial stages of addition. Thus, the procedure was modified, such that, the added I_2 was predissolved in carbon tetrachloride. The small mixing time of the two reactants was found to yield satisfactory results.

Reaction Order with Respect to Iodine

In addition of iodine to the double bond, in the various C_5 olefins studied, proceeds smoothly when the reaction is exposed to ambient light at 25°C. Several kinetic runs were made in which the iodine concentration was varied and the initial velocity of the reaction as a function of iodine concentration was determined. A double-logarithmic plot of the velocity versus the concentration of the added I_2 yielded a straight line with the slope equal to the order of the reaction with respect to iodine. The reaction was found to be 3/2 order with respect to iodine.

Since all kinetic runs were made with the respective alkene in excess, the rate of disappearance of iodine with respect to the concentration of iodine at time t, can be expressed by

$$-d(I_2)_t/dt = k(I_2)^{3/2} \qquad (1)$$

Integration of equation yields the following expression

$$1/2kt = 1(a_o - x)^{1/2} - (1/a_o^{1/2}) \qquad (2)$$

where a_o is the initial concentration of iodine at zero time, $(a_o - x)$ the concentration of iodine at time t, and t the time in minutes. Rate constants, k, were determined from the slopes of the straight lines obtained by plotting the values of $1/(a_o - x)^{1/2}$ vs $1/2t$. The data for a representative run in each of the five pentene isomers studied is presented in Table II to VI and summerized in Fig. 20. As demonstrated by the data, deviation of the reaction rates from equation 2 did not become serious until the reactions had proceeded to 75% completion or greater.

Within a few hours after the start of a reaction an equilibrium was established. At that point the reaction was 75-99% complete, depending on

the original concentrations of the reactants and the nature of the alkene. This observed equilibrium could result from either or both of the following: (1) a true equilibrium established by the previously demonstrated[20] iodine atom catalyzed decomposition of the products, and/or (2) competition for the unreacted iodine via the formation of a charge transfer complex of iodine with the product, whose effect would be to decrease the concentration of uncombined iodine. The well-established photo-accelerated decomposition of various vicinal diiodides[21-23] would suggest that the decomposition of the product predominantly accounts for the observed equilibrium.

Although the reactions become complex in their later stages, the kinetics can be studied readily up to at least 75% completion, ad demonstrated by the data in Fig. 20.

TABLE II

Rate of Addition of Iodine to 1-Pentene at 25° C[a]

Time (sec)	Organic Yield (%)	$\frac{1}{(a_o-x)^{\frac{1}{2}}}$ (moles$^{-\frac{1}{2}}$ l)	(min^{-1} $\underline{k}$ x 10^{2} moles$^{-\frac{1}{2}}$ l$^{\frac{1}{2}}$)[b]
30	14.2	28.1	13.8
120	37.0	32.8	11.3
300	65.1	44.1	12.0
600	82.7	62.6	12.2
900	88.7	77.6	11.5
1200	92.6	96.1	11.7
1800	95.5	122.9	10.8
2700	96.1	132.7	7.9
3600	96.7	143.5	6.5
4500	96.3	135.5	4.7

a Concentrations of I_2 and 1-pentene were 1.47 x 10^{-3} M and 8.78 M, respectively.

b Computed for each point using equation 2.

TABLE III

Rate of Addition of Iodine to cis-2-Pentene at 25° C[a]

Time (sec)	Organic Yield (%)	$\frac{1}{(a_o-x)^{\frac{1}{2}}}$ (moles^{-1} l)	$\frac{k}{}$ x 10^2 (min^{-1} mole$^{-\frac{1}{2}}$ l$^{\frac{1}{2}}$)[b]
30	13.1	31.2	14.2
120	27.9	34.3	8.6
300	50.0	41.2	8.0
600	67.6	51.2	7.4
900	77.3	61.2	7.1
1200	83.5	71.6	7.0
1800	86.2	78.5	5.5
2700	90.1	92.4	4.7
3600	99.5	396.2	20.4
4500	99.5	400.0	16.5
39600	99.0	291.2	1.3

a Concentrations of I_2 and cis-2-pentene were 1.18 x 10^{-3} M and 8.99 M, respectively.

b Computed for each point using equation 2.

TABLE IV

Rate of Addition of Iodine to 2-Methyl-1-Butene at 25° C[a]

Time (sec)	Organic Yield (%)	$\frac{1}{(a_o-x)^{\frac{1}{2}}}$ (moles^{-1} l)	$\underline{k} \times 10^2$ (min^{-1} moles$^{-\frac{1}{2}}$ l$^{\frac{1}{2}}$)[b]
30	7.1	30.2	7.3
120	25.4	33.7	7.6
300	41.6	38.1	6.0
600	67.9	54.5	7.4
900	77.0	60.8	7.0
1200	83.7	72.1	7.2
1800	88.0	83.9	6.1
2700	88.5	85.9	4.2
3600	87.9	83.7	3.0
4500	88.8	86.8	2.6

a Concentrations of I_2 and 2-methyl-1-butene were 1.18×10^{-3} M and 8.92 M, respectively.

b Computed for each point using equation 2.

TABLE V

Rate of Addition of Iodine to 2-Methyl-2-Butene at 25° C[a]

Time (sec)	Organic Yield (%)	$\frac{1}{(a_o-x)^{\frac{1}{2}}}$ (moles^{-1} l)	$\underline{k} \times 10^2$ (min^{-1} moles$^{-\frac{1}{2}}$ l$^{\frac{1}{2}}$)[b]
30	4.2	29.7	4.2
120	10.2	30.7	2.6
300	21.2	32.8	2.5
600	39.3	37.4	2.8
960	53.7	42.8	2.8
1200	59.0	45.5	2.7
1800	70.0	53.0	2.7
2700	79.3	64.0	2.6
3600	82.0	68.7	2.2
4500	84.6	74.3	2.0
5400	85.9	77.5	1.8
86400	82.4	69.4	0.1

a Concentrations of iodine and 2-methyl-2-butene were 1.18×10^{-3} M and 9.08 M, respectively.

b Computed for each point using equation 2.

TABLE VI

Rate of Addition of Iodine to trans-2-Pentene at 25° C[a]

Time (sec)	Organic Yield (%)	$\frac{1}{(a_o-x)^{\frac{1}{2}}}$ (moles^{-1} l)	$\underline{k} \times 10^2$ (min^{-1} moles$^{-\frac{1}{2}}$ l$^{\frac{1}{2}}$)[b]
30	6.5	26.8	5.0
120	13.6	28.0	3.3
300	20.4	29.2	2.1
600	34.9	32.3	2.1
900	47.1	35.9	2.2
1200	53.3	38.1	2.0
1800	63.5	43.2	1.9
2700	74.9	52.0	1.9
2660	78.9	56.8	1.7
4680	81.8	61.1	1.5
5400	84.8	66.8	1.5
7200	86.5	70.8	1.2
9000	84.4	66.1	.9
10800	88.5	76.9	.9
93600	84.3	65.8	.1

a Concentrations of iodine and trans-2-pentene were 1.18×10^{-3} M and 9.02 M, respectively.

b Computed for each point using equation 2.

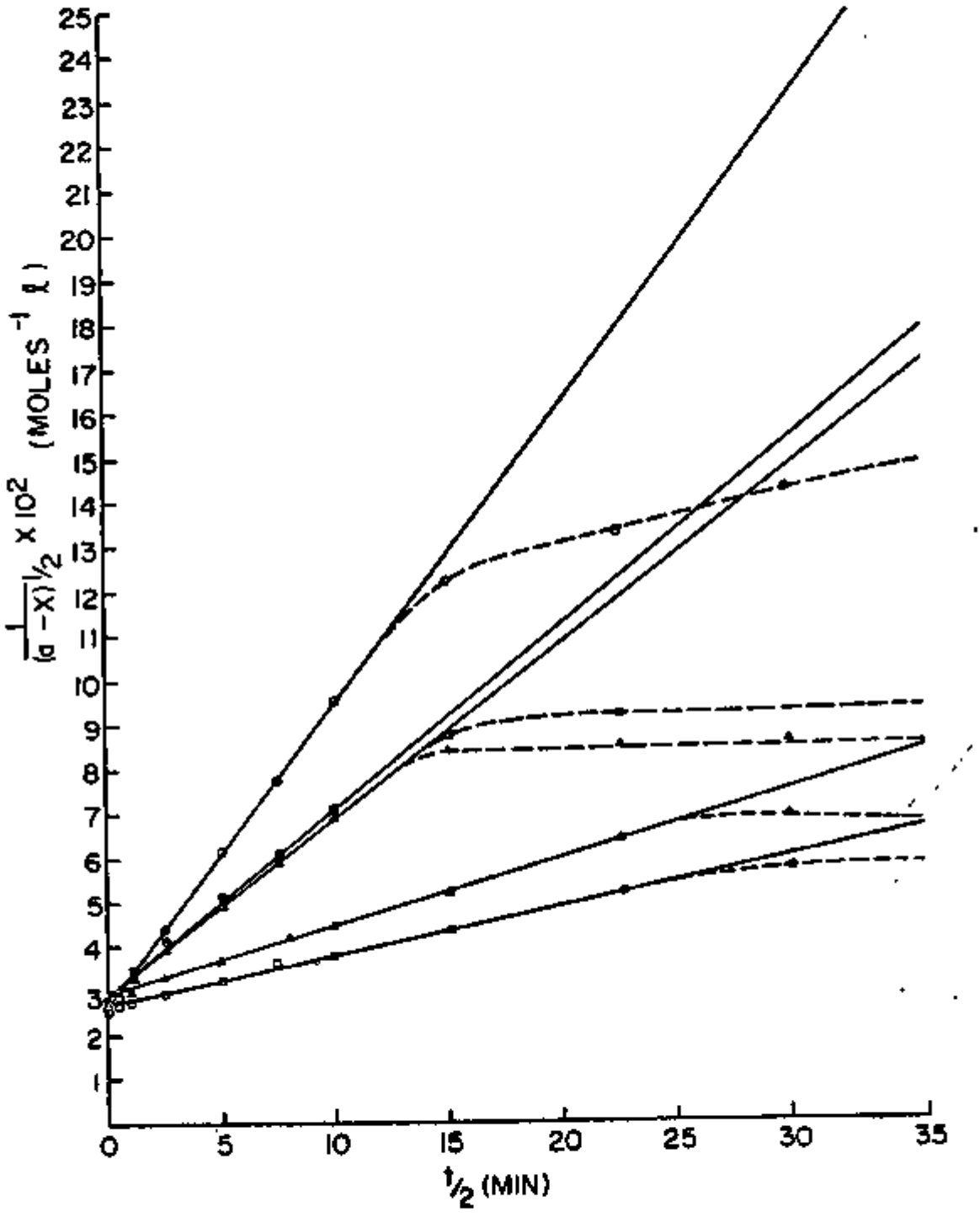

Figure 20. Rate curves for the addition of iodine to olefins as a function of time. 1-pentene, O; cis-2-pentene,; 2-methyl-1-butene, Δ; 2-methyl-2-butene, Δ; and trans-2-pentene, .

The reaction between the labeled iodine and 1-pentene was studied as a function of the initial concentrations of iodine and/or 1-pentene. The results of the individual runs are summarized in Table VII. The 2/3 dependence of the reaction rate on the iodine concentrations is demonstrated by the results of runs 1-5.

Reaction Order with Respect to the Alkene. If the reaction was first order in 1-pentene concentration then the values of (1-pentene/k) should have been independent of 1-pentene concentration. That this is not so is indicated in the last column of Table VII, runs 5-9. As the concentration of 1-pentene was decreased there was also a marked decrease in the ratio. This suggests that the order with respect to 1-pentene is more complex. A more complex order would be expected if a 1-pentene-iodine charge transfer complex was involved in the rate limiting step of the reaction (vide infra).

Additional evidence suggesting the importance of the iodine-olefin charge transfer complex, with respect to the addition of iodine to the double bond, was obtained by comparison of the reaction rates of a series of C_5 alkenes with their relative equilibrium constants for complex formation with iodine. Table VIII lists the rate constants obtained in this study along with the relative equilibrium constants obtained by Cvetanovic and his coworkers.[24] It can be seen from the Table that there a rough correlation between the rate of the reaction and the ability of the olefin to act as a donor toward iodine. Because of the complexity of the kinetic relationships one would not expect an exact correlation but it is gratifying that an overall trend in the anticipated direction is observed. This is precisely what would be expected if the iodine-olefin charge transfer complex was involved in the rate determining step.

TABLE VII

Rate Constants for the Addition of Iodine to 1-Pentene in Carbon Tetrachloride at 25° C

Run	(I_2) mole/liter $\times 10^3$	(1-pentene) mole/liter	$\underline{k}$ min^{-1} moles$^{-\frac{1}{2}}$ liters$^{\frac{1}{2}}$ $\times 10^2$	(1-pentene)/$\underline{k}$ min moles$^{3/2}$ liters$^{-3/2}$
1	21.89	9.12	10.9	83.26
2	8.83	9.13	10.9	83.26
33	0.076	9.11	11.5	79.2
4	0.152	9.10	12.1	75.2
5	0.147	8.78	11.2	78.4
6	1.18	7.02	9.7	72.6
7	1.18	5.27	8.0	65.8
8	1.18	3.51	6.4	54.8
9	1.18	1.76	4.01	44.1

TABLE VIII

Comparison of Rate Constants of Iodination with the Relative Equilibrium Constants of Charge-Transfer Complexes

Olefin	k^a min moles$^{-½}$ l^{½} x 10^2	Relative K_c [b]
1-pentene	11.0	12.7
cis-2-pentene	7.04	4.0
2-methyl-1-butene	6.74	.80
2-methyl-2-butene	2.59	.45
trans-2-pentene	1.03	.56

a Obtained with initial concentration of iodine of 1.8×10^{-3} mol/l. in neat pentenes.

b Obtained from ref. 24. The values are relative to *cis*-2-butene, which was taken as unity. It should be pointed out that Cvetanovic' *et. al.* gave several values to choose from. The values quoted here possibly the best values although the other choices showed the same general trend. cf. W. E. Falconer and R. J. Cvetanovic', *J. Chromat.*, 27, 20 (1967).

However, as pointed out by Furuyama, et. al.[28], I atoms would also be expected to complex with the alkene bond. Although there is no data on the relative equilibrium constants of the I-atom-olefin charge transfer complexes for the various pentene isomers studied, one might expect these constants to follow the same general trend as the corresponding molecular iodine complexes. Based on this assumption the earlier argument for the importance of the iodine-olefin charge transfer complex would be equally applicable to the I-atom-olefin complexes.

Mechanisms and Rate Laws

The effects of alkene concentration and complexing ability on the observed k values can be explained by the following reaction scheme in which steps 5 and 6, either singly or in combination, are rate determining where i and f refer to the initiation and termination steps.

$$I_2 + h\nu \xrightarrow{i} 2I\cdot \qquad 1$$

$$I_2 + C_5 \underset{}{\overset{K_c}{\rightleftharpoons}} C_5\cdot I_2 \qquad 2$$

$$I\cdot + C_5 \overset{K'_c}{\rightleftharpoons} C_5\cdot I \qquad 3$$

$$C_5\cdot I_2 + h\nu \xrightarrow{i} C_5\cdot I + I\cdot \qquad 4$$

$$C_5\cdot I_2 + I \xrightarrow{k_1} (C_5I_3) \qquad 5$$

$$C_5\, I + I_2 \xrightarrow{k'_1} (C_5I_3) \qquad 6$$

$$(C_5I_3) \longrightarrow C_5I_2 + I \qquad 7$$

$$I + I \xrightarrow{f} I_2 \qquad 8$$

$$I + C_5\, I \xrightarrow{f} C_5 + I_2 \qquad 9$$

Examing the proposed reaction scheme a number of factors need to be considered:

(1) The $I_2 \cdot$ olefin complex absorbs as well or better, than the free iodine, therefore, step 4 would be expected to contribute just as much, if not more, to the I atom formation as step 1;

(2) I atoms probably form just as strong a π-complex with olefins as I_2, so that the formation of the diiodide products from either step 5 or step 6 could be equally probably;

(3) Both steps 5 and 6 lead to the same transition state (C_5I_3), thus the kinetic data would not be expected to distinguish between the two possibilities.

Assuming the rate determining step to be step 5 and that the $I_2 \cdot$ olefin complex contributes equally to the $I \cdot$ atom formation, then a mechanism of this type requires a rate law of the form

$$d(C_5I_2)/dt = \underline{k}_1 K_c (I_2)^{3/2}(C_5)/[1 + K_c(C_5)] \qquad (3)$$

where K_c is the equilibrium constant for complex formation as defined by

$$K_c = (C_c \cdot I_2)/(C_5)(I_2)_f \qquad (4)$$

and where $(I_2)_f$ is the concentration of uncomplexed iodine. The observed rate constant $\underline{k}$ should then be related to $\underline{k}_1$ by the expression

$$(C_5)/\underline{k} = 1/(\underline{k}_1 K_c) + (C_5)/\underline{k}_1 \qquad (5)$$

According to equation 5 a plot of the experimental values of $(C_5)/\underline{k}$ vs. (C_5) should then yield a straight line, the slope and intercept of which should yield the values of K and $\underline{k}_1$, respectively. The data of Table XV were treated graphically according to equation 5. From the resultant plot (Fig. 21) values of $K = 1.0 \times 10^{-2}$ moles^{-1} liters and $\underline{k}_1 = 2.38 \times 10^{-1}$ min^{-1}

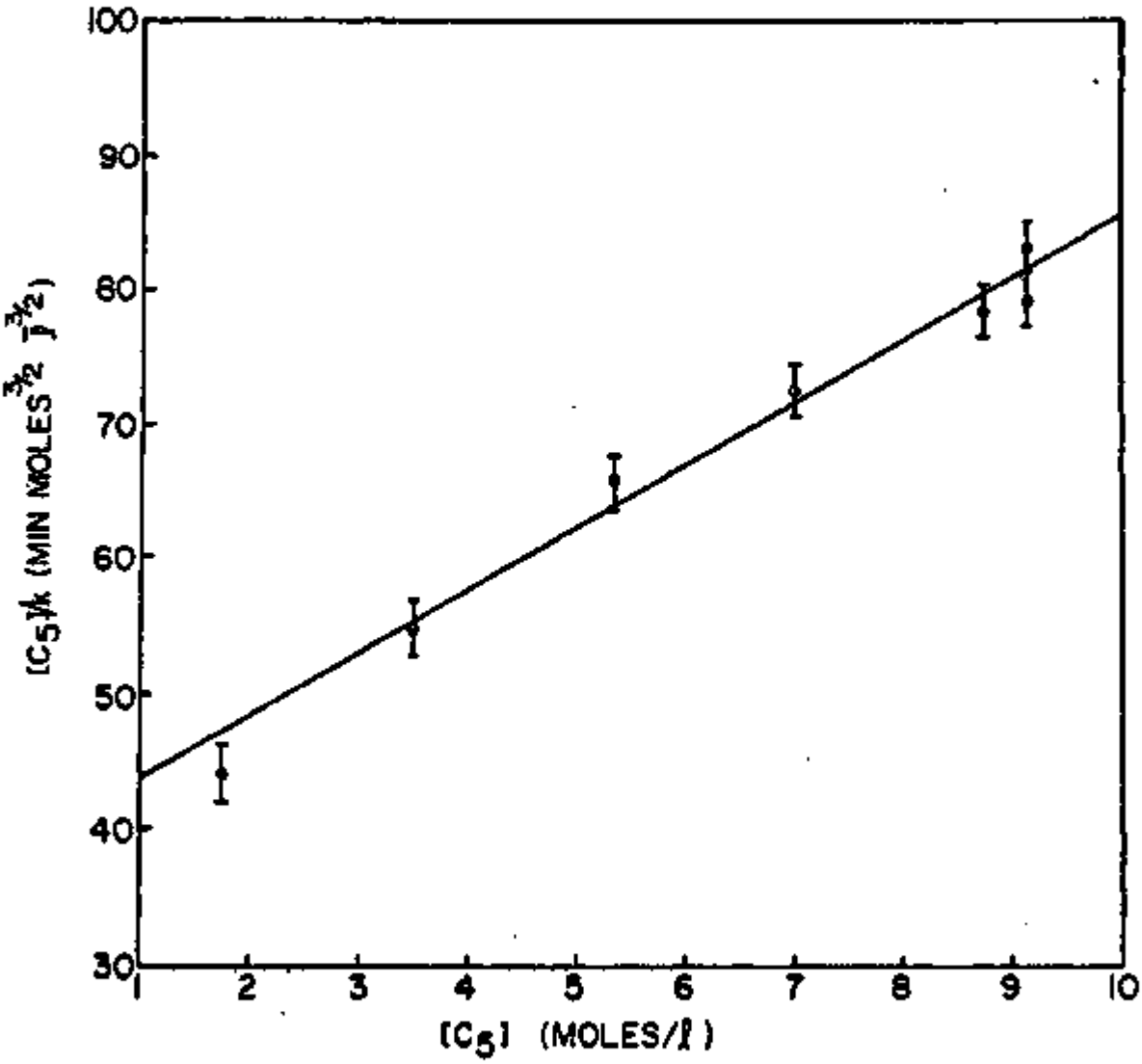

Figure 21. Plot used in the determination of K_c and $\underline{k}$, according to equation $\underline{5}$.

liters were obtained.

Alternately if step 6 is considered to be the rate determining step the required rate law is

$$d[C_5I_2]/dt = \underline{k}_1' K_c' [C_5][I_2]^{3/2}/(1 + K_c[C_5]) \qquad (6)$$

where K_c' is the equilibrium constant for the I-atom-olefin complex formation as defined by

$$K_c' = [C_5 \cdot I]/[C_3][I] \qquad (7)$$

The above rate expression, with the exception of K_c' in the numerator, is the same as the previously derived rate law for the $I\cdot + C_5 \cdot I_2 \rightarrow C_5I_3$ mechanism. Thus the slope and intercept of the plot of $[C_5]/\underline{k}$ *vs.* $[C_5]$ would be equal to $K_c/\underline{k}_1' K_c'$ and $1/\underline{k}_1' K_c'$, respectively. The value of $\underline{k}_1'$ is dependent on the value assumed for K_c', but the value of K_c obtained from the solution of the two equations is independent of the value of K_c'. If $K_c' = K_c = 0.10$ moles^{-1} l, then the value of $\underline{k}_1'$ is the same as that obtained previously.

We could also re-evaluate the first rate law, assuming that the $C_5 \cdot I_2$ complex does not contribute to the formation of I-atoms. This would require a rate law of the form

$$d[C_5I_2]/dt = \underline{k}_1 K_c (I_2)^{3/2}(C_5)/(1 + K_c[C_5])^{3/2} \qquad (8)$$

The observed rate constant $\underline{k}$ should then be related to $\underline{k}_1$ by the expression

$$[(C_5)/k]^{2/3} = 1/(\underline{k}_1 K_c)^{2/3} + K_c(C_5)/(\underline{k}_1 K_c)^{2/3} \qquad (9)$$

According to equation 9 a plot of the experimental values of $[(C_5)/\underline{k}]^{2/3}$ *vs.* (C_5) should then yield a straight line, the slope and intercept of which should yield the value of K and $\underline{k}_1$, respectively. The data of Table VII were treated graphically according to equation 9. From the resultant plot (Fig. 22) values of $K = 7.07 \times 10^{-2}$ moles^{-1} liters and $\underline{k}_1 = 3.58 \times 10^{-1}$ min^{-1} moles$^{-1/2}$

liters$^{1/2}$ were obtained.

Andrews and Keefer[25] reported that the absolute value of the equilibrium constant for the cyclohexene/iodine complex was 0.34 mole^{-1} liter. Cvetanović et al.[24] gave a relative value for cyclohexene. Combining these data with the relative equilibrium constant for 1-pentene allows the calculation of the absolute value for 1-pentene. This comes out to be 9.0 x 10^{-2} mole^{-1} liter. This compares very favorably with the independent value of 10.0 x 10^{-2} mole^{-1} liter obtained in this study, assuming the iodine olefin complex contributes equally to the formation of I-atoms. The value of K_c obtained when the contribution of the complex is neglected (7.07 x 10^{-2} moles^{-1} liters) results in poorer agreement, thus supporting the expected importance of the complex in contributing to the formation of I-atoms.

Equilibrium

A series of five solutions, containing varying concentrations of iodine between 1.0 x 10^{-2} and 1.0 x 10^{-3} moles liter^{-1} in neat 1-pentene, were allowed to stand for 48 hrs. and the equilibrium concentrations of the respective reactants and products were determined. These values are listed in Table IX. The expression for the overall equilibrium constant for step 5 assuming the reaction was reversible, would be

$$K = (C_5I_2)/(C_5 \cdot I_2) \qquad (10)$$

and from equation 4. $(C_5 \cdot I_2)$ is equal to $K_c(C_5)(I_2)$. Then the expression for the observed equilibrium constant, K_{obs}, would be

$$K_{obs} = KK_c = (C_5I_2)/(C_5)(I_2) \qquad (11)$$

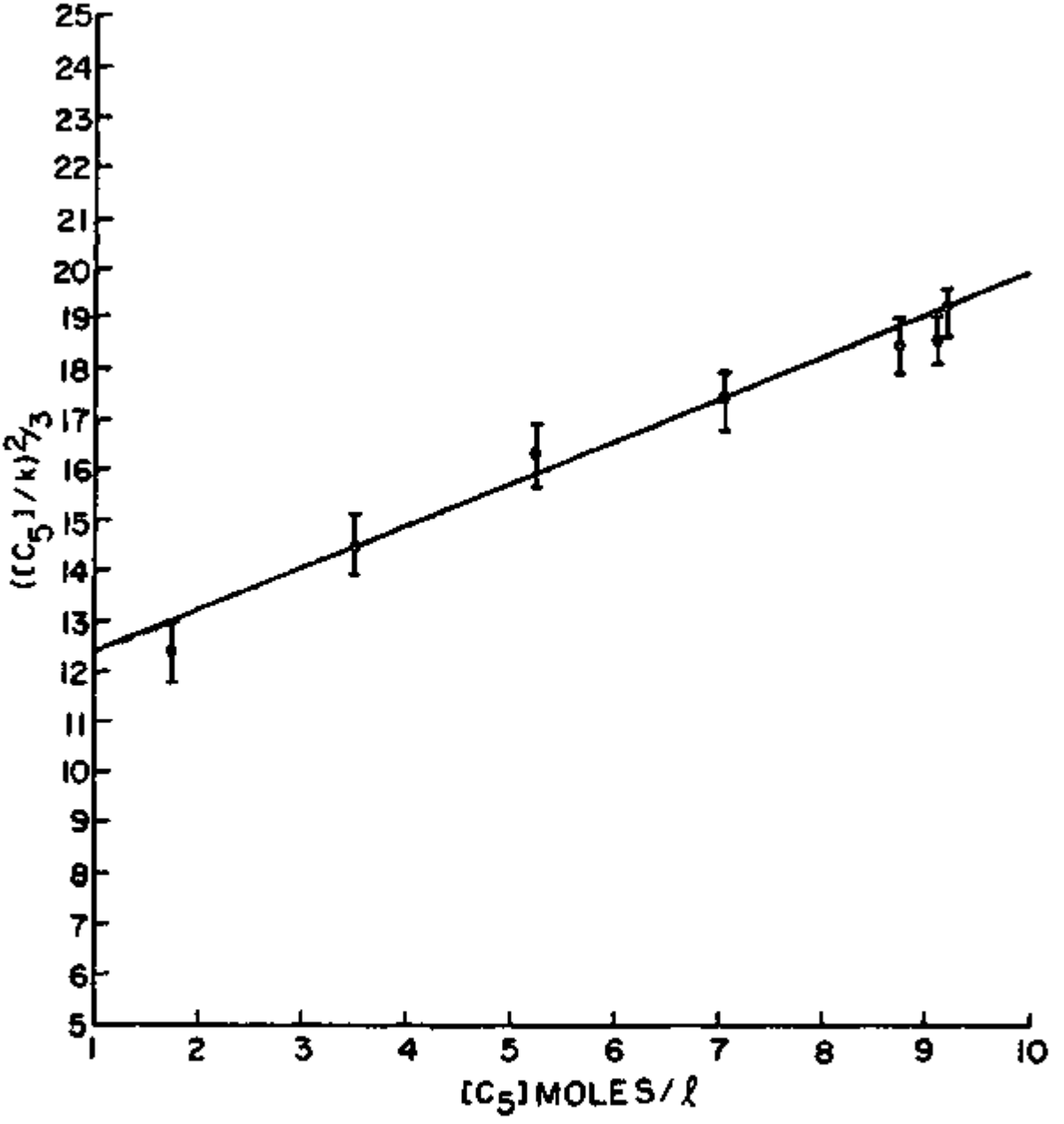

Figure 22. Plot used in the determination of K_c and $\underline{k}_1$ according to equation 9.

Using equation 11, the average value of the observed equilibrium constant, K_{obs}, was found to be 2.51 ± 0.20. Using this value and the value determined previously for K_c the value of K was found to be 25.10.

The observed deviation of the experimental values from the straight line plots in Fig. 20, which occur in the later stages of the reaction, and the subsequent attainment of an equilibrium suggest that the proposed mechanisms and the resultant kinetic expressions do not fully describe the iodine interaction with the alkene. For example step 5 would be more correctly expressed as follows

$$C_5 \cdot I_2 + I \underset{k_2}{\overset{k_1}{\rightleftharpoons}} C_5I_2 + I \qquad (12)$$

allowing for the reversible decomposition of the products. Thus the kinetic expression should include an additional term allowing for the reversible step. Polissar[21], and others[22,23] have shown that the decomposition of vicinal diiodides to proceed by an I atom catalyzed concerted process, i.e., essentially the reverse of the addition mechanism. Thus equation 3 could be rewritten to give:

$$d(C_5I_2)/dt = k_1K_c(I_2)^{3/2}(C_5)/[1 + K_c(C_5)] - k_2(C_5I_2)(I_2)^{1/2} \qquad (13)$$

which includes the expression for the product decomposition. By the inclusion of the decomposition term in the overall kinetic expression the observed data should cover the entire range of the reaction. This, however, is not necessary in order to describe the addition mechanism. As demonstrated by the data the decompostion term may be neglected and sufficient data can be obtained from the initial stages of the reaction in order to identify the most probable rate determining step and, nature of the activated complex. A similar treatment of step 6 would be equally valid.

Stereochemistry of the Addition-Elimination Reactions

Identification of the products of addition of iodine to 1-pentene and cis and trans-2-pentene were made on the basis of their characteristic nmr spectra.[26] A representative spectra of each of the pentene isomers and their corresponding diiodo products is shown in Figures 23 to 28. The nmr spectra of the respective starting olefins were identical with the products of elimination of iodine from the corresponding diiodides. The 1,2-diiodopentane was readily converted to 1-pentene by stirring with zinc dust in methanol. Similar treatment of the dl- and meso-2,3-diiodopentanes, however, produced considerable quantities of pentane. The iodine catalyzed conversion of an alkene to its corresponding alkane has been reported previously.[27] However, conversion of the 2,3-diiodopentanes back to their respective cis and trans-2-pentenes was successfully accomplished by stirring with magnesium in ethyl ether. Although pentane was also produced in this reaction it was in a much smaller amount and sufficient quantities of the cis and trans-2-pentenes were recovered to confirm the reported[9] stereospecific nature of the addition and elimination of iodine.

Attempts to convert the respective diiodo-products back to their starting materials by thermal decomposition were also unsuccessful. When 1,2-diiodopentane and the 2,3-diiodopentanes were heated, without prior removal of the small quantities of excess iodine, decomposition occurred at ca. 35° which resulted in the formation of HI and a dark polymeric material of unknown composition. However, if the excess iodine was removed prior to heating by an aqueous sulfite extraction, the respective diiodides could be distilled at ca. 130° with little accompanying thermal decomposition.

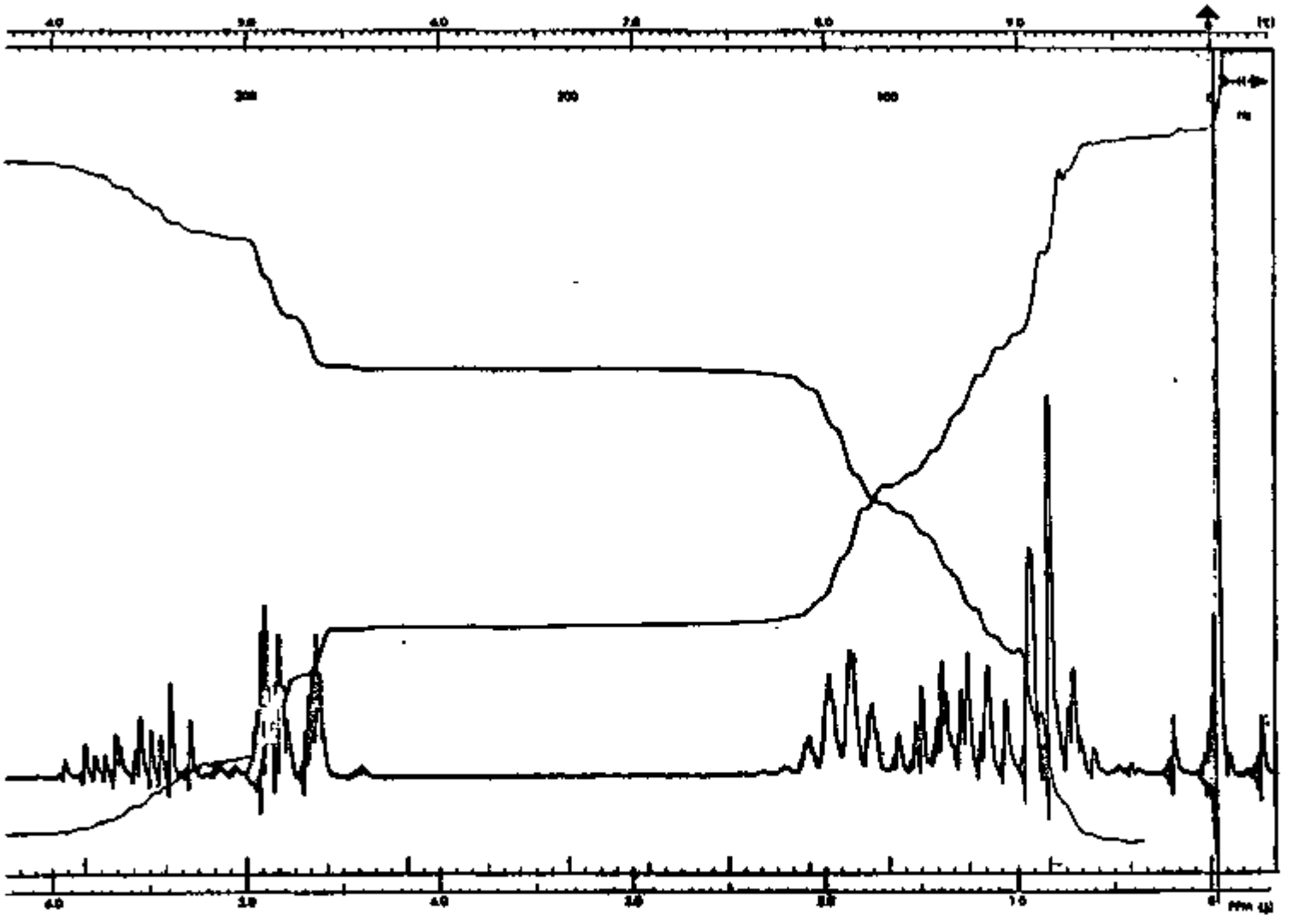

Figure 23. NMR spectra of pure 1-pentene.

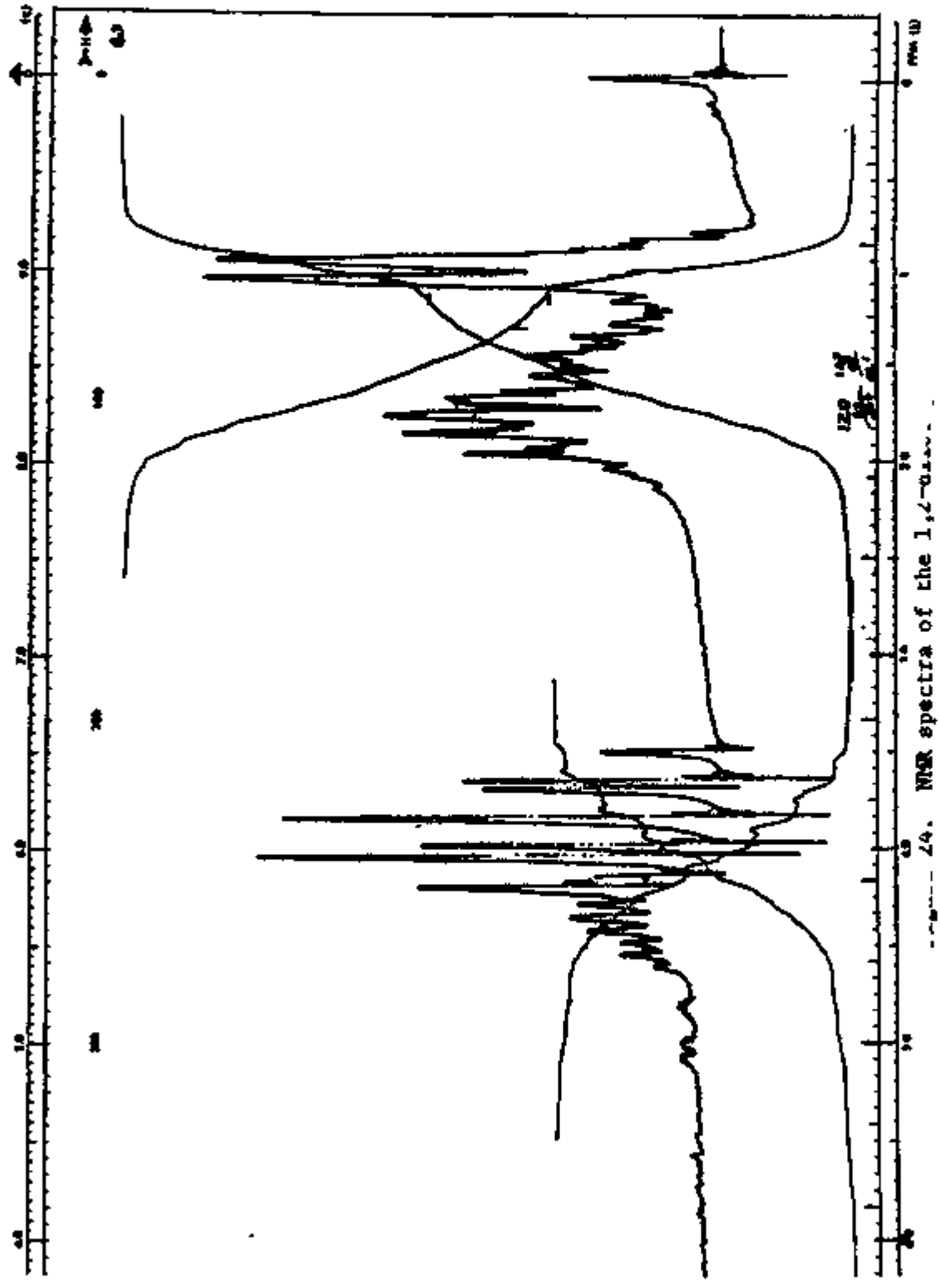

Fig. 24. NMR spectra of the 1,4-...

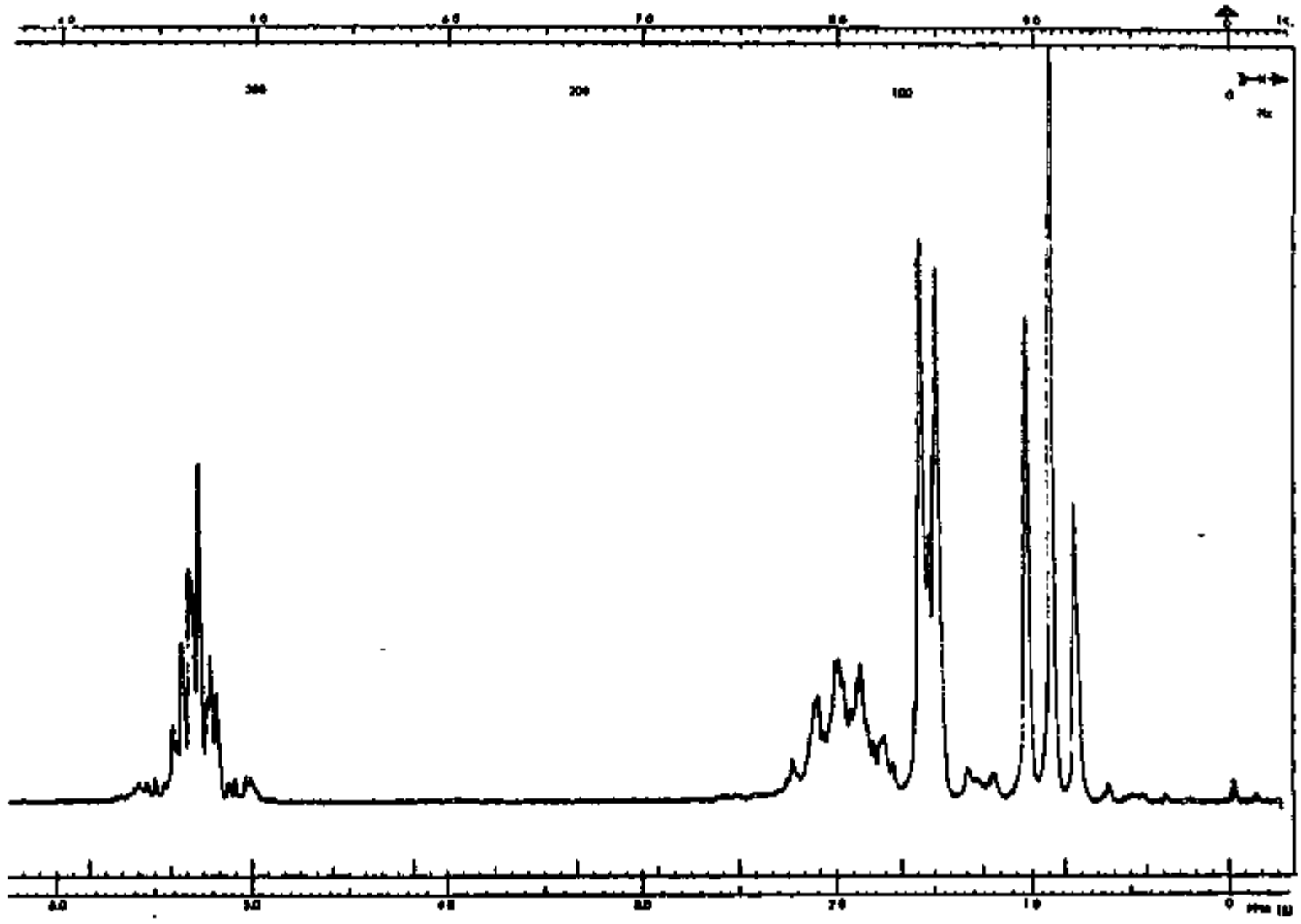

Figure 25. NMR spectra of pure cis-2-pentene.

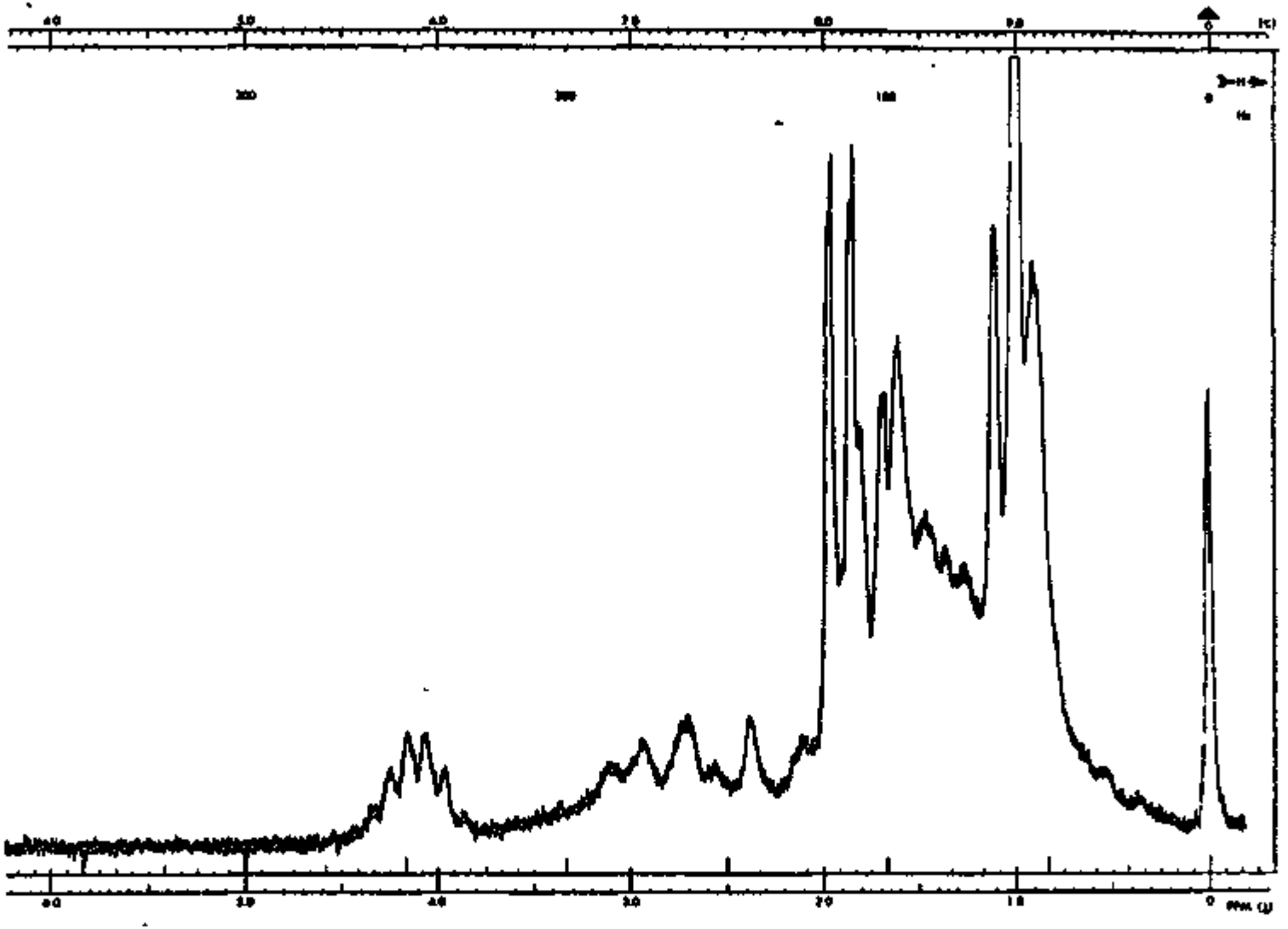

Figure 26. NMR spectra of dl-2,3-diiodopentane.

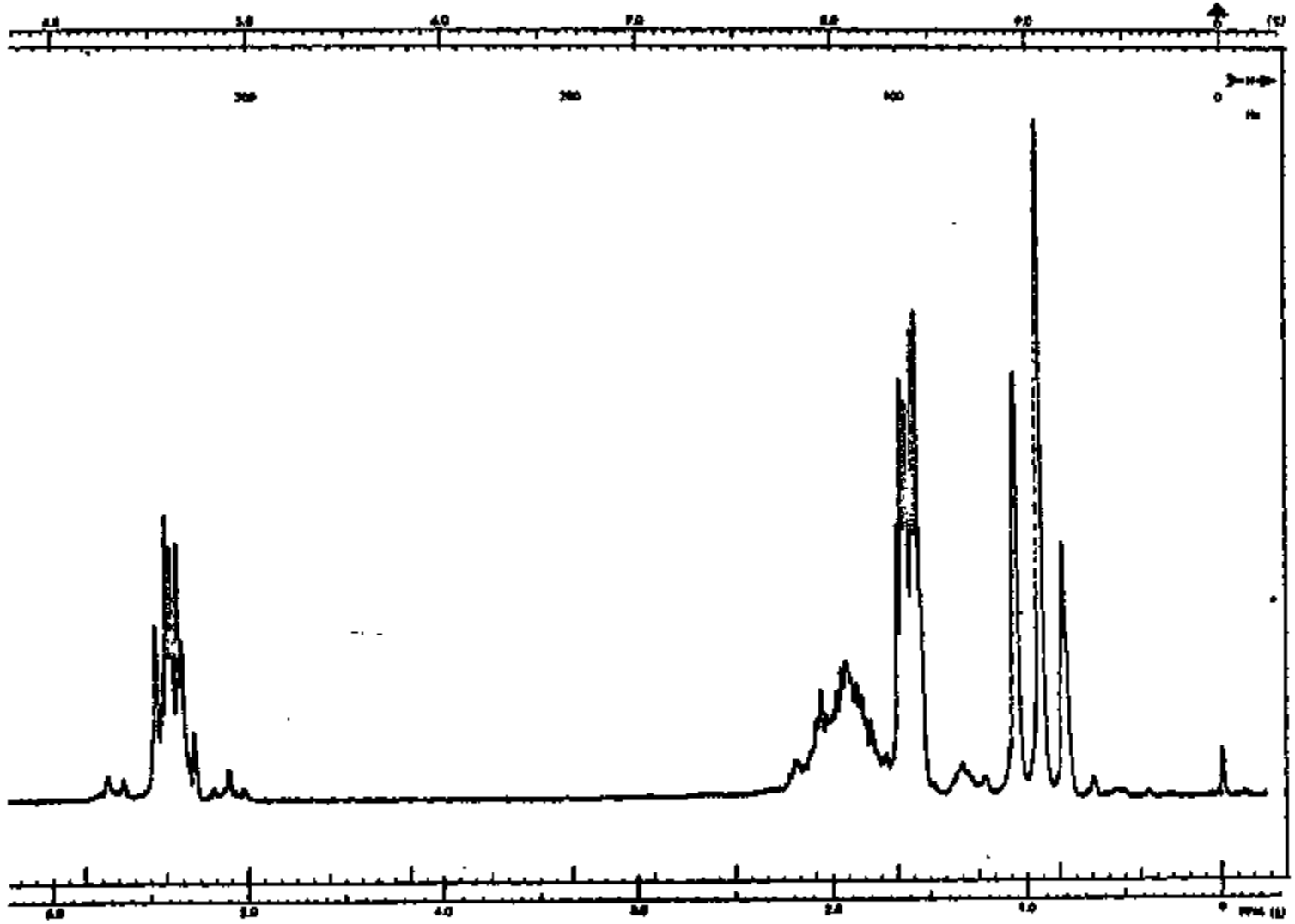

Figure 27. NMR spectra of pure trans-2-pentene.

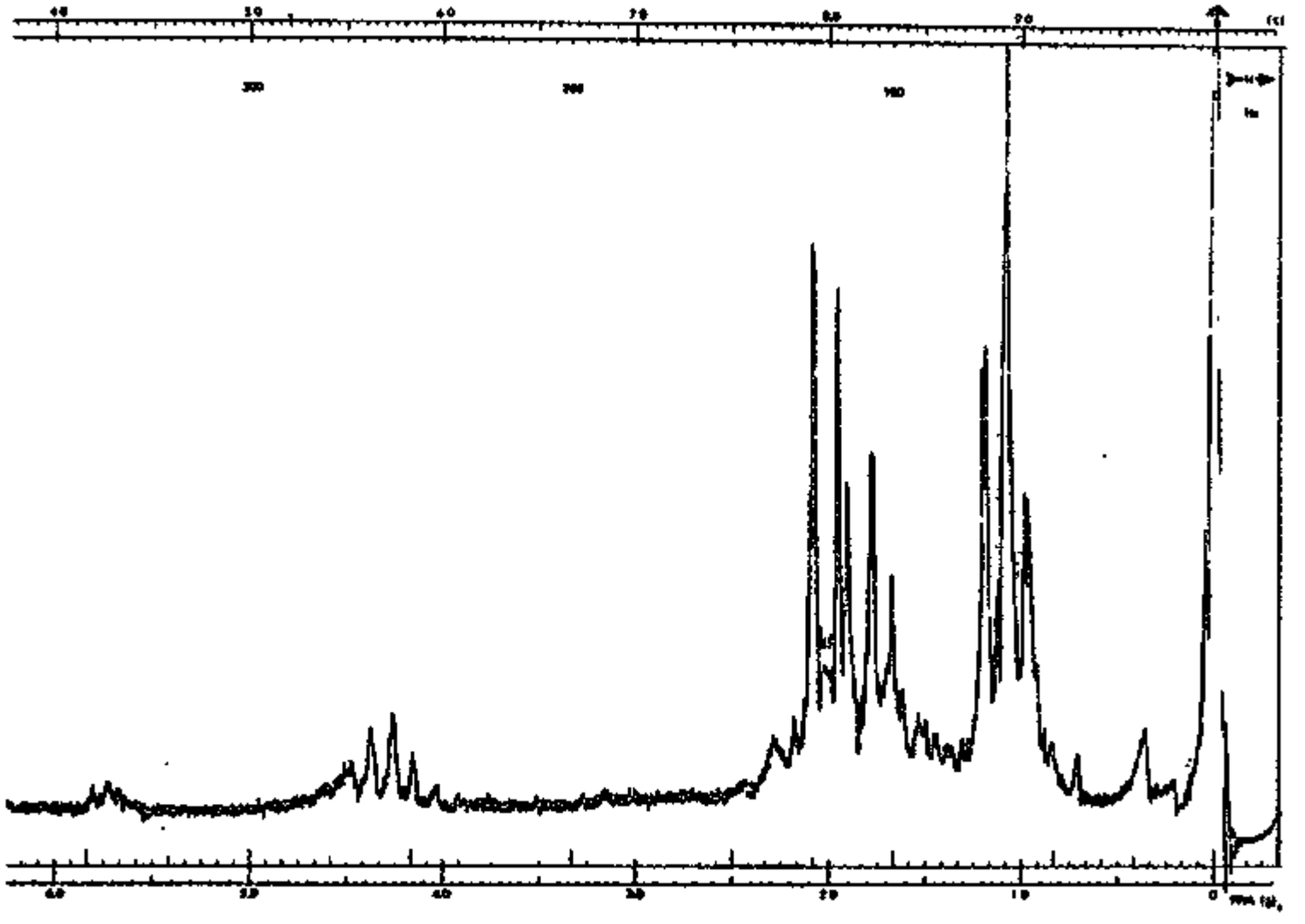

Figure 28. NMR spectra of meso-2,3-diiodopentane.

Discussion

Assuming a mechanism based on either steps 5 or 6, it was possible to obtain reproducible experimental values for the rate constant consistant with the rate laws for either of the respective mechanisms. As both steps 5 and 6 require activated complexes having identical configurations, the kinetic measurements would not be expected to distinguish between the two proposed alternate reaction paths. In addition the expected correlation between reaction rates and complexing ability of the respective olefins was found. The value obtained for the charge transfer equilibrium constant for the 1-pentene/iodine complex was consistant with the reported value for the iodine-cyclohexene complex.[25] It would therefore appear that, assuming similar complexing abilities of the olefins with I-atoms, either postulated mechanism is sufficiently justified by the experimental data.

The mechanism in step 5 is also in complete agreement with other studies which suggested that a concerted addition mechanism was required for the addition of iodine to alkenes. Most of these studies dealt with the reverse of the addition reaction[21,22] and with isomerization of olefins by iodine.[19,20,27,28] Agreement with the reported stereospecific nature of the iodine addition and elimination, found in this study and reported previously by Skell, et. al.[9], is also consistant with the proposed mechanism, as the pi-complex would be expected to collapse stereospecifically. Although our observations can be explained without assuming the existance of bridged radicals we can offer no definitive evidence to either prove or disprove the importance of the $C_5I\cdot$ radical in the formation of the diiodo products. However, the stereospecific nature of the iodine addition and elimination require the iodine atom to bridge the two carbons.

As discussed previously the diiodo products were converted back to their respective olefins and the stereospecific nature of the addition-elimination cycle of iodine was confirmed. The dependence of the thermal stability of the products on the presence of iodine and the conversion of the pentenes to their respective pentanes, while interesting were not pursued further.

CHAPTER IV CHEMICAL EFFECTS OF THE (n,γ)-ACTIVATION OF IODINE IN LIQUID ALKENE-IODINE SYSTEMS

The chemical effects of the (n,γ) induced reactions in condensed systems may involve a large number of factors, the relative importance of which is not well understood as yet. The currently accepted hypothesis employed in the interpretation of the chemical effects of the nuclear transformation induced reactions of heavy halogens in condensed systems is the "Auger Electron Hypothesis".[36] This hypothesis suggests that the recoil halogens react with the solvent radicals which are formed at high localized concentration in their immediate vicinity by reactions such as $RX + e^- \rightarrow R + X^-$ and $RX + H \rightarrow R + HX$, made possible by the localized radiation chemistry induced by the internal conversion and Auger electrons emitted by the recoil atoms.

Because of the complicated nature of radiation chemistry itself, such as the well known production of approximately equal quantities of radicals and ionized species, the "Auger Electron Hypothesis" proposed by Willard[36] fails to predict the identity of the reaction species responsible for the incorporation of the halogen into the solvent molecule and/or one of its fragments. In fact, the "Auger Electron Hypothesis" does not even consider the activated iodine species is directly participating in the formation of the observed products. For instance the formation of organic iodides could proceed <u>via</u> charged and/or excited iodine atoms, as found to occur in the gas phase[31-39], or by radicals produced by the internal conversion and Auger processes. However, the previously described hypothesis would not be expected to differentiate between the formation of products by either process.

In the past nearly all studies of the (n,γ) induced reactions of iodine in condensed systems have been carried out in various alkane and alkyl halide solvents. These solvents (target molecules), with the possible exception of some of the alkyl halides, would be expected to exhibit little chemical selectivity toward an ion or radical attack and, therefore, yield no information on the identity of the reactive species. There have been a few studies, however, with aromatic systems liable to attack by positive halogens at particular positions, thus leading to more specific modes of reaction.[40] Attempts to discover such effects have generally led to somewhat ambiguous results.

It would therefore be desirable to find and employ a system which would inhibit a chemical selectivity toward either an ion or a radical attack that could be detected by the formation of a product or products characteristic of an attack by a particular species. Alkenes with their electron rich double bond, could exhibit an internal chemical selectivity to attack by a positive iodine ion. If such is the case one would expect the ion to attack the molecule at the position of the double bond and as result observe an increase in the formation of products with the labeled iodine attached to this position, as compared to the product distribution of the corresponding alkane. Thus by studying the (n,γ) induced reactions of iodine in liquid alkenes, it may be possible to determine if ionic precursors are important to the incorporation of iodine into the solvent molecules in condensed media.

Although there exists little information with respect to the ion-molecule reactions of alkenes and halogens, the thermal (iodine free radical) reactions of iodine with alkenes in both the gas[14,29] and liquid[8,9,30] have been investigated in some detail. Golden and Benson[29] in a recent review

of the gas phase reactions have shown that these reactions do not lead to the incorporation of iodine into the alkene. Similar studies in the liquid state show that the formation of the respective 1,2-diiodo- products occurs rapidly when illuminated by ordinary white fluorescent light.[8,9] As discussed in Chapter III, it was found that the addition to the alkene double bond proceeds through a I atom catalyzed conserted addition process. It has been noted however, that negligable addition occurs in the absence of light[9,30] as would be expected for a free radical process. Thus, the (n,γ) induced hot atom studies of the addition of iodine to olefins may be performed in the dark, in either the gaseous or condensed state, with little or no interference expected from thermal addition reactions.

If, contrary to what would be expected, significant interference with the "hot atom" studies by thermal processes did occur, then a less reactive source of iodine such as CH_3I could be employed. The feasibility of using methyl iodide as a source of "hot" iodine has been demonstrated.[31,32] Although this would not permit the effects of I_2 scavenger to be determined and complicate the product determinations, no other experimental problems would be expected.

Organic Yields

Previous studies (Chapter III and Refs. 8,9,30) have shown that, while molecular iodine readily adds to the double bond in a number of simple olefins when in the presence of light, the addition reaction is neglible in the dark. In fact less than 10% addition was found to occur after three hrs. of standing in the dark for a 1.5×10^{-5} M solution of I_2 (^{131}I) in 1-pentene at 25°C. Therefore, all the iodine-olefin samples, for subsequent neutron activation, were

prepared in a completely darkened room with only a dim red light present to supply the necessary illumination. Quadruplicate one ml. samples of each concentration were prepared immediately ($\leq$ 1 min.) after mixing of the I_2 with the pentene isomer of interest. After placing the samples in individual quartz ampoules, the ampoules were shielded with an aluminum foil shroud to further protect them from any incident light during the degassing procedure described previously. Immediately after preparation the samples were wrapped in foil and frozen in liquid N_2. Just prior to activation of the individual samples in the reactor they were removed from the liquid N_2 and wrapped in carbon paper and then allowed to liquify. The carbon paper wrap was employed to shield the samples from any incident light during irradiation as the more durable aluminum foil wrap, used previously, would present an unnecessary radiation hazard as a result of its high cross section for thermal neutrons. Immediately after activation the samples were refrozen, unwrapped, and then extracted while solid. Thus, throughout the sample preparation, activation, and extraction procedures, little or no photo-induced addition reactions would be expected.

The $^{127}I(n,\gamma)^{128}I$ induced yield of iodine in 1-pentene, trans-2-pentene, and cis-2-pentene were determined as a function of I_2 concentration. The results are tabulated in Table X and represented graphically in Fig. 29. It was found that the organic yields of 1-pentene and cis-2-pentene were the same within experimental error and, that the trans-2-pentene yields were slightly lower than the corresponding 1-pentene and cis-2-pentene yields.

The organic yields of 1-pentene as a function of added CH_3I were then determined to test for any thermal contribution to the observed organic yields in the I_2-1-pentene system. Of the three olefins used, 1-pentene possesses

TABLE X

Radiative Neutron Capture Induced Yields of ^{128}I in Various C_5 Isomers as a Function of Additive Concentration

Additive	Concentration	Organic Yield			
		Pentane	1-pentene	trans-2-pentene	cis-2-pentene
I_2	4.8×10^{-2}				29.02
					29.11
					32.13
					29.19
					29.89
I_2	1×10^{-2}		36.78	31.58	40.88
			38.35	31.61	42.63
			40.25	32.47	37.41
			39.03	32.18	38.50
			38.60	31.96	39.86
I_2	1×10^{-3}	39.39	46.58	38.57	46.55
		40.45	47.82	41.97	48.26
		41.88	44.66	38.42	49.18
		40.88	43.71	35.02	42.90
			45.69	38.50	46.72
I_2	1×10^{-4}	45.42	49.30	45.77	58.73
		45.54	46.34	44.74	54.85
		50.65	48.48	43.46	56.79
		42.07	47.68	44.66	
			47.95		

TABLE X (cont.)

Additive	Concentration	Pentane	1-pentene	trans-2-pentene	cis-2-pentene
I_2	5×10^{-5}		53.35		
			52.54		
			55.76		
			53.88		
I_2	1×10^{-5}	48.53	54.05	54.04	60.66
		54.62	51.95	51.41	60.03
		47.95	55.87	64.26	60.30
		55.91	58.60	64.21	57.83
			55.12	61.71	59.71
				59.36	
				59.17	
I_2	5×10^{-6}			69.82	86.39
				66.84	80.52
				69.78	88.66
				73.67	77.99
				66.20	75.07
					41.49
I_2	1×10^{-6}	86.52	81.37	74.50	66.97
		88.51	66.69	59.68	71.82
		90.45	71.43	73.39	90.05
			88.59	89.55	91.73
				92.99	91.83
				90.46	85.24
				65.24	
				59.82	

TABLE X (cont.)

Additive	Concentration	Pentane	1-pentene	trans-2-pentene	cis-2-pentene
CH_3I	1×10^{-1}	53.28			
		54.58			
		57.65			
		61.62			
		56.78			
CH_3I	1×10^{-2}	56.55			
		57.39			
		58.11			
		58.44			
		58.56			
		59.17			
		59.91			
		62.78			
		58.86			
CH_3I	1×10^{-3}	56.55			
		60.00			
		60.52			
		63.53			
		64.37			
		66.11			
		62.15			
CH_3I	1×10^{-4}		57.80		
			59.95		
			61.91		
			62.73		
			63.30		
			65.13		
			62.48		

TABLE X (cont.)

Additive	Concentration	Pentane	1-pentene	trans-2-pentene	cis-2-pentene
CH_3I	1×10^{-5}		54.95		
			56.15		
			61.76		
			61.92		
			64.51		
			70.52		
			72.06		
			63.12		

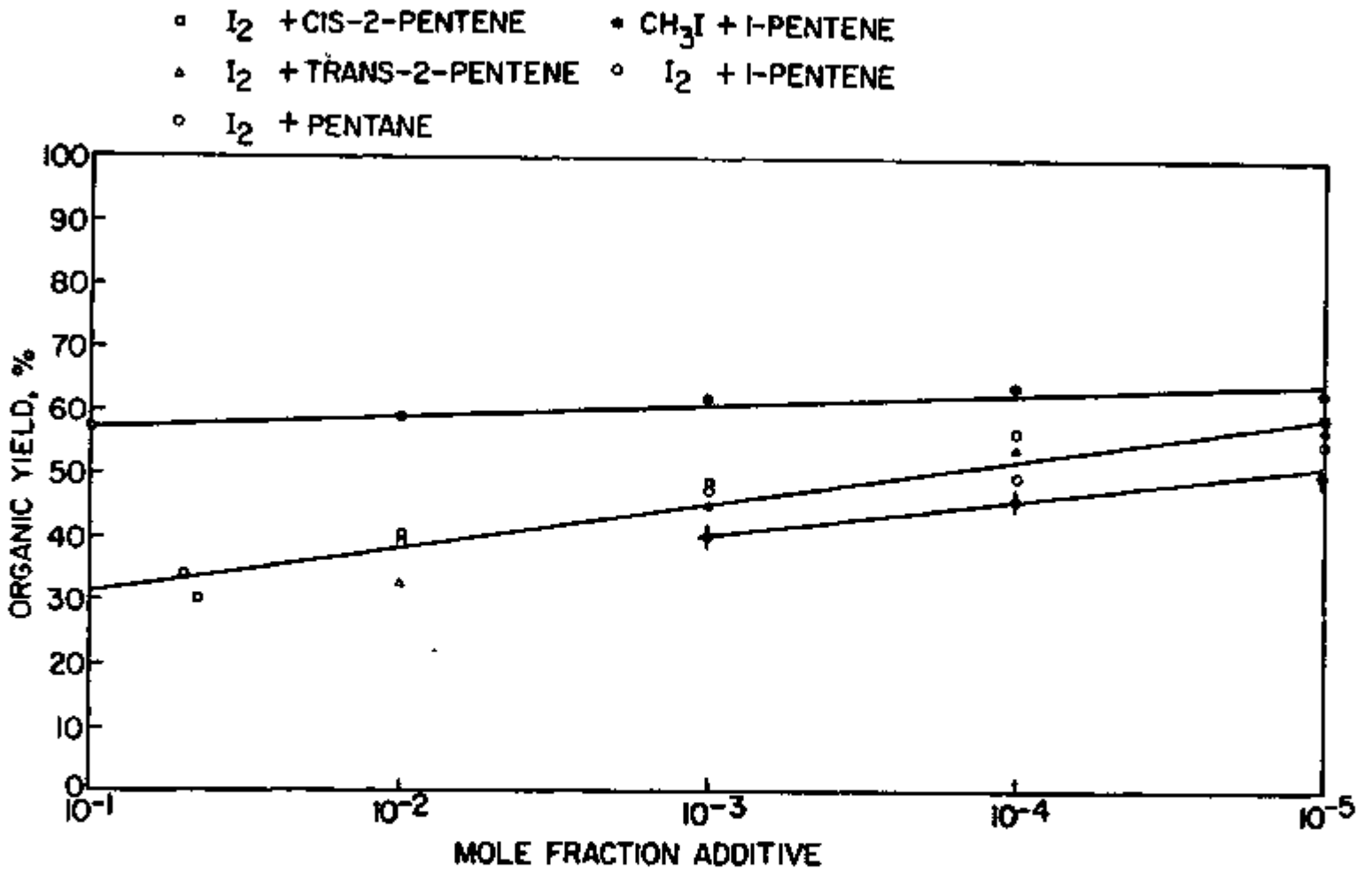

Figure 29. $^{127}I(n,\gamma)^{128}I$ induced organic yields in pentane and various pentene isomers as a function of I_2 or CH_3I concentration.

the fastest rate of thermal iodine addition[30], and was, therefore, selected as the system for this comparison.

Since CH_3I would not be expected to react thermally, with the various olefins studied the radiative neutron capture induced organic yields of dilute CH_3I-1-pentene solutions would be expected to reflect the organic yield in an iodine-1-pentene system in the absence of any thermal reactions and iodine scavenger effects. Thus, if there exists no contribution by thermal processes to the observed organic yields in very dilute iodine-olefin systems (where scavenger effects would be expected to be negligable) the radiative neutron capture induced yields of iodine in both the dilute CH_3I-olefin and I_2-olefin systems would be expected to be the same.

The experimentally determined organic yields obtained in the CH_3I-1-pentene system as a function of the methyl iodide concentration are presented in Table XVIII and compared with the I_2-1-pentene system in Fig. 29. After correction for the reported[123] 1.09% failure to bond rupture for the CH_3I, the CH_3I + 1-pentene organic yields were found to ca. 3 per cent higher than the corresponding I_2 + 1-pentene organic yields at 1×10^{-5} mole fraction added I_2 or CH_3I. The slightly lower yields for the I_2 + 1-pentene system can be attributed to the scavenging effect of the small amount of I_2 present; as comparison of the organic yields (and the trend of the yields with concentration) of the two systems at even lower additive concentrations suggest that they are identical for infinitely dilute solutions, as would be expected if there was no contribution to the observed I_2 + 1-pentene yields from thermal processes. However, the extremely low activities and radiolytic damage accompanying the longer irradiation times (~ 1 min.) preclude any accurate experimental values below 1×10^{-5} mole fraction additive.

The ^{128}I organic yields in the I_2 + pentane system, as a function of iodine concentration, were determined for comparison with the corresponding yields obtained in the pentene systems. The results of this study are also reported in Table X and compared with the pentene systems in Fig. 29. The ^{128}I organic yields were consistently lower than the corresponding pentene values and showed a smaller dependence on added iodine (scavenger) concentration. This smaller dependence on scavenger concentration indicates the $^{127}I(n,\gamma)^{128}I$ induced organic yields in the pentane system are less dependent on diffusive radical reactions than those in the unsaturated pentene systems.

The most important information obtained from the study of the organic yields in these varied C_5 isomers is the great similarity in the observed yields under identical conditions. Although the four C_5 isomer studied possess widely varying thermal reactivities with molecular iodine, varying from essentially zero to nearly complete addition in one hour, the radiative neutron capture induced yields vary less than 10 per cent over the entire concentration range studied. However, this information is not particularly useful in terms of any mechanistic interpretations; but, merely reflects the high energy nature of the nuclear activiation process.

The higher pentene yields do suggest, however, that the more thermally reactive double bond possessed by these isomers, also exhibits a greater reactivity toward the activated iodine species. The slightly smaller values obtained for the organic yields of the trans-2-pentene isomer could be the result of increased steric inhibition to attack at the position of the double bond by the reactive iodine species or compared to the 1-pentene and cis-2-pentene isomers. The importance of steric factors in the inhibition of $^{127}I(n,\gamma)^{128}I$

induced yields has been previously demonstrated in halocarbon systems.[33]

Product Distributions

As discussed previously, the organic yields of a system as a function of various parameters are insufficient, by themselves, for any adequate interpretation of the mechanism of product formation. As in any type of chemical reaction, it is essential that the final reaction product or products are known before any reasonable consideration can be given to the mechanism of their formation. Therefore, the I_2 + pentane, CH_3I + 1-pentene and I_2 + 1-pentene, cis-2-pentene, and trans-2-pentene systems were analyzed by radiogas chromatography in order to identify and measure the relative quantities of the various products formed by the nuclear activation of ^{127}I in these systems. With the exception of increased irradiation times, the preparation and irradiation of the various systems for product analyses was identical to the procedures employed for the organic yield samples.

The qualitative and quantitative product analyses for the various systems studied were determined as functions of additive (I_2 or CH_3I), additive concentration, and irradiation time. The product distributions obtained for the various C_5 isomers as functions of these parameters are tabulated in Table XI. The yields of the individual products are reported relative to the total organic activity detected. The qualitative identification of the saturated and unsaturated C_1-C_5 iodides and the relative abundances of these products were determined by the radiogas chromatography procedures as discussed in Chapter II.

As shown in Table XI the ^{128}product distributions for the various C_5 isomers exhibit considerable differences from isomer the isomer, particularly with respect to the relative quantities of methyl and the various C_5 iodides.

TABLE XI

Relative Yields[a] of Organic ^{128}I Products Formed by the $^{127}I(n,\gamma)^{128}I$ Activation of Iodine in Solutions of Various C_5 Hydrocarbon Isomers[b]

Isomer	I_2 mole fraction	Irrad. Time	CH_3I	C_2H_3I	C_2H_5I	i- and n- C_3H_5I	i- and n- C_3H_7I	C_4H_9I	C_5H_9I	2- and 3- $C_5H_{11}I$	1- $C_5H_{11}I$
Pentane[d]	1×10^{-2}	10 min.	6.4	2.0	13.7	1.8	12.3	3.1	0.8	34.8	25.0
	1×10^{-3}	10 min.	11.2	3.4	8.2	1.7	9.6	3.1	2.3	30.1	27.8
1-pentene[d]	1×10^{-3}	10 min.	5.0	4.6	10.5	0.9	7.7	2.8	3.7	35.3	27.1
	1×10^{-2}	10 min.	5.7	4.4	13.3	2.2	4.8	5.5	6.1	23.6	34.2
	1×10^{-2}	30 sec.	7.4	6.3	8.8	0.8	6.3	5.5	5.3	23.8	31.6
	d	10 min.	40.4	2.6	5.2	--c	3.9	--c	--c	14.6	10.6
	e	10 min.	28.1	3.7	6.8	1.5	5.9	2.4	2.9	24.7	18.8
	f	10 min.	21.8	5.4	10.1	1.0	6.3	2.8	4.0	18.6	24.9
trans-2-pentene	1×10^{-3}	10 min.	21.0	4.1	11.3	1.0	8.0	5.4	--c	38.9	6.3
	1×10^{-2}	10 min.	17.3	4.2	10.7	2.1	6.8	1.5	2.2	41.7	10.9
	1×10^{-2}	30 sec.	21.6	4.2	11.1	1.6	4.7	5.3	--c	34.5	6.3
cis-pentene	1×10^{-3}	10 min.	17.2	3.9	16.5	2.3	7.9	2.3	2.6	37.0	12.1
	1×10^{-2}	10 min.	21.1	4.7	10.6	1.1	5.8	--c	--c	43.8	12.9
	1×10^{-2}	30 sec.	25.9	4.7	10.3	1.1	7.4	5.2	--c	31.1	4.3

[a] Expressed as the percent total organic activity.

[b] All irradiations performed at 25° C in carbon wrapped ampoules.

[c] no peak detected.

[d] reference 75.

The product distributions of the cis and trans-2-pentene isomers are, however, identical within experimental error as might be expected.

Assuming that all positions were equally liable to attack by the reactive iodine species one would then expect a statistical distribution of the observed 1-,2-, and 3-iodopentanes and/or pentenes. In this case the relative product distributions for the C_5 iodides would be 2:1:2 for the 1-,3-, and 2-iodo products respectively. As the 2- and 3-iodopentanes were not separated in this study then the observed relative product distributions assuming a statistical distribution, would be 1.5:1 for the combined 2- and 3-iodopentanes and the 1-iodopentane, respectively.

Examining of experimental data in Table XI, the values for the relative product distributions for combined 2- and 3-iodo products and the 1-iodo product were found to be ca. 1.4, 0.7, 7.2, and 5.8 for pentane, 1-pentene, trans-2-pentene, and cis-2-pentene respectively. Thus, the I_2 + pentane system possesses a nearly statistical distribution of the respective C_5 iodides as would be expected due to the uniform bonding throughout this molecule. However, the 1- and 2-pentene isomer exhibit considerable deviation from a statistical distribution of iodination of the respective pentene molecules, with the 1-pentene isomer favoring iodination at the 1-position and the 2-pentene isomer favoring iodination at the 2- and/or 3-positions. This is precisely the expected result if the respective pentene isomers possessed an internal chemical selectivity towards attack by the reactive iodine species at the position of the double bond.

The greater CH_3I yields observed for the 2-pentene isomers over that found for 1-pentene and pentane systems could be the result of cleavage of the carbon to carbon single bond containing the methyl group adjacent to the double bond

with the subsequent attachment of the attacking iodine species, contained in the activated complex,* to the methyl radical produced. The lower total C_5 iodide yields for the 2-pentene isomers as compared to the pentane and 1-pentene systems would seem to support this hypothesis.

Comparison with Radiolysis Produced Products

The currently accepted hypothesis used to account for the chemical distribution of the active atoms produced by the nuclear activation is the autoradiolysis theory proposed by Geissler and Willard.[36] This hypothesis is based upon the observed similarity between the yields of radioactive products formed either by neutron capture in the system: aliphatic iodide + iodine + pentane, or by radiolysis of the same system tagged with $^{131}I_2$ with ^{60}Co γ-rays.[36]

In order to test the validity of the "autoradiation hypothesis" in describing the observed ^{128}I product distributions in our systems, the ^{131}I product distributions produced by radiolytic processes in similar systems, are required for purposes of comparison with the product distributions resulting from the nuclear activation process. There 1-pentene, trans-2-pentene, and cis-2-pentene samples containing 1×10^{-3} mole fraction of ^{131}I tagged molecular iodine were prepared for irradiation. These samples were then irradiated in the "lazy susan" of the TRIGA reactor for a period of two hours, during this time they received an accumulated γ-dose* of 3.6×10^{19} e.v. g^{-1} per sample. Little or no ^{132}I, produced by the nuclear activation of ^{131}I in the reactor, would be expected because of the extremely small quantity of ^{131}I in the sample (~ 1 mCi or $< 4 \times 10^{-11}$ moles) and the small thermal neutron cross section of 0.7 barns for the ^{131}I. Thus, after allowing $\geq$ 4 hours for the ^{128}I produced in these samples to decay, the only labeled products remaining would be the

desired ^{131}I labeled products produced by the γ-radiolysis during the sample irradiation.

The results obtained from the radiogas chromatographic analyses of the respective I_2 (^{131}I)-pentene systems are reported in Table XII and compared with the corresponding ^{128}I product distributions. For the purposes of comparison with the ^{131}I labeled radiolysis products the ^{128}I product distributions obtained in the short irradiation time, high iodine scavenger concentration systems were chosen, as they would be expected to possess the smallest contribution to the ^{128}I products formed by the accompanying radiolysis of the sample.

The comparison of the ^{131}I radiolytic product distributions with the ^{128}I product distributions from the (n,γ) activation of ^{127}I in Table XII shows two major differences between the relative quantities of the various products produced by the dissimiler processes. The major difference being a considerable decrease in the total quantity of the various obeerved fragmentation products (C_4-C_1 iodides) for the radiolysis produced products as compared to the ^{128}I product distributions, produced by the nuclear activation. In addition, the C_5 iodides produced by the radiolysis process tend to favor a more statistical distribution over those produced by the nuclear activation.

The increase in fragmentation products observed for the (n,γ) activation would suggest that the product formation proceeds through a higher energy process than the corresponding radiolysis processes. While the increased randomness in the formation of the various C_5 iodide isomers for the radiolytic process could be the result of decreased chemical selectivity in the formation of radicals by ionizing radiation and/or rearrangements occurring after the formation of the various hydrocarbon radicals.

TABLE XII

Comparison of the Radiolysis Produced ^{131}I Organic Products[a] from the Reactor Irradiation of I_2 (^{131}I) Solutions of the Various C_5 Hydrocarbon Isomers with the Corresponding ^{128}I Products[a] Produced by the Nuclear Activation of ^{127}I[b]

System	CH_3I	C_2H_3I	C_2H_3I	i- and n- C_3H_5I	i- and n- C_3H_7I	C_4H_9I	C_3H_9I	2- and 3- $C_5H_{11}I$	1- $C_5H_{11}I$	CH_2I_2
Pentane-^{131}I[c],	6.1	__d	14.1	__d	10.9	1.0	__d	51.0	17.0	__d
-^{128}I[h],	6.4	2.0	13.7	1.8	12.3	3.1	0.8	34.8	25.0	__d
1-pentene-^{131}I[f],	3.0	2.7	7.8	0.5	5.6	3.2	7.6	42.2	25.5	1.7
-^{128}I[e],	7.4	6.3	8.8	0.8	6.3	5.5	5.3	23.8	31.6	4.4
cis-2-pentene-^{131}I[f]	9.3	0.6	5.2	__g	4.0	0.8	__g	58.3	15.6	6.3
-^{128}I[e]	25.9	4.7	10.3	1.1	7.4	5.2	__g	31.1	4.3	6.6
trans-2-pentene-^{131}I[f]	10.1	__g	4.9	__g	4.3	1.3	__g	60.8	15.8	1.4
-^{128}I[e]	21.6	4.2	11.1	4.2	4.7	5.3	__g	34.5	6.3	7.2

TABLE XII (cont.)

a Expressed as per cent of total organic activity detected.

b All ^{128}I organic yields determined with 1×10^{-2} mole fraction of I_2 present and 30 sec. irradiation time to minimize any radiolytic contributions.

c Obtained from ref. 36

d No peak reported.

e 1×10^{-2} mf I_2

f 1×10^{-3} mf I_2 (^{131}I)

g No peak detected.

h 1×10^{-2} mf I_2

These differences between the product distributions of the organic iodides produced by radiolysis and the radiative neutron capture of ^{127}I, clearly indicate that the "autoradiation hypothesis" does not adequately explain the total product distributions for the (n,γ) activation of iodine in the various pentene systems studied. Therefore, other processes must account, either partially or completely, for the formation of the observed products in these systems.

Discussion

As discussed previously, the (n,γ) activation of ^{127}I produces chemical effects which are not only profound but quite varied in character. The energy released in the transformation manifests itself in the kinetic energy of the particle formed, in electromagnetic radiation, in ionization, and in electronic and other excitations. Most of this energy is dissipated in the surrounding medium, along tracks of promary and secondary particles, and produces normal radiolytic changes in the system. However, the iodine ion or atom incorporating the transformed nucleus is in itself a highly reactive entity and should not be neglected in an overall consideration of the mechanism or mechanisms of final product formation. Thus the number of reactive species capable of participating in the formation of products are many and varied.

The "autoradiation hypothesis" attributes the formation of all products to reactions between the activated halogen and solvent radicals which are formed by the localized radiation chemistry induced by the internal conversion and Auger electrons emitted by the recoil atoms; thereby, completely neglecting any possible contribution to the overall product formation by the potentially reactive iodine atom or ion produced by the nuclear transformations.

Two other possible processes, not considered by the "autoradiation hypothesis", are displacement reactions whereby the iodine atom or ion replaces a hydrogen atom or radical from a solvent molecule in a bimolecular process by virtue of its excess kinetic energy and the formation of products through ion-molecule reaction with ions produced by the vacancy cascade associated with the internal conversion of the activated iodine and/or the subsequent neutralization of this highly charged specie by charge exchange with the surrounding media.

Gas phase studies have shown[34,37,38,39,126] the bimolecular replacement reactions of species attacked by ^{128}I to result in total organic yields of only a few percent, except in CH_4 systems. Thus this type of process would not be expected to contribute, appreciably to the total yields observed in condensed systems unless the probability for this type of reaction is greatly altered by the change in phase. The reactions of iodine atoms at elevated temperatures with various saturated and unsaturated hydrocarbons do not lead to the production of organic iodides but instead produce HI by a hydrogen abstraction mechanism.[14,29,35] In addition, the studies[9,30] of the photo and thermochemical reactions of iodine atoms and molecules in the various liquid pentenes of interest reveal no formation of the various mono-iodo products found in this study. On the basis of the accumulated evidence presented above the formation of the organic products observed in this study via bimolecular displacement reactions would appear to be unimportant.

In the I_2 + pentene liquid systems employed in this study, the highly charged iodine atom produced by the nuclear activation process will first share its charge with the molecule to which it is attached and then abstract electrons from the surrounding solvent molecules producing considerable ion-

ization and fragmentation of these molecules in close proximity to the activated iodine. During this stage chemical combination would be improbable between the activated iodine and the charged solvent molecules, and will occur only after the charge density has been reduced by neutralization or by diffusion of the ions away from each other. Because of their lower mass, protons dissociated from the solvent molecules by this process would be expected to diffuse further than any other groups under the action of the field, so that the center of the ionic cluster containing the activated iodine would be rich in hydrogen deficient species with which the active atom may react. This type of mechanism, previously advanced by Mia and Shaw[41] to explain the product distributions associated with neutron capture processes in liquid bromoethane systems, could be expected to produce both ionic and radical iodine and hydrocarbon precursors leading to the eventual organic combination of the activated iodine species.

In a recent study of the ion-molecule reactions of various simple olefins, Henis[42] was able to account for the observed products distributions in all of the reactions studied by assuming the following selection factors:

1. no significant rearrangement of parent ions;
2. positive charge located at a secondary carbon in the parent ion;
3. site of the unpaired electron may be considered the active or attacking site on the ion;
4. addition occurs at either double-bond site (seric factors may favor primary sites when they are available);
5. fragmentation involving more than one bond is not possible;
6. fragmentation occurs most favorably at the tertiary carbon in the intermediate;

7. loss of CH_3 radicals generally will not occur (possibly due to un favorable thermo-chemistry).

Assuming these qualitative rules also apply to ion-molecule reactions between iodine atoms or ions with olefin ions or atoms, respectively, the observed product distributions found for the (n,γ) induced reactions of ^{128}I in the C_5 pentene isomer could be accounted for. In particular rules 3 and 4 would account for the preferential addition of iodine at the double bond site and rule 5 for the extremely small quantities of di-iodo products observed. Although rule 7 conflicts with the large quantities of methyl iodide found in our systems, particularly for the 2-pentene systems, the potentially higher energy nature of the ion-molecule reactions in our systems could account for this violation. In fact, the high CH_3I^{128} yields obtained in the 2-pentenes show a strong preference for loss of CH_3 radicals adjacent to the double bond. It would therefore seem that the ionization associated wit the nuclear activation of the iodine leads to subsequent ion-molecule reactions between the activated iodine and the solvent or its fragmentation products; thereby, accounting for the differences found between products distributions produced by nuclear activation and radiolytic processes found in this study.

V. REACTIONS OF SELECTED HALOGENS AND INTERHALOGENS BY RADIATIVE NEUTRON CAPTURE AND ISOMERIC TRANSITION WITH CONDENSED STATE CYCLOPENTANE AND AROMATIC HYDROCARBONS

Progress in this area was previously reported in Chapter V of our Progress Report No. 3 and Chapters IV and VI of our Porgress Report No. 4.

Previous studies of nuclear activated halogen reactions have been mainly with alkyl halide and aliphatic hydrocarbon systems. Much of this work was hampered by a lack of knowledge concerning experimental parameters and metastable states, by the limited availability of carrier-free nuclides of interest, and by the lack of instrumentation capable of resolving multiisotope system assays. With most of these problems taken care of, it has become possible to study multi-isotope systems in most of the hydrocarbons, especially those of relatively low molecular weight.

With the availability of organic yield and labeled organic product distribution probes in halogen hot atom chemistry, the possibility of investigating compounds of biological interest was considered. The iodothyronines, which are synthesized and used in the body, seemed to be a natural choice for an introductory study. Several studies have been reported in this area but essentially nothing in depth has been done in the area of hot atom reactions with the iodothyronines.

Due to the complexity of the iodothryonine molecules, only preliminary work was performed to ensure a solid foundation for such a project in the future. For a relatively comprehensive study, benzene and alkyl benzenes were probed with a number of halogen nuclides at 298° K and 77° K. Cyclopentane,

a strained aliphatic ring system, was also studied for a broader picture of hot atom reactions with ring systems.

The primary goals of this research were to investigate the following:

1. (a) The reactions of $^{127}I_2$, $^{129}I_2$, and ICl activated by radiative neutron capture and isomeric transition in liquid and solid (77° K) cyclopentance; (b) the possibility of an isotope effect among the various isotopes of iodine activated by the two nuclear processes; (c) the labeled product distribution in camparison with cyclohexane.
2. (a) The reactions of $^{127}I_2$, $^{129}I_2$, Br_2, IBr, and ICl activated by radiative neutron capture and isomeric transition in liquid and solid (77° K) benzene; (b) the possibility of an isotope effect among the various isotopes of bromine (and iodine) activated by the two nuclear processes; (c) the correlation between organic yield plateaus and the crystalline structure of the bromine-benzene system (77° K); (d) the labeled product distribution of the various halogen nuclides in benzene.
3. (a) The reactions of $^{127}I_2$ and ICl activated by radiative neutron capture in selected alkylbenzenes at 77° K and 298° K; (b) the role of a side chain on an aromatic nucleus in organic yield andisotope effect studies; (c) the effect of the alkyl side chains in the labeled product distribution of selected alkylbenzenes.

Cyclopentane, benzene and selected alkylbenzenes were probed both in the liquid and solid phases with nuclear processes induced by the neutron activation of one or more of the following species: $^{127}I_2$, $^{129}I_2$, Br_2, ICl and

IBr. Of particular interest in each of the systems were the following: (1) isotope effects due to (n,γ) and (IT) processes; (2) individual and comparative scavenging effects in the liquid phase systems of the various halogens and interhalogens; (3) crystalline structure at 77° K, and; (4) product distributions of organic halides.

As in previous studies of the ^{127}I (n,γ) ^{128}I, ^{129}I (n,γ) ^{130}I and $^{130}I^{m}$ (IT) ^{130}I processes in aliphatic hydrcarbons, the ^{128}I and ^{130}I (by IT) organic yields in cyclopentane were essentially the same and in the range of 1.2 to 1.4 times higher than the ^{130}I (by n,γ) organic yields. Of further similarity was the product distribution which was seemingly independent of the nuclear process and phase. The major organic product was found to be iodocyclopentane although in the iodine-cyclohexane system the major product was reported to be the hexyl iodides. In comparing the ^{128}I and ^{38}Cl organic yields in the solid state I_2- and ICl- cyclopentane systems, it was found that although the ^{128}I O.Y. plateaus cover about the same concentration range (2×10^{-5} and lower mf of I_2 and ICl) the ^{38}Cl O.Y. plateau starts somewhat lower, approximately 10^{-4} mf ICl, thus indicating that the ^{38}Cl organic yields are probably a better guide to fractional crystallization.

All of the nuclear processes used in this study were used in the study of benzene in order to thoroughly probe this aromatic system found in thyroxine and related compounds. The study of the alkylbenzenes was made to further lay the groundwork for future study of certain amino acids and hormones containing one or more aromatic nuclei.

It was found that essentially no scavenging effect occurred in liquid I_2- and Br_2- benzene systems, and ^{38}Cl organic yields were not affected by

either ICl concentration of phase effects in benzene. In liquid benzene systems containing two halogens both bromine and iodine showed a significant scavenging effect ($^{80}Br^{m}$, $^{82}Br + {}^{82}Br^{m}$, ^{128}I and ^{82}Br organic yields). The nuclear processes of both chlorine and bromine tended to increase the ^{128}I organic yields in liquid benzene while the $^{127}I\ (n,\gamma)\ ^{128}I$ process generally lowered the bromine isotope organic yields and had no effect on the ^{38}Cl O.Y.s. In liquid I_2-alkylbenzene systems, a self-scavenging effect was quite evident in all of them. The ^{128}I organic yields were generally higher at 10^{-5} mf I_2 that in the I_2-benzene system but became approximately equal in saturated solutions.

The product distribution studies along with the comparative organic yield studies in the liquid systems indicated that the number of different products produced by the nuclear processes of the halogens increases as one goes from iodine to bromine to chlorine, whereas relative "scavenging" ability is in the reverse order. The increased ^{128}I O.Y.s.in mixed systems is apparently due to thermal reactions of ^{128}I species with excited species produced by either bromine or chlorine nuclear processes. The decreased bromine isotope organic yields appear to be caused by the enhanced scavenging of excited species by I_2 and ^{38}Cl O.Y.s are constant since there are no thermal reactions of ^{38}Cl atoms (or ions).

In solid state systems of benzene and the various halogens and interhalogens, isotope effects occurred between $^{129}I\ (n,\gamma)\ ^{130}I + {}^{130}I^{m}$ and $^{129}I\ (n,\gamma)\ ^{130}I + {}^{130}I^{m}\ (IT)\ ^{130}I$ processes and the various nuclear processes of bromine studied. There was also an appreciable difference in the $^{79}Br\ (n,\gamma)\ ^{80}Br^{m}$ and $^{81}Br\ (n,\gamma)\ ^{82}Br$ processes in liquid benzene. Since the presence of extremely small quantities of impurities were found to cover up or indicate isotope effects when the reverse was found at

higher purity levels, only the isotope effect studies in the Br_2-benzene systems were regarded with a high degree of confidence. The alkylbenzenes could not be purified well enough for such a study nor were such purities available commercially as was benzene.

Organic yield studies of Br_2 in benzene at 77° K produced two O.Y. plateaus, the various isotopes producing different but parallel curves. The lower curves between 5×10^{-1} and 5×10^{-2} mf Br_2 have been interpreted to indicate a region of uniform 1:1 complex to a mixture of complex plus pure solvent. The upper curves were interpreted here to be a monomolecular dispersion of Br_2 in benzene. Due to limitations in solubility, 5×10^{-2} mf I_2 in benzene was probably not reached in the solid state. Although ^{128}I organic yields in both the I_2- and ICl-benzene systems indicated a monomolecular dispersion at 10^{-4} and lower mf I_2 and ICl, the ^{38}Cl O.Y.s remained at about 21% throughout the concentration range studied. Thus, although the ^{128}I O.Y.s dropped rapidly at higher concentrations of I_2 and ICl, apparently no significant clustering occurred. Iodine O.Y.s are seemingly a misleading guide to structure in aromatic systems at the present.

^{128}I and ^{38}Cl organic yields in solid state I_2- and ICl-alkylbenzene systems resemble those in the analogous benzene systems, indicating complex formation with a probable difference between the ICl and I_2 systems since the ^{128}I O.Y.s from ICl are consistently lower than those from I_2 except at 10^{-2} mf halogen. Product distribution of the I_2-alkylbenzene systems indicate that alkyl side chains are quite vulnerable to attack by hot atom processes. Methyl iodide was the major product by far in several alkylbenzenes studied except in the case of ethylbenzene where ethyl iodide

essentially equalled the methyl iodide formed. Also a large amount of an unstable organic iodide was formed in the I_2-ethylbenzene, I_2-cumene and I_2-tert-butylbenzene systems.

VI. Isotope and Pressure Effects of (n,γ) and (I.T.) - Activated Bromine Reactions in Gaseous CH_3Br, CH_3Cl and CH_3F

The main purpose of studying the (n,γ) and (I.T.) activated reactions of bromine in CH_3Br, CH_3Cl and CH_3F is to better understand bromine reactions in systems other than CH_4 or CD_4, to evaluate the role of target molecule parameters on the product yields, to determine the relative importance of charge and hot atom kinetic energy on the reaction products by both (I.T.) and (n,γ)-activation, to evaluate the applicability of the E strip-Wolfgang kinetic theory to those systems, and to evaluate decomposition probabilities of the various products as a function of target molecule. Our broad goal is to develop mechanisms for these reactions.

By employing radiogas chromatography we are studying reaction systems at various systems pressures and varying concentrations of rare gas or halogen additives. The study at the present time is incomplete. We have only partially studied the reactions of bromine in CH_3Br and CH_3F. At this time we will only summarize some of our CH_3Br systems data.

The CH_3Br System

While (n,γ)-activated ^{80}Br[43] reacts with CH_4 to yield CH_3Br mainly as a result of the recoil kinetic energy acquired by the ^{80}Br, (I.T.)-activated ^{82}Br reacts with CH_4 by both [44] excess kinetic-energy processes (utilizing the kinetic energy acquired by Coulombic repulsion) and thermal (kinetic-energy-independent) processes to yield both [45,46] CH_3Br and CH_2Br_2. The CH_3Br system is interesting in that, unlike CH_4, the environment for the (I.T.)-activated ^{82}Br ions has a lower ionization potential (10.29)[47] than that of the bromine atom (11.84)[5]. From moderator studies on the ^{82}Br-CH_3Br system, the relative importance of kinetic energy and positive charge (as well as importance of ion-molecule and charge neutralization) can be readily determined.

In preliminary studies of reactions of (I.T.) and (n,γ)-activated reaction of ^{80}Br with alkanes and haloalkanes, Spicer and Gordus[48] found that the organic yields of ^{80}Br by (I.T.) and (n,γ)-activation are 2.4 ± 0.3 and 2.8 ± 0.2 respectively. Okamoto and Tachikawa [49] report a total organic yield for (I.T.)-activated ^{82}Br of 5.93% in CH_3Br systems containing 50 mm Hg of Br_2 with a total system pressure of 510 mm Hg. If a difference in organic yields between (I.T.)-activated ^{80}Br and ^{82}Br exists, we do not believe it would be of the magnitude presently reported in the literature.

EXPERIMENTAL

Bromine prepared from Mallinchrodt reagent-grade $K_2Cr_2O_7$, KBr, and H_2SO_4 was used after three distillations over P_2O_5. Matheson CH_3Br and Airco assayed reagent Ar were used directly.

Sextuplicate quartz ampules contained either (a) Br_2 (5mm), Ar, and CH_3Br, with a total system pressure of 700 mm Hg, or (b) CH_3Br with varying quantities of Br_2, with a total system pressure of 200 or 700 mm Hg. Sample preparation, handling, and neutron irradiation in the Omaha, Nebraska V.A. Hospital reactor employing an "in-reactor technique" have been described previously.[44] Most systems were irradiated for 20 seconds, which corresponded to a total radiation absorbed by a sample of about 2×10^{-5} e.v. per molecule.

All relative product distributions were determined by radiogas chromatography employing a modified flow-through proportional counter of the type described by Wolf et. al.[1] for the detection of the labeled products. All product determinations were carried out on a 1/4 in. x 10 ft. column containing a 5% loading of Di(2-ethylhexyl) sebacate on 50/60 mesh C-22 support at a flow rate of 100 ml/min. Individual samples were analyzed by direct introduction into the pre-column carrier gas streams, with ballistic temperature programming from 0°C to 110°C. A 1/4 in. x 4 in. pre-column packed with potassium ferro-

cyanide was used to remove all inorganic bromine prior to passage of the sample through the analytical column. Under these conditions the observed adjusted retention volumes were 280, 700, 1150 and 2100 ml. for CH_3Br, C_2H_5Br, CH_2Br_2, and $CHBr_3$ respectively. The product yields reported in this paper are the percent individual activities relative to the total organic activities observed, multiplied by the total organic yield. All ^{82}Br samples were analyzed at least 48 hours after irradiation. The major products observed were $CH_3{}^{82}Br$ and $CH_2{}^{82}BrBr$, although several minor products such as $CHBr_2Br^{82}$ and $C_2H_4BrBr^{82}$ were observed.

RESULTS AND DISCUSSION

The effects of Ar moderator and Br_2 additive on the individual product yields (labeled CH_3Br and CH_2Br_2) of the reaction of CH_3Br with ^{82}Br activated by the (I.T.) process are depicted in Fig. 30. Using procedures described previously[9] we determined the failure to bond rupture of ^{82}Br from the $^{81}Br(n,\gamma)^{82}Br^m$ and $^{82}Br^m(I.T.)^{82}Br$ processes to be 0.28%. All reported data are corrected for this observed failure to bond rupture.

The data appear to extrapolate for both Ar and Br_2, to $2.6 \pm 0.2\%$ for $CH_3{}^{82}Br$ and to $1.3 \pm 0.2\%$ for $CH_2{}^{82}BrBr$ at zero mole fraction additive. At one mole fraction of either additive, the data appear to extrapolate to $0 \pm 0.3\%$ for both products. This suggests that the products $CH_3{}^{82}Br$ and $CH_2{}^{82}BrBr$ are both formed via excess kinetic-energy processes.

We investigated for possible isotope effects between (n,γ) and (I.T.)-activated ^{82}Br reactions in CH_3Br by comparing the total ^{82}Br organic yields for the two nuclear processes as a function of mole fraction additive. At zero mole fraction additive, the ^{82}Br organic yield resulting from (n,γ) activation was $4.3 \pm 0.2\%$, while that for (I.T.) activation was $3.9 \pm 0.2\%$. The organic yield for each activation process was $0 \pm 0.3\%$ at one mole fraction

additive. For the two processes there were no real differences in the organic yields as a function of mole fraction additive.

In comparing the total (I.T.)-activated ^{82}Br organic yields for the $CH_3Br + Br_2$ systems at 200 and 700 mm Hg pressure, we found no differences within experimental error.

Several conclusions can be drawn from this study.

1. Within experimental error, no isotope effect exists between (n,γ) and (I.T)-activated ^{82}Br reactions with CH_3Br. Our value for the total (I.T.)-activated ^{82}Br organic yield ($3.9 \pm 0.2\%$) is significantly lower than the value (5.93%) reported by Okamoto and Tachikawa.[7] A possible reason for this discrepency is that, in their preparation of $^{82}Br^m$ systems, 80 to 90% of the $^{82}Br^m$ decayed prior to their mixing the $^{82}Br^m$ with CH_3Br. Correcting to zero decay could produce a significant error in the results. If an isotope effect does exist for (I.T.)-activated reactions of ^{80}Br and ^{82}Br, it does not appear to be as large as suggested by previous results.[48, 49]
2. Both the (I.T.)-produced products, $CH_3{}^{82}Br$ and $CH_3{}^{82}BrBr$, seem to be formed by excess kinetic-energy processes. This could indicate that there is no contribution to the observed organic yields by thermal ion-molecule reactions. The energetically favored charge exchange process ($CH_3Br + {}^{82}Br^+ \rightarrow CH_3Br^+ + {}^{82}Br + 1.3$ e.v.) supports the contention that thermal $^{82}Br^+$ ions do not contribute to the observed organic yields.
3. Preferential replacement of the Br atom over the H atom in the CH_3Br molecule by the "hot" ^{82}Br is similar to results found by Spicer and Wolfgang[51, 52] in "hot" Cl and F reactions with halocarbons.
4. No pressure effect appears to exist between 200 and 700 mm Hg for the (I.T.)-activated ^{82}Br reaction with CH_3Br. Okamoto and Tachikawa reported[7]

a pressure effect in systems containing 5 cm Hg Br_2 and a pressure of CH_3Br varying from 1.8 to 76.6 cm Hg. Their observed effect is merely a result of varying Br_2 additive concentration, and not a true pressure effect. This type of effect has been reported previously in the reactions of (n,γ)-activated ^{80}Br [3] with CH_4 and (I.T.)-activated ^{82}Br [2] reactions with CH_4.

PERSONNEL, PUBLICATIONS, TALKS AND MEETINGS

A. PERSONNEL LISTING:

1. Project Director

E. P. Rack

2. Graduate Students

R. L. Ayres (Ph.D., August 1970)

O. Gadeken

H. K. J. Hahn

E. J. Kemnitz (Ph.D., August 1970)

D. Oates

J. B. Nicholas

R. Pettijohn

K. Swartz

M. Yoong

3. Undergraduate Students

F. E. Ming

4. Manuscript Typing and Progress Report Preparations

Sondra Kernmoade

B. PUBLICATIONS

1. E. J. Kemnitz, H. K. J. Hahn and E. P. Rack, Isotope and Concentration Effects of Bromine in Polycrystalline Benzene at 77° K, Radiochim Acta, 13, 112 (1970).

2. H. K. J. Hahn, M. Yoong and E. P. Rack, Radiometric Analysis of Serum and Tissue Proteins, In Press, J. Lab. and Clin. Medicine (Dec., 1970).

3. R. L. Ayres and E. P. Rack, Szilard-Chalmers Organic Yields in Liquid and Solid Alkyl Iodides, Radiochem. Radioanal. Letters, 3, (3) 213 (1970).

4. D. W. Oates, R. L. Ayres, R. W. Helton, K. S. Schwartz and E. P. Rack, Isomeric Transition Activated Reactions of ^{82}Br with Gaseous Methyl Bromide, Radiochem. Radioanal. Letters, 4 (3), 123 (1970).

5. O. C. Gadeken, R. L. Ayres, and E. P. Rack, Application of Isotopically-labeled Br4mine for the Determination of Trace Unsaturation in Alkanes, Analytical Chemistry, 42, 1105 (1970).

6. R. L. Ayres, C. J. Michejda and E. P. Rack, Reactions of Iodine with Olefins: I. Kinetics and Mechanism of Iodine Addition to Pentene Isomers, J. American Chemical Society, (Feb. 1971) in Press.

7. Reactions of Iodine with Olefins. II. Radiative Neutron Capture Induces Reactions of ^{128}I with Various C_5 Isomers: Evidence for the Participation of Ion-Molecule Reactions in the Condensed State, J. Phy. Chem. (submitted for publication).

C. TALKS

1. R. W. Helton (with E. P. Rack), "Isotope and Pressure Effects of (n,γ) - Activated Bromine Reactions in Gaseous CH_3F." Los Angeles, California, March 1971. Divisions of Nuclear Chemistry and Technology, Am. Chem. Soc.)

2. M. Yoong (with E. P. Rack). "Decomposition Probabilities for Products formed by (n,γ) and (I.T.) Activated Iodine in CH_4, CD_4 and Halomethanes." Los Angeles, California, March 1971, Division of Nuclear Chemistry and Technology, Am. Chem. Soc.

ACKNOWLEDGEMENTS

We greatly appreciate the kind cooperation of Mr. A. Bloctky and the staff of the Omaha V. A. Hospital reactor in assisting with the many neutron irradiations. Special thanks to Mr. Tim Crouer and Mr. Lloyd Moore who fabricated all the special vacuum lines, radio-gas chromatography hardware and quartz bulblets. Without their help much of the progress would not be possible.

LIST OF REFERENCES

1. M. Welch, R. Withnell, and A. P. Wolf, Anal. Chem., 39, 275 (1967).
2. Progress Report No. 3, (No. COO-1617-13), Feb. 15, 1969.
3. J. A. Merrigan, Ph.D. Thesis, The University of Nebraska, 1966.
4. R. D. Peterson, J. Gas Chromatog., 1, 19 (1963).
5. R. L. Tecsak, Ed., "Principles and Practice of Gas Chromatography," John Wiley and Sons, Inc., London, (1959).
6. R. E. Young, H. K. Pratt, J. B. Baile, Anal. Chem., 24, 551 (1952).
7. D. M. Coulson, Anal. Chem., 31, 906 (1959).
8. G. Sumrell, B. M. Wyman, R. G. Howell and M. C. Harvey, Can. J. Chem., 42, 2710 (1964).
9. P. S. Skell and R. R. Pavlis, J. Am. Chem. Soc., 86, 2956 (1964).
10. T. S. Paterson and J. Robertson, J. Chem. Soc., 125, 1526 (1964).
11. A. Fairbourne and D. W. Stevens, ibid., 1973 (1932).
12. M. P. Cava and D. R. Napier, J. Am. Chem. Soc., 79, 1701 (1957).
13. F. R. Jensen and W. F. Coleman, J. Org. Chem., 23, 869 (1958).
14. S. W. Benson, D. M. Golden, and K. W. Egger, J. Chem. Phys., 42, 4265 (1965).
15. R. L. Burwell, Jr., and R. G. Pearson, J. Phys. Chem., 70, 300 (1966).
16. R. M. Noyes, D. E. Applequist, S. W. Benson, D. M. Golden, and P. S. Skell, J. Chem. Phys., 46, 1221 (1967).
17. P. S. Skell, D. L. Tuleen, and P. D. Readio, J. Am. Chem. Soc., 85, 2850 (1963).
18. P. S. Skell and P. D. Readio, J. Am. Chem. Soc., 86, 3334 (1964).
19. P. S. Skell, "Organic Reaction Mechanisms" (The Chemical Society, London, 1964), Special Publ. No. 19, pp. 131-145.
20. S. W. Benson, K. W. Egger, and D. M. Golden, J. Am. Chem. Soc., 87, 468 (1965).
21. M. J. Polissar, J. Am. Chem. Soc., 52, 956 (1930).

22. L. B. Arnold, Jr. and G. B. Kistiakowsky, J. Chem. Phy., 1, 166 (1933).

23. A. Abrams and T. W. Davis, J. Am. Chem. Soc., 76, 5593 (1954).

24. R. J. Cvetanovic, D. J. Duncan, W. E. Falconer, and W. A. Sunder, J. Am. Chem. Soc., 88, 1602 (1966).

25. L. J. Andrews and R. M. Keefer, J. Am. Chem. Soc., 74, 458 (1952).

26. The nmr data in Ref. 1 was used to identify 1, 2-diiodopentane. The meso and d, l-2, 3-diiodopentanes were identified on the basis of comparison of their nmr spectra with the spectra of the chloro- and bromo- analogs found in Sadtler NRM Spectra, Sadtler Research Laboratories, Philadelphia, Pa.

27. K. W. Egger and S. W. Benson, J. Am. Chem. Soc., 88, 236 (1966).

28. S. Furuyama, D. M. Golden, and S. W. Benson, Int. J. Chem. Kin., 1, 147 (1969).

29. D. M. Golden and S. W. Benson, Chem. Rev., 69, 125 (1969).

30. R. L. Ayres, C. J. Michejda, and E. P. Rack, J. Am. Chem. Soc., (In Press).

31. A. A. Gordus and Chi-Hua Hsiung, J. Chem. Phys., 36, 954 (1962).

32. R. L. Ayres and E. P. Rack, Radiochem. Radioanal. Letters, 3, 213 (1970).

33. N. J. Parks and E. P. Rack, Radiochim, Acta, 10, 26 (1968).

34. A. A. Gordus and J. E. Willard, J. Am. Chem. Soc., 79, 4609 (1957).

35. J. H. Raley, R. D. Mullineaux, and C. W. Bittner, J. Am. Chem. Soc., 85, 3174 (1963).

36. P. R. Geissler and J. E. Willard, J. Phys. Chem., 67, 1675 (1963).

37. E. P. Rack and A. A. Gordus, J. Chem. Phys., 34, 1855 (1961).

38. E. P. Rack and A. A. Gordus, J. Chem. Phys., 36, 287 (1962).

39. G. Levey and J. E. Willard, J. Chem. Phys., 25, 904 (1956).

40. A. G. Maddock and R. Wolfgang in "Nuclear Chemistry", Vol. 2, L. Yaffe, ed., Academic Press, New York, 1968, pp. 185-248.

41. M. D. Mia and P. D. F. Shaw, Radiochim. Acta, 6, 172 (1966).

42. J. M. S. Henis, J. Chem. Phys., 52, 282 (1970).

43. E. P. Rack and A. A. Gordus, J. Phys. Chem., 65, 944 (1961).

44. (a) J. B. Nicholas, J. A. Merrigan, and E. P. Rack, J. Chem. Phys., 46, 1996 (1967).
(b) J. B. Nicholas and E. P. Rack, J. Chem. Phys., 48, 4085 (1968).

45. E. Tachikawa, Bull. Chem. Soc. Japan, 42, 2404 (1969).

46. D. W. Oates, Unpublished Data.

47. R. W. Kiser, "Tables of Ionization Potentials," Office of Technical Services, Department of Commerce, Washington D. C., U. S. Atomic Energy Commission, Dept. TID-6142 (1960).

48. L. D. Spicer and A. A. Gordus, "Chemical Effects of Nuclear Transformations," Vol. I, IAEA, Vienna (1965), p. 185.

49. J. Okamoto and E. Tachikawa, Bull, Chem. Soc. Japan, 42, 1504 (1969).

50. A. A. Gordus and C. Hsiung, J. Chem. Phys., 36, 954 (1962).

51. L. Spicer and R. Wolfgang, J. Am. Chem. Soc., 90, 2426 (1968).

52. L. Spicer and R. Wolfgang, J. Am. Chem. Soc., 90, 2425 (1968).